Journal of the
OPTICAL SOCIETY
of AMERICA

VOLUME 32 NOVEMBER, 1942 NUMBER 11

The Dispersion of Silicate Glasses as a Function of Composition. II*

MAURICE L. HUGGINS, KUAN HAN SUN, AND DOROTHY O. DAVIS
Kodak Research Laboratories, Rochester, New York

(Received August 10, 1942)

A previously proposed refraction and dispersion equation, containing two empirical constants per component oxide, is improved by the addition, for each component, of a term containing a single new constant (the same for all components) and, for each of the components PbO, CaO, and BaO, of another term containing two additional constants characteristic of the component. Tests of the new equation with experimental data, both for simple (crystalline and vitreous) oxides and for 2-, 3-, and multicomponent glasses, show agreement, practically within the probable error of the experimental data, over the visible range of wave-lengths.

ONE of the authors[1,2] has shown that the dispersion of silicate glasses in the visible region of the spectrum can be fairly well represented as a function of the composition and density by a simple relation involving two empirical constants per component. In this paper we show how the agreement can be bettered considerably, principally as a result of the addition, for each component, of another term, involving a single additional constant—the same for all components. We also compare our dispersion equations with those recently published by Young and Finn[3] and by Herzberger.[4]

DEDUCTION OF A NEW DISPERSION FORMULA

As before,[1,2,5] we use the relation

$$\mu_\lambda = n_\lambda - 1 = R_{0,\lambda}/V_0 = \sum R_{M,\lambda}/V_0 = \sum a_{M,\lambda} \cdot N_M/V_0, \quad (1)$$

where n_λ is the index of refraction for the wave-length λ, V_0 is the volume and R_0 the refraction per gram atom of oxygen, and N_M is the number of atoms of the element M per atom of oxygen. The constants $a_{M,\lambda}$ depend on the kind of element M and on the wave-length λ in a manner to be described below. μ_λ is defined by its relationship to n_λ. $R_{M,\lambda}$ is the contribution of a single component M_mO_n to the total $R_{0,\lambda}$.

V_0 can be determined from the density ρ and the weight fractions f_M and molecular weights W_M of the component oxides by means of the equation

$$V_0 = [\rho \sum (n_M f_M / W_M)]^{-1}. \quad (2)$$

Alternatively, it can be computed[6] from the

* Communication No. 875 from the Kodak Research Laboratories.

[1] M. L. Huggins, J. Opt. Soc. Am. **30**, 514 (1940). Certain errors in the figures of this paper may be noted here: Figures 1 and 2 should be interchanged. The decimal points in the numbers in the ordinate scales of these figures should all be moved one place to the left. (The actual agreement is 10 times as good as that indicated.) The ordinates of Figs. 1 and 2 should be labeled n_λ(obs.)$-n_\lambda$(calc.); that of Fig. 3 should be labeled $10^{-10}\, g_{Pb}$.

[2] M. L. Huggins, Ind. Eng. Chem. **32**, 1433 (1940).

[3] J. C. Young and A. N. Finn, J. Research Nat. Bur. Stand. **25**, 759 (1940).

[4] M. Herzberger, J. Opt. Soc. Am. **32**, 70 (1942).

[5] M. L. Huggins, J. Opt. Soc. Am. **30**, 495 (1940).

[6] M. L. Huggins, J. Opt. Soc. Am. **30**, 420 (1940).

BOSTON UNIVERSITY
COLLEGE OF LIBERAL ARTS
LIBRARY

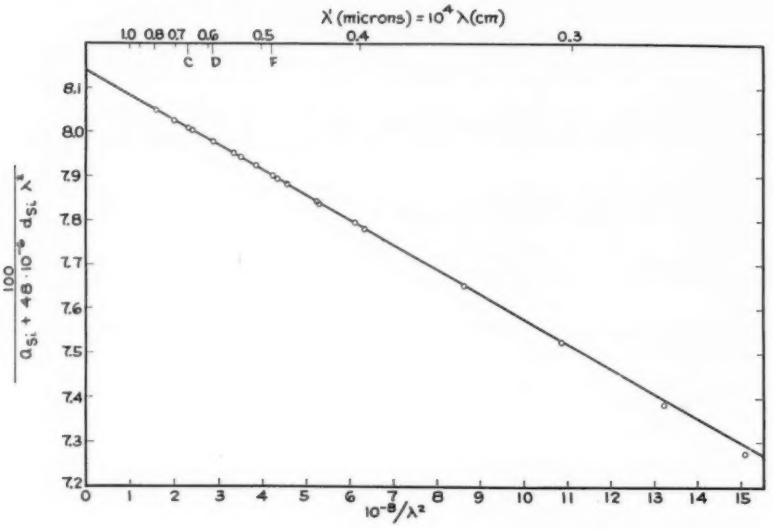

FIG. 1. To show agreement with Eqs. (11) and (12) for vitreous silica. The dots represent the most probable refractive index values, according to Sosman (reference 8).

compositions, using the equation

$$V_0 = k + b_{Si} + c_{Si}N_{Si} + \sum' c_M N_M, \qquad (3)$$

where k, b_{Si}, c_{Si}, and c_M denote empirical constants previously determined. The summation in this equation is over all of the components except silica.

N_M in Eqs. (1) and (3) is calculated from the weight fractions, formulas, and molecular (formula) weights by means of the equation

$$N_M = \frac{m_M f_M / W_M}{\sum (n_M f_M / W_M)}. \qquad (4)$$

Equation (1) has been shown[2,5] to hold well for the wave-length of the D line of sodium. If it holds for *all* wave-lengths of interest, there must be, for each component, a quantity $a_{M,\lambda}$ which varies with the wave-length but not with the kinds or amounts of other components. This variation with wave-length can be approximately represented[1,2] by the equation

$$a_{M,\lambda} = \frac{d_M}{g_M - (1/\lambda^2)}, \qquad (5)$$

in which d_M and g_M are independent of wave-length.

The published values of the empirical constants d_M and g_M were deduced almost entirely from data on the refractive indices of glasses for the D, F, and C lines. Moreover, this relation was tested almost exclusively, except for pure vitreous SiO_2, by comparing calculated with experimental values of the indices for these lines or of the difference between the index for F and that for C.

One should not expect a relation as simple as Eq. (5) to hold accurately over a large range of wave-lengths. From well-known optical theory one would expect a term, similar in form to the right side of Eq. (5), for each absorption band which has an appreciable effect on the dispersion. If there were but one such absorption band for each component, the g_M value would be the reciprocal of the square of the effective mean wave-length λ_M of that band:

$$g_M = 1/\lambda_M^2. \qquad (6)$$

The empirical g_M values correspond to absorption bands in the ultraviolet.

An obvious extension of Eq. (5), which might be expected to give somewhat better agreement with experiment, would be the addition of a term for the effect of an absorption band in the infra-red, thus:

$$a_{M,\lambda} = \frac{d_M}{1/\lambda_M^2 - 1/\lambda^2} + \frac{d_{M,i}}{1/\lambda_{M,i}^2 - 1/\lambda^2}. \qquad (7)$$

Here, λ_M and $\lambda_{M,i}$ are the effective mean wave-lengths of supposed absorption bands in the

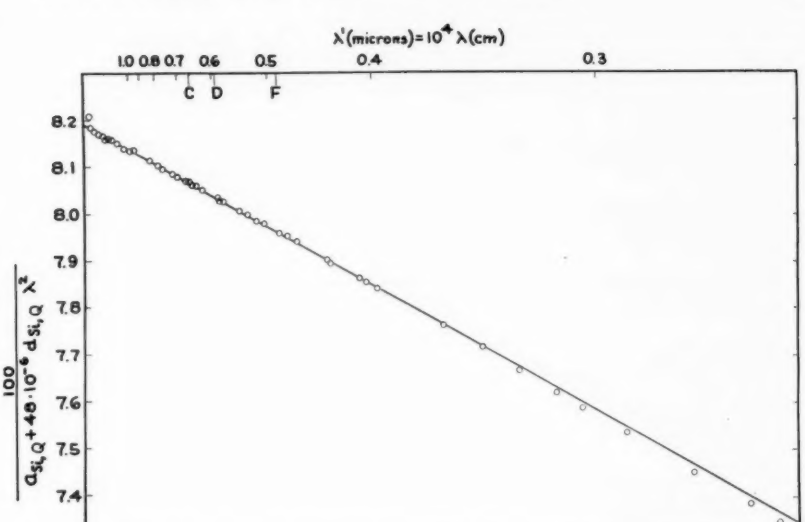

FIG. 2. To show agreement with Eqs. (11) and (12) for quartz. The dots represent mean indices of refraction, computed by means of Eq. (25) from Sosman's (reference 8) most probable values for the ordinary and extraordinary rays.

ultraviolet and infra-red, respectively, and d_M and $d_{M,i}$ are related to the probabilities of absorption for these bands.

For most ordinary glasses at least, the infra-red absorption band nearest the visible region occurs[7] at wave-lengths greater than 7 microns, i.e., much longer than those of visible light. We shall tentatively assume that for *all* the components of interest

$$\lambda_{M,i} \gg \lambda \tag{8}$$

and so

$$\frac{d_{M,i}}{1/\lambda^2_{M,i} - 1/\lambda^2} \approx -d_{M,i}\lambda^2. \tag{9}$$

We thus arrive at the equation

$$a_{M,\lambda} = \frac{d_M}{g_M - 1/\lambda^2} - d_{M,i}\lambda^2. \tag{10}$$

Rearranging this equation, we obtain

$$\frac{1}{a_{M,\lambda} + d_{M,i}\lambda^2} = \frac{g_M}{d_M} - \frac{1}{d_M \lambda^2}. \tag{11}$$

If this relation holds, a plot of $1/(a_{M,\lambda}+d_{M,i}\lambda^2)$ against $1/\lambda^2$ for any given component should show the points following a straight line, having a slope equal to $-1/d_M$ and an intercept, at $1/\lambda^2=0$ equal to g_M/d_M.

For vitreous and crystalline (quartz) SiO_2, vitreous B_2O_3, and crystalline MgO, accurate data are available for testing this. In each of these cases a value of $d_{M,i}$ has been found which will give this rectilinear relationship accurately over the visible spectrum. (See Figs. 1–4.[8–10])

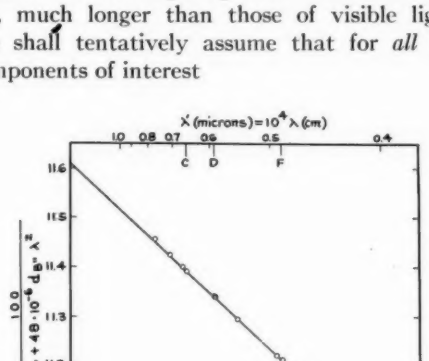

FIG. 3. To show agreement with Eqs. (11) and (12) for vitreous B_2O_3. The dots represent experimental refractive indices by Morey and Merwin (reference 9).

[7] F. Matossi and H. Bluschke, Zeits. f. Physik **108**, 295 (1938).

[8] R. B. Sosman, *The Properties of Silica* (Reinhold, New York, 1927).

[9] G. W. Morey and H. E. Merwin, J. Am. Chem. Soc. **58**, 2248 (1936).

[10] J. Strong and R. T. Brice, J. Opt. Soc. Am. **25**, 207 (1935).

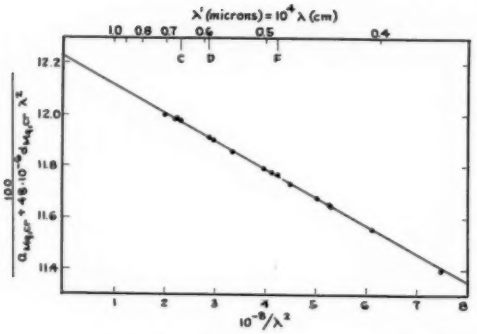

FIG. 4. To show agreement with Eqs. (11) and (12) for crystalline MgO. Experimental data by Strong and Brice (reference 10).

Obtaining the constants empirically in this way, it is found, surprisingly, that

$$d_{M,i}/d_M = k_i = 48 \cdot 10^{-6}, \tag{12}$$

practically within experimental error, in each instance. Because of this result and because the calculation of three independent constants per component is not at present possible—since only n_D and $n_F - n_C$ are known for most of the glasses of simple, accurately analyzed composition—we make the tentative assumption that Eq. (12) holds, to a sufficient degree of accuracy for our purpose, for *all* components. As more data become available it will doubtless become necessary to modify this assumption.

Another justification for this procedure is the following. Herzberger[4] has used a dispersion equation, applicable to ordinary silicate glasses, which can be written

$$\mu_\lambda = K' + K''\lambda^2 + \frac{K'''}{\lambda^2 - \lambda_1^2} + \frac{K''''}{(\lambda^2 - \lambda_1^2)^2}, \tag{13}$$

with

$$K' = \alpha'\mu_D + \alpha(\mu_F - \mu_C), \tag{14}$$

$$K'' = \beta'\mu_D + \beta(\mu_F - \mu_C), \tag{15}$$

$$K''' = \gamma'\mu_D + \gamma(\mu_F - \mu_C), \tag{16}$$

$$K'''' = \delta'\mu_D + \delta(\mu_F - \mu_C), \tag{17}$$

α, β, γ, δ, α', β', γ', δ', and λ_1 being empirical constants. Since Eq. (13) holds well for glasses of widely varying composition, we may reasonably assume it to hold, at least approximately, for each component separately. Applying Eq. (1), then,

$$a_{M,\lambda} = k_M' + k_M''\lambda^2 + \frac{k_M'''}{\lambda^2 - \lambda_1^2} + \frac{k_M''''}{(\lambda^2 - \lambda_1^2)^2}, \tag{18}$$

with

$$k_M' = \alpha' a_D + \alpha a_{F-C}, \tag{19}$$

$$k_M'' = \beta' a_D + \beta a_{F-C}, \tag{20}$$

etc. (a_{F-C} is an abbreviation for $a_F - a_C$.)

Comparing Eqs. (10) and (18), it seems reasonable to assume that the coefficients of λ^2, in the second term of each, are approximately equal. Using Herzberger's values of his constants,

$$d_{M,i} \approx -k_M'' = 70.58 \cdot 10^4 a_D - 889 \cdot 10^4 a_{F-C}. \tag{21}$$

(The constants given in reference 4 are for use with refractive indices for the *d*, *F*, and *C* lines. Dr. Herzberger has kindly furnished us with the corresponding constants pertaining to *D*, *F*, and *C*.) Table I gives the values of the ratio $d_{M,i}/d_M$, computed by means of this relation, using either the d_M, a_D, and $a_F - a_C$ values previously published[1,2] or those deduced in the present study. Except for Fe_{III}, the variation is not large. (The reason why Fe_{III} is so irregular in this respect will be discussed further on in this paper.)

TABLE I. Rough values of the ratio $d_{M,i}/d_M$, using $d_{M,i}$ values computed from Eq. (21).

	$10^6 d_{M,i}/d_M$			$10^6 d_{M,i}/d_M$	
M	Using d_M from ref. 1	Using d_M from Table II	*M*	Using d_M from ref. 1	Using d_M from Table II
Li		57	*B'*	30	32
Na	64	62	*B''*		46
K	57	55	Al	45	47
Rb		51	Y		59
Cs		47	La		57
Tl_I		6	Ga		61
			In		62
Be		34	As_{III}	69	53
Mg	57	55	Sb_{III}	72	70
Ca	57	53	Bi_{III}	57	64
Sr		51	Fe_{III}	−2767	−1927
Ba		46			
Zn	66	64	Si	44	40
Pb_{II}	69	70	Ti		62
			Ge		59
			Sn_{IV}		66
			Zr		69
			Th_{IV}		66
			P_V		33
			Cb_V		71
			Ta_V		71
			W_{VI}		71

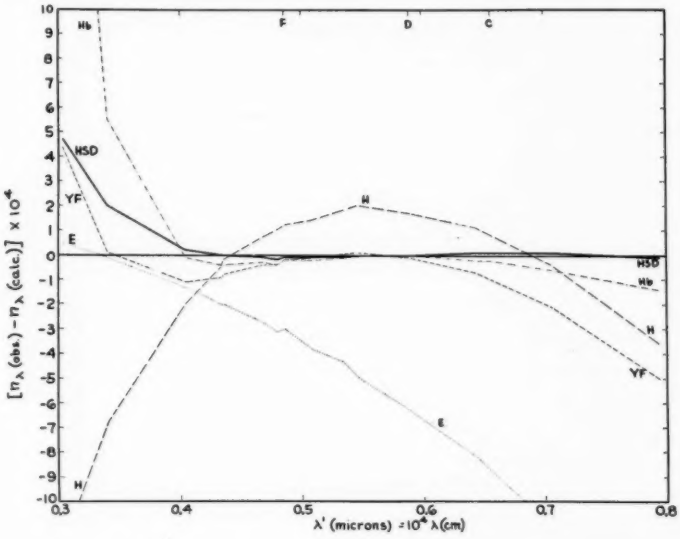

FIG. 5. Differences between observed and calculated indices of refraction for vitreous silica. The "observed" indices are Sosman's "most probable" values (reference 8). HSD ——— Huggins, Sun, and Davis, Eqs. (1), (22), and (12); H — — — — — Huggins, Eqs. (1) and (5); YF – – – – – – – – Young and Finn, Eq. (23); E ---------- Engl, Eq. (24); Hb —·—·—·— Herzberger, Eqs. (13)–(17).

Therefore, since the infra-red term is relatively small, we believe that the assumption of a constant ratio [Eq. (12)] will not lead to much error. At any rate, this is better than our previous hypothesis that it is uniformly zero.

In place of Eq. (5), therefore, we adopt the equation

$$a_{M,\lambda}=\frac{d_M}{g_M-1/\lambda^2}-k_i d_M\lambda^2, \qquad (22)$$

with k_i equal to $48\cdot10^{-6}$.

COMPARISON OF DISPERSION EQUATIONS FOR CERTAIN VITREOUS AND CRYSTALLINE OXIDES

Figure 5 shows (curve HSD) the deviations between the observed refractive indices for vitreous silica and those calculated by means of Eqs. (1), (22), and (12). Over practically the whole visible region ($\lambda=0.4$ to $0.8\cdot10^{-4}$ cm) the agreement with the values considered by Sosman[8] to be most probable (at 18°C) is within one or two units in the fifth decimal place—somewhat better than the agreement between Sosman's most probable values and either of the two most accurate sets of experimental data.[11,12,13]

[11] J. W. Gifford and W. A. Shenstone, Proc. Roy. Soc. London **73**, 201 (1904).
[12] J. W. Gifford, Proc. Roy. Soc. London **A84**, 193 (1910.)
[13] H. Trommsdorff, Die Dispersion Jenaer Gläser im ultravioletten Strahlengebiet, Inaug.-Diss. Jena (1901); see reference 8, pp. 595–6.

It may be noted that our constants for Si have been derived from n_λ values reduced to vacuum by multiplying the values (N_λ) for the index in air by 1.000275 (see reference 16, p. 366). Our constants for other elements have been deduced from indices given by Morey as n_λ. If they are really *vacuum* values (as implied by this notation), the index values calculated from our constants are also vacuum values (n_λ); on the other hand, if they are really *air* values, those calculated from our constants should also be considered as air values (N_λ), except for pure or nearly pure SiO_2. Practically speaking, the difference between the vacuum and air indices is considerably less than the probable error introduced due to inaccuracies in the experimental indices and compositions and in our characteristic constants, except in the case of pure silica. (See the footnote to Table III.)

As would be expected, the deviations (curve H) from the indices computed from our older[1,2] two-constant-per-component relation [Eqs. (1) and (5)] are considerably larger. This is also true of the deviations (curve YF) from Young and Finn's[3] two-constant-per-component equation

$$\frac{n_\lambda-1}{\rho}=\sum 100 f_M\left(\alpha_M+\frac{\beta_M}{\lambda^2}\right), \qquad (23)$$

in which f_M is (as in Eqs. (2) and (4)) the weight

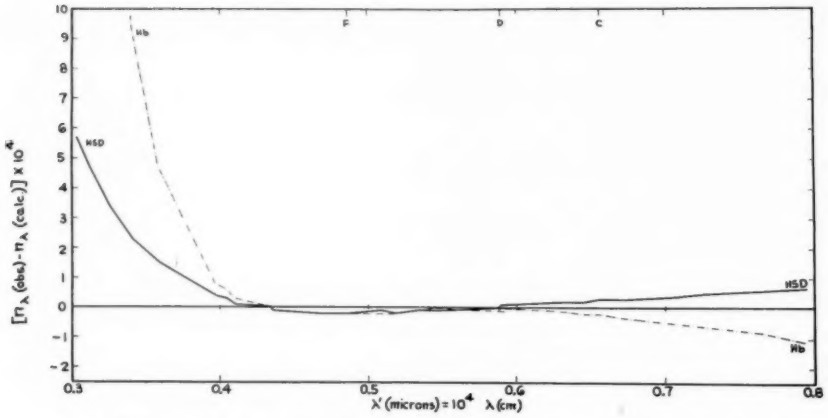

FIG. 6. Differences between experimental and calculated mean refractive indices for quartz. HSD ———— Huggins, Sun, and Davis; $d_{Si,\,Q}=1829.29\cdot10^8$; $g_{Si,\,Q}=149.819\cdot10^8$; Hb —·—·—·— Herzberger.

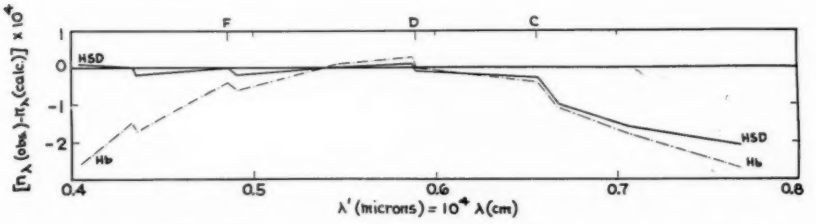

FIG. 7. Differences between experimental and calculated refractive indices for vitreous B_2O_3. HSD ———— Huggins, Sun, and Davis; $d_{B''}=1066.0\cdot10^8$; $g_{B''}=123.752\cdot10^8$; Hb —·—·—·— Herzberger.

fraction of component M_mO_n (here SiO_2) and α_M and β_M are empirical constants characteristic of this component. (α_M and β_M values for the components SiO_2, Na_2O, K_2O, and CaO have been published.)

The four-constant equation [cf. Eq. (7)],

$$\frac{n_\lambda^2-1}{n_\lambda^2+2}=\frac{A}{a-c^2/\lambda^2}+\frac{B}{b-c^2/\lambda^2}, \qquad (24)$$

in which A, B, a, and b are empirical constants and c is the velocity of light, has recently been tested for silica glass by Engl.[14] Using the constants he has deduced, the agreement with the experimental data is somewhat better than for our equation in the ultraviolet, but poorer in the visible and infra-red. (See curve E of Fig. 5.)

Herzberger's[4] relation [Eqs. (13–17)], although deduced for ordinary silicate glasses, gives agreement for vitreous silica over most of the visible range which is nearly as good as that obtained with our new equations. (Compare curves HSD and Hb.)

(References to Herzberger's equations, here and elsewhere in this paper, are to his equations for the calculation of n_λ values for various wavelengths from *two* experimental values, e.g., n_d and n_{F-C}. His published expressions for calculating n_λ values from *four* experimental measurements, e.g., n_d, n_{F-C}, $n_{A'}$, and n_h, as well as an unpublished expression of his for calculating them from *three* known refractive indices, give agreement, apparently within the probable experimental error, over the whole visible range.)

Figure 6 shows a comparison of the differences between (mean) observed and calculated refractive indices for quartz. The mean experimental values were computed by means of the

[14] J. Engl, Ann. d. Physik [5] **25**, 600 (1936).

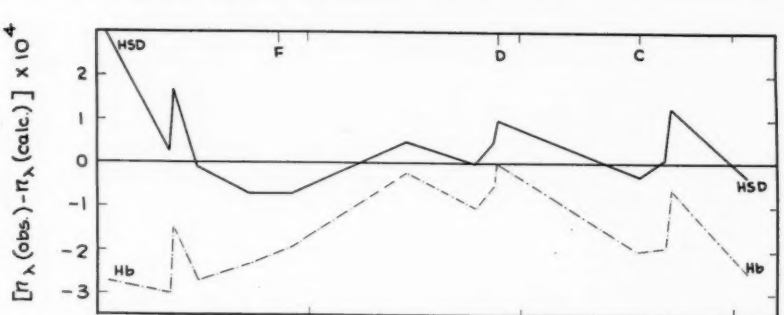

FIG. 8. Differences between observed and calculated indices of refraction for crystalline MgO. HSD ——— Huggins, Sun, and Davis; $d_{Mg}=912.26\cdot 10^8$; $g_{Mg}=111.55\cdot 10^8$; Hb —·—·—·— Herzberger.

equation[15]

$$\bar{n}=\left(\frac{2n_\omega^2+n_\epsilon^2}{3}\right)^{\frac{1}{2}} \tag{25}$$

from the most probable indices for the ordinary and extraordinary rays, at 18°C, as given by Sosman.[8] The heavy curve (HSD) shows the deviations from indices computed with the aid of Eqs. (1), (22), and (12) of this paper. The other (Hb) shows the deviations from the indices computed by Herzberger's procedure. The equations used by Huggins and by Young and Finn (using the constants computed for SiO_2 glass) give much larger deviations. No curve is given for Engl's equation, since he has published the constants only for n_ω and n_ϵ, not for the mean index $\bar{n}$.

Figure 7 is a similar graph for vitreous B_2O_3. Appropriate constants for substitution in Huggins' older equation and in Young and Finn's and Engl's equations are not available. Our new relation leads to fairly large deviations ($\sim 2\times 10^{-4}$) at the infra-red end of the visible; Herzberger's expression gives deviations of this order of magnitude at both ends of the visible spectrum.

Figure 8 gives similar comparisons for magnesium oxide crystals. The experimental data are here more erratic. Our new equation seems to give agreement within the probable experimental error from about 0.43 to 0.71 micron.

CALCULATION OF THE $a_{M,\lambda}$, d_M, AND g_M CONSTANTS

The d_M and g_M values published[1,2] for use with Eq. (5) are obviously not correct for use with Eq. (22). New values have therefore been deduced. In doing this we have revised and extended the previous $a_{M,D}$ and $a_{M,F-C}$ values. The new values for all these constants are collected in Table II. Our general procedure in deducing these will now be outlined.

As before, we start with vitreous SiO_2. The d_{Si} and g_{Si} values are obtained with the aid of Eq. (11). After obtaining approximate values from a graph of the type of Fig. 1, a plot of

$$\frac{1}{a_{Si,\lambda}+k_i[d_{Si}]\lambda^2}-\frac{[g_{Si}]}{[d_{Si}]}+\frac{1}{[d_{Si}]\lambda^2}$$

(in which the square brackets denote the approximate values) *vs.* $1/\lambda^2$ yields more precise values. Another approximation of this sort gives them very accurately. From d_{Si} and g_{Si}, $a_{Si,D}$, $a_{Si,F-C}$, and other desired $a_{Si,\lambda}$ values are then readily computed from Eq. (22).

Treating next the Na_2O-SiO_2 system, we compute $R_{Na,D}$ and $R_{Na,F-C}$ for each Morey and Merwin glass[16] by means of the equations

$$R_{Na,D}=\mu_D V_0-R_{Si,D}=\mu_D V_0-a_{Si,D}N_{Si} \tag{26}$$

and

$$R_{Na,F-C}=(\mu_F-\mu_C)V_0-R_{Si,F-C}$$
$$=(\mu_F-\mu_C)V_0-a_{Si,F-C}N_{Si}. \tag{27}$$

Weighted average values of $a_{Na,D}$ and $a_{Na,F-C}$ are then computed from the relations

$$a_{Na,D}=\sum R_{Na,D}/\sum N_{Na} \tag{28}$$

and

$$a_{Na,F-C}=\sum R_{Na,F-C}/\sum N_{Na}. \tag{29}$$

[15] S. B. Hendricks and W. E. Deming, Zeits. f. Krist. **A91**, 290 (1935).

[16] The experimental data for these glasses, as well as most of the other data we have used, are collected in G. W. Morey, *The Properties of Glass* (Reinhold, New York, 1938). This book has been invaluable to us in this work.

Weighted averages are taken because, other things being equal, a value of a_M calculated from the experimental data by subtracting terms for the other components is more accurate the larger the value of N_M. This is shown by the greater scattering of the experimental points at low N_M values in plots of a_M *vs.* N_M, such as Figs. 13–16 of this paper. However, if the data are meager and the scattering is great or if the a_M values show a trend with N_M, graphical determination of a_M is preferable.

TABLE II. Characteristic refraction and dispersion constants.

M	$10^{-8}d_M$	$10^{-8}g_M$	a_D	a_{F-C}
Li*	406.1	91.0	4.60	0.105
Na	463.655	79.844	6.017	.1554
K	900.965	97.202	9.537	.2035
Rb*	1293.1	106.7	12.43	.243
Cs*	2024.4	118.5	17.47	.310
Tl_I*	768.9	27.33	31.43	2.55
Be*	1027.6	176.4	5.90	.075
Mg	786.91	95.75	8.46	.183
Ca†	1228.	99.7	12.66	.264
	$d^\circ=1246.6$	$g^\circ=101.2$	$a_D^\circ=12.66$	$a^\circ_{F-C}=0.260$
	$d'=1.21$	$g'=10.9$	$a_D'=0.15$	$a'_{F-C}=0.04$
Sr	1701.38	105.81	16.50	0.325
Ba†	2136.	109.	20.1	.39
	$d^\circ=2380.7$	$g^\circ=122.87$	$a_D^\circ=19.8$	$a^\circ_{F-C}=0.34$
	$d'=72.52$	$g'=17.38$	$a_D'=5$	$a'_{F-C}=0.7$
Zn	868.20	73.96	12.20	0.340
Pb_{II}†	1220.	45.8	28.4	1.3
	$d^\circ=1220.1$	$g^\circ=45.81$	$a_D^\circ=28.40$	$a^\circ_{F-C}=1.30$
	$d''=196$	$g''=11.5$	$a_D''=22.74$	$a''_{F-C}=5.61$
B′	1413.49	190.75	7.50	0.090
B″	1067.18	123.90	8.80	.150
Al	1200.0	118.15	10.39	.185
Y*	1629.0	86.63	19.42	.463
La*	2111.1	91.50	23.79	.538
Ga*	1120.3	80.91	14.34	0.366
In*	1460.1	79.03	19.15	.500
As_{III}	2078.	100.5	21.	.44
Sb_{III}	1379.	47.8	31.	1.34
Bi_{III}	1301.1	40.57	34.5	1.80
Fe_{III}	259.0	11.15	31.3	8.1
Si	1790.480	145.685	12.508	0.1853
Ti	918.	39.6	25.	1.34
Ge*	1453.9	85.99	17.47	0.419
Sn_{IV}*	1490.4	68.74	22.61	.678
Zr*	1539.0	62.58	25.75	.850
Th_{IV}*	2023.4	70.60	29.85	.872
P_V*	2545.6	179.90	14.34	.180
Cb_V*	1382.8	48.08	30.57	1.33
Ta_V*	1561.8	55.60	29.60	1.10
W_{VI}*	1586.0	51.00	32.93	1.35

The units of d_M and g_M are cm and cm^{-3}, corresponding to λ values in cm. The units of the constants a_D and a_{F-C} are cm^3.
The * identifies components for which the constants were computed from Young and Finn's r_M and g_M values.
The Ca, Ba, and Pb constants in the rows marked † are approximately valid up to N_M =0.25, 0.10, and 0.10, respectively.

Values of $a_{M,D}$ and $a_{M,F-C}$ for most of the components listed in Table II (other than those designated by an *) are similarly obtained. The general equation, of which Eq. (26) is a special case, is

$$R_{M,D}=\mu_D V_0-\sum{}' a_{M,D}N_M, \qquad (30)$$

the summation being over all the components other than the one whose a_D value is being calculated. [Cf. Eq. (3).] Equation (27) is correspondingly generalized.

The constant g_M can be computed from a_M values at two wave-lengths by means of the relation

$$g_M=\left[\frac{a_{M,\lambda_1}/\lambda_1{}^2-a_{M,\lambda_2}/\lambda_2{}^2}{a_{M,\lambda_1}-a_{M,\lambda_2}}\right]\phi, \qquad (31)$$

where

$$\phi=\frac{1+k_i-k_i\lambda_1{}^2g_M}{1+k_i-k_i\lambda_2{}^2g_M}. \qquad (32)$$

As a first approximation, ϕ is put equal to unity. Further approximations are made until successive computations yield g_M values which are identical within the accuracy desired.

A similar procedure, with more complicated equations, enables one to calculate g_M from the ratio $(a_{M,\lambda_2}-a_{M,\lambda_3})/a_{M,\lambda_1}$, for instance, from $(a_{M,F}-a_{M,C})/a_{M,D}$. Abbreviating the latter ratio as θ, the expressions corresponding to (31) and (32) are

$$\theta g_M{}^2+\left(\frac{\phi-\theta}{\lambda_C{}^2}-\frac{\phi+\theta}{\lambda_F{}^2}\right)g_M+\left(\frac{\theta}{\lambda_F{}^2\lambda_C{}^2}+\frac{\phi}{\lambda_D{}^2\lambda_F{}^2}-\frac{\phi}{\lambda_D{}^2\lambda_C{}^2}\right)=0 \qquad (33)$$

and

$$\phi=\frac{1-k_i(\lambda_F{}^2-\lambda_C{}^2)\Big/\left(\dfrac{1}{g_M-1/\lambda_F{}^2}-\dfrac{1}{g_M-1/\lambda_C{}^2}\right)}{1-k_i\lambda_D{}^2(g_M-1/\lambda_D{}^2)}. \qquad (34)$$

The g_M values listed in Table II were computed with the aid of these equations, the d_M constants being then calculated by means of Eq. (22).

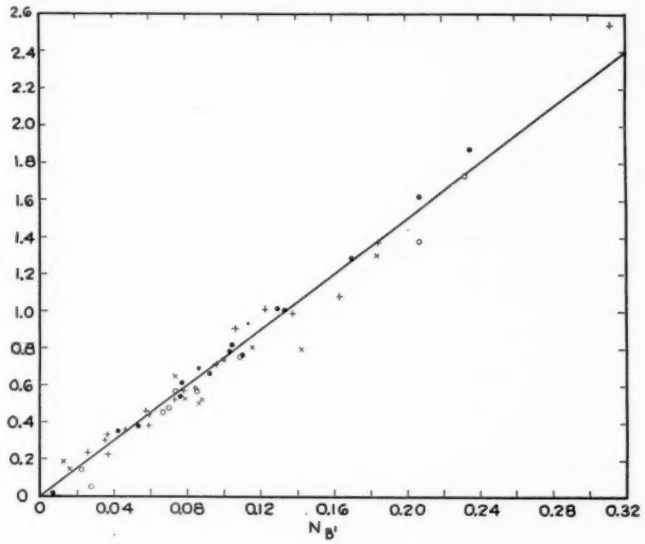

FIG. 9. Variation of $R_{B',D}$ ($=a_{B',D}N_{B'}$) with $N_{B'}$. + Ordnance Dept. Document 2037, Superintendent of Documents, Washington, D. C. (1921); ○ Chance Brothers; × Parra-Mantois; ● Turner and co-workers.

Following our previous procedure, we compute separate constants for B′ ("tetrahedral" boron atoms, each with four oxygen neighbors) and for B″ ("triangular" boron atoms, each with three oxygen neighbors), assuming[6] the amounts of these two kinds of boron in a given glass to be given by the following relations:

If $N_{Si}+N_B<0.50$,

$$\begin{aligned} N_{B'} &= N_B \\ N_{B''} &= 0. \end{aligned} \tag{35}$$

If $N_{Si}+N_B>0.50$,

$$\begin{aligned} N_{B'} &= 2-4N_{Si}-3N_B \\ N_{B''} &= 4N_{Si}+4N_B-2. \end{aligned} \tag{36}$$

Graphs of the data used for getting the $a_{B,D}$ and $a_{B,F-C}$ values are shown in Figs. 9–12. The scattering of the experimental points in the first two of these is somewhat greater than for most other components, probably due in part to different relative amounts of B′ and B″ from those assumed in Eqs. (35) and (36), which give the *equilibrium* distribution (on the basis of certain reasonable assumptions). The distribution in actual glasses will deviate from this more or less, depending primarily on the annealing treatment.

Figures 11 and 12 show that the B″ constants applicable to glasses in the $B_2O_3-SiO_2$ system and in the $Na_2O-B_2O_3-SiO_2$ system are also satisfactory for pure B_2O_3 and for $Na_2O-B_2O_3$ glasses containing no silicon.

For three components, CaO, BaO, and PbO, an increase—very slight in the first two instances—in the a_M values at large values of N_M is evident. For CaO and BaO (see Figs. 13 to 16), equations of the form

$$a_{M,\lambda}=\overset{\circ}{a}_{M,\lambda}+a'_{M,\lambda}N_M \tag{37}$$

fit the data, while for PbO better agreement is obtained with

$$a_{Pb,\lambda}=\overset{\circ}{a}_{Pb,\lambda}+a''_{Pb,\lambda}N_{Pb}{}^2. \tag{38}$$

In this case we may write, in good agreement with the data (Fig. 17),

$$\overset{\circ}{a}_{Pb,\lambda}=\frac{d_{Pb}{}^\circ}{g_{Pb}{}^\circ-1/\lambda^2}-k_1 d_{Pb}{}^\circ\lambda^2 \tag{39}$$

and

$$a''_{Pb,\lambda}=\frac{d_{Pb}{}''}{g_{Pb}{}''-1/\lambda^2}. \tag{40}$$

For the CaO and BaO glasses we have good data only for $a_{M,D}$ and $a_{M,F-C}$. Although these are obviously insufficient to test the assumption, the $d_M{}^\circ$, $g_M{}^\circ$, $d_M{}'$ and $g_M{}'$ constants for these components in Table II have been computed on the supposition that equations like Eqs. (39) and (40)—except for the substitution of Ca or Ba for Pb and of ′ for ″—are applicable.

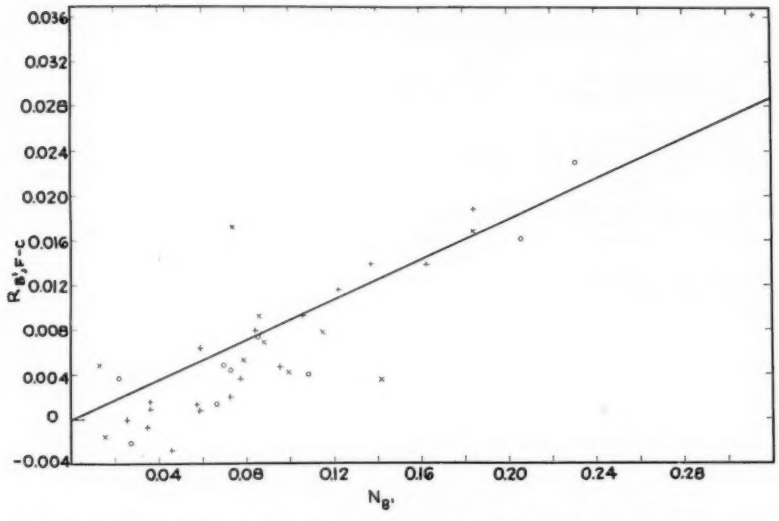

FIG. 10. Variation of $R_{B',F-C}(=a_{B',F-C}N_{B'})$ with $N_{B'}$. + Ordnance Dept. Document 2037, Superintendent of Documents, Washington, D. C. (1921); ○ Chance Brothers; × Parra-Mantois.

The n_D data by Larsen[16] and Safford[17] for glasses containing Al_2O_3 suggest that $a_{Al,D}$ also increases with increasing N_{Al} (Fig. 18). Safford's results, exclusive of those for a series of glasses of low SiO_2 content (represented by the six highest dots on this figure), are fairly well represented by an expression for a_D of the form of Eq. (37), with $a^{\circ}_{Al,D}=10.24$ and $a'_{Al,D}=2.4$. Because of the scattering of the experimental points and the differences between the results reported by different observers, however, we are perhaps not justified in using a variable value for $a_{Al,D}$. The constant value included in Table II is an average, deduced from the glasses studied by Finn and co-workers.

The dispersion data for aluminum-containing glasses are even less satisfactory for our purposes. The measurements of Merwin and Morey[18] are for unannealed glasses of unknown density. We have nevertheless used these (together with the indices for 3 wave-lengths for six glasses studied by Larsen), with the aid of calculated densities and a correction factor introduced to

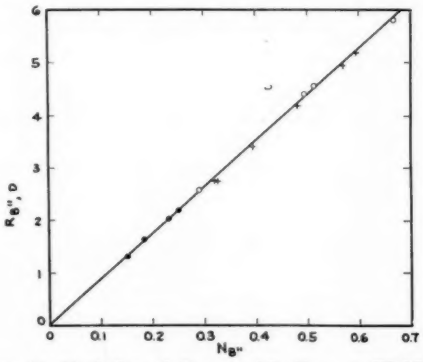

FIG. 11. Variation of $R_{B'',D}$ with $N_{B''}$. + Wulff and Majumdar ($Na_2O-B_2O_3$ glasses); ○ Merwin and Morey (B_2O_3 and unannealed $B_2O_3-SiO_2$ glasses); ● English and Turner ($Na_2O-B_2O_3-SiO_2$).

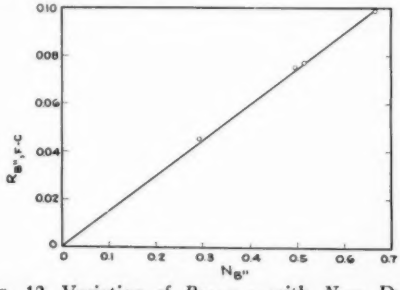

FIG. 12. Variation of $R_{B'',F-C}$ with $N_{B''}$. Data by Merwin and Morey on B_2O_3 and unannealed B_2O_3—SiO_2 glasses.

[17] H. W. Safford, Univ. of Pittsburgh Bulletin, **38** (1942).

[18] Reference 16, p. 393, Table XVI. 14. According to a private communication from Dr. Morey, the headings of the last six columns of this table should be: $c-b$, $d-c$, $e-d$, $F-e$, $g-F$, $h-g$. The + signs indicate a 5 in the next decimal place.

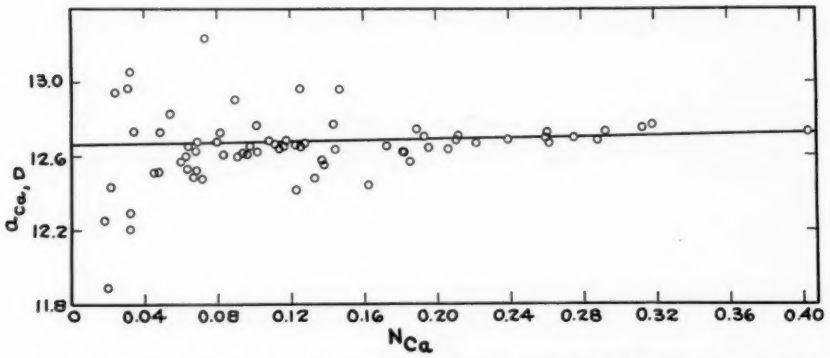

FIG. 13. Variation of $a_{Ca,D}$ with N_{Ca}. Data on $Na_2O-CaO-SiO_2$ glasses by Morey and Merwin. To avoid confusion, only half of the experimental points are shown.

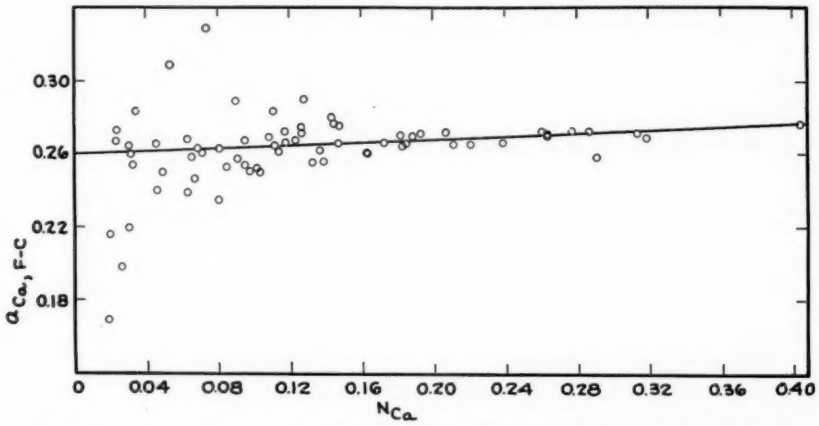

FIG. 14. Variation of $a_{Ca,F-C}$ with N_{Ca}. Data on $Na_2O-CaO-SiO_2$ glasses by Morey and Merwin. Only half of the experimental points are shown.

give agreement between observed and computed n_D values, to deduce the $a_{Al,F-C}$, d_{Al} and g_{Al} values listed in Table II. These constants are not to be trusted too much.

The mutual inconsistency of the experimental data for aluminum glasses is probably attributable in part to insufficient annealing and in part to the fact that—as has been shown by crystal structure studies—an aluminum atom can be stably surrounded by either 4 or 6 (or 5?) oxygens. The situation resembles that in boron-containing glasses, discussed above. Before a really adequate theoretical treatment can be given, more accurate experimental data are needed.

If the amount of Ca, Ba, Pb (or Al) in a glass is relatively small, little error is introduced into the calculation of n_D and n_{F-C} by assuming $a_{M,D}$ and $a_{M,F-C}$ to be constant (for each component). This has been done, for example, in the derivation of some of the constants for other components. The constant values we have used, with the approximate limits of validity of each, are included in Table II.

Morey gives n_D values in his book for many glasses containing Fe_2O_3 as one of the components. No densities are given, however, and all of these glasses seem to have been unannealed. Moreover, most of them also contain FeO, usually in an unknown amount. Dispersion data on analyzed glasses seem to be entirely lacking. In view of this situation we have resorted to the

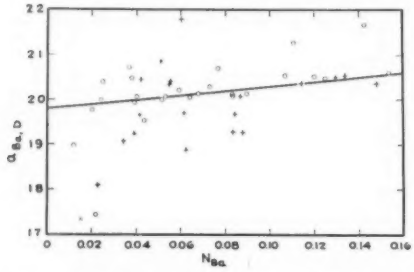

FIG. 15. Variation of $a_{Ba,D}$ with N_{Ba}. + Ordnance Dept. Document 2037, Superintendent of Documents, Washington, D. C. (1921); ○ Peddle. Points are omitted for a few glasses of low barium content, which would fall outside the range of $a_{Ba,D}$ covered by the figure.

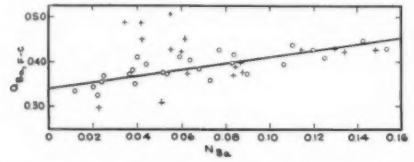

FIG. 16. Variation of $a_{Ba,F-C}$ with N_{Ba}. + Ordnance Dept. Document 2037, Superintendent of Documents, Washington, D. C. (1921); ○ Peddle. A few points are omitted, as for Fig. 15.

use of data on *crystalline* Fe_2O_3 (hematite). We have found experimental values[19, 20] for only five wave-lengths ($\lambda = 0.66$ to 0.76 micron). These agree quite well with Eqs. (11) and (12) as shown in Fig. 19. Nevertheless, in view of the proximity of an absorption band one must be careful about using the d_{Fe} and g_{Fe} values deduced from these data for wave-lengths outside the range mentioned. Extrapolation to the wave-length of the *F* line (~ 0.49) would certainly not be justified. This is doubtless the reason why the values of $d_{Fe,i}/d_{Fe}$ computed from d_{Fe}, $a_{Fe,D}$, and $a_{Fe,F-C}$ (see Table I) are so different from the values of this ratio for other elements.

Shortly after the publication of our previous papers[1, 2, 5] on refraction and dispersion of glasses, Young and Finn[3] published an interesting and useful paper dealing with this subject, in which they gave, for a large number of oxide components, "specific refraction and dispersion factors," $r_{M,D}$ and $r_{M,F-C}$ (designated by them as r and q), so defined as to satisfy the relations

$$(n_D - 1)/\rho = \sum r_{M,D} f_M \qquad (41)$$

and

$$n_{F-C}/\rho = (n_F - n_C)/\rho = \sum r_{M,F-C} f_M. \qquad (42)$$

As they later[21] pointed out, $r_{M,D}$ and $r_{M,F-C}$ are closely related to our a_D and a_{F-C}, according to the equations

$$a_{M,D} = r_{M,D} W_M / m_M \qquad (43)$$

and

$$a_{M,F-C} = r_{M,F-C} W_M / m_M. \qquad (44)$$

As in Eqs. (2) and (4), W_M is the molecular (formula) weight of the oxide and m_M is the number of M atoms represented in its formula (M_mO_n).

Values of $a_{M,D}$ and $a_{M,F-C}$ computed from Young and Finn's $r_{M,D}$ and $r_{M,F-C}$ values are included in Table II. As they have noted, the agreement between our results and theirs is, in general, good, where comparison is possible. Unfortunately, the data on which many of their constants (for the more unusual components) are based remain unpublished and unavailable to us. Nevertheless, we have used their values of $r_{M,D}$ and $r_{M,F-C}$ for these components to compute d_M and g_M and have included the results (identified by *) in Table II. Until the experimental data—in most instances on a very small number of glasses, each containing only a small proportion of the component in question—are published, we

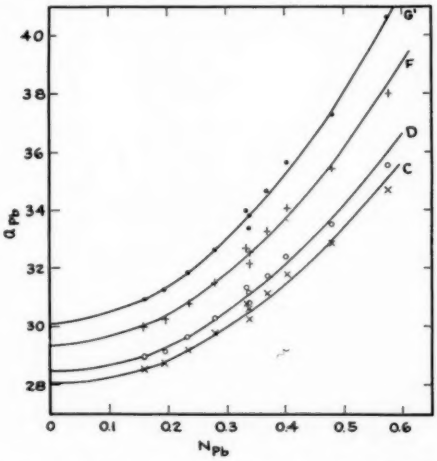

FIG. 17. Variation of $a_{Pb,\lambda}$ with N_{Pb}, for four wave-lengths. Experimental data by Merwin and Andersen (reference 16) on glasses in the $Na_2O-PbO-SiO_2$ system. The curves represent Eqs. (38–40).

[19] Wülfing, *Tschermak's Mineralog. petrog. Mitt.* **15**, 29, 49 (1896); quoted in *Int. Crit. Tables* **7**, 21.
[20] H. E. Merwin, Proc. A. S. T. M. **17**(2), 497 (1917).
[21] J. C. Young and A. N. Finn, J. Opt. Soc. Am. **31**, 383 (1941).

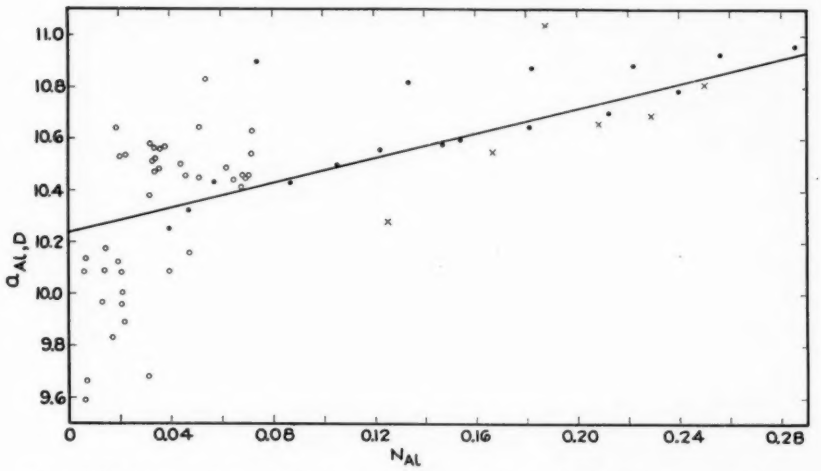

FIG. 18. Variation of $a_{Al,D}$ with N_{Al}. ○ Faick, Young, Hubbard, and Finn; × Larsen (reference 16); ● Safford (reference 17).

have no means of estimating the reliability of these constants.

The $a_{As,D}$ and $a_{Sb,D}$ values we have listed are from data on pure vitreous As_2O_3 and Sb_2O_3 by Kordes.[22] We consider these to be more reliable than the much smaller $a_{M,D}$ values deduced from Young and Finn's $r_{M,D}$ values for these components—which, in turn, were deduced from data on glasses containing either very small amounts of arsenic or antimony or large amounts of boron. Our other constants for As_2O_3 and Sb_2O_3 were deduced from the $a_{M,D}$ values and the assumption that the ratio $a_{M,F-C}/a_{M,D}$ $(=r_{M,F-C}/r_{M,D})$ is the same as calculated by Young and Finn.

It should be pointed out that Young and Finn's specific refraction and dispersion constants are directly applicable only to the calculation of n_D and n_{F-C}. For other wave-lengths and wave-length intervals, one might use their $r_{M,D}$ and $r_{M,F-C}$ constants to compute α_M and β_M values for their dispersion equation [Eq. (23)] and then use this equation to calculate $r_{M,\lambda}$ and $r_{M,\lambda_1-\lambda_2}$ values for other wave-lengths and wave-length differences. Since Eq. (23) is considerably less accurate than Eq. (22) (see Figs. 5 and 20–22, curves YF and 3), however, it seems better to transform Young and Finn's $r_{M,D}$ and $r_{M,F-C}$ values to $a_{M,D}$ and $a_{M,F-C}$ [Eqs. (43) and (44)] and from these to compute d_M and g_M. This we have done (Table II). One can now use Eq. (22) to compute $a_{M,\lambda}$ and $a_{M,\lambda_1-\lambda_2}$ values for any other desired wave-lengths within the range for which this equation is valid. Then, if one prefers, he can change these to $r_{M,\lambda}$ and $r_{M,\lambda_1-\lambda_2}$ values by means of equations similar to Eqs. (43) and (44) and use equations like Eqs. (41) and (42) to compute n_λ and $n_{\lambda_1-\lambda_2}$.

[22] E. Kordes, Zeits. f. physik. Chemie **B43**, 173 (1939).

COMPARISON WITH EXPERIMENTAL DATA

Several types of comparison with experimental data are of interest. These differ with respect to the data available and with respect to the quantities desired. For example, one may have the following data available:

(1) Accurate composition only (e.g., for a glass which is not available for measurement of its properties);

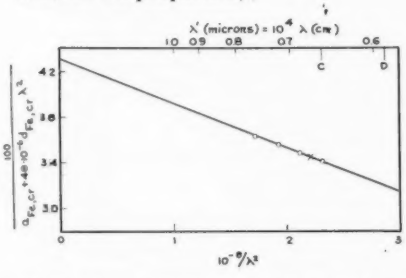

FIG. 19. To show agreement with Eqs. (11) and (12) for hematite (Fe_2O_3) crystals. ○ Wülfing (reference 19); × Merwin (reference 20).

(2) Accurate composition and density;
(3) Accurate composition and n_D;
(4) Rough or accurate composition and accurate n_D and n_{F-C}.

One may wish to calculate:

(*a*) Density;
(*b*) n_D;
(*c*) n_λ (with λ other than D);
(*d*) n_{F-C};
(*e*) $n_{\lambda_1-\lambda_2}$ (with λ_1 and λ_2 not F and C).

To give here detailed comparisons between experimental and calculated quantities for all possible combinations of the above would be a lengthy procedure and unnecessary for our present purpose. We shall, however, discuss briefly certain of the more important cases. For illustration, Table III and Figs. 20–22 give some pertinent comparisons for analyzed glasses in the $Na_2O-CaO-SiO_2$ system, whose dispersions over a large range of wave-lengths have been measured by Morey and Merwin.[23]

Combination 1a

The calculation of the density of a glass from its composition has been treated previously.[6] The experimental density of a well-annealed glass of accurately known composition and the density calculated for it by means of Eqs. (2) and (3) differ, in general, by one- or two-tenths of one percent of the actual value.

Combinations 1b, 1c, 1d, and 1e

Calculated and experimental V_0 values differ by about this same percentage, on the average. Because both μ_λ and $n_{\lambda_1-\lambda_2}$ are inversely proportional to V_0, the use of a calculated value of V_0 (or ρ) instead of an accurate experimental value can be expected to lead to about the same percentage error in these quantities. For average well-annealed glasses, this means about 0.001 error in n_D and 0.00002 error in n_{F-C}.

Combination 2b

(Cf. the last 4 rows of Table III.) The average differences between calculated and experimental refractive indices for the D line, for glasses of known density, are slightly less with our new equations and constants than with our old ones or with Young and Finn's [Eq. (41)]. With good density and composition data, these differences average somewhat less than 0.001. Without a knowledge of the density, n_D can still be calculated to within an average error of about 0.002.

Combination 2c

Except for wave-lengths near the borders of the visible spectrum, n_λ values for wave-lengths other than D can be calculated by our new equations with not much larger average error than those for the sodium D line. (See curves 3 of Figs.

[23] Reference 16, p. 389, Table XVI. 12. It may be noted that there are several minor discrepancies between the n_D and n_{F-C} values in this table and those in Table XVI. 11 for the same glasses.

TABLE III. Comparisons of observed and calculated refractive indices and dispersions for certain analyzed glasses.

Weight fractions f_{Si}		0.999	0.6650	0.5568	0.5080	0.5174	0.4880	0.4417	0.7425	0.6039	0.5332	
f_{Na}		—	.3350	.4432	.4920	—	—	—	.0573	.0744	.0518	Average
f_{Ca}		—	—	—	—	.4826	.5120	.5583	.2002	.3217	.4150	
n_{b-g} (obs.)−n_{b-g} (calc.) using	Hb	0.00005	0.00011	−0.00009	−0.00008	−0.00009		0.00001	−0.00004	−0.00002	0.00000	0.00005
expti. n_D and n_{F-C}	HSD	.00005	.00025	.00013	.00024	.00000		.00006	.00005	.00007	.00005	.00010
Same, using only expti. n_D	HSD	.00004	.00022	.00013	.00026	.00001		.00005	.00005	.00005	.00004	.00009
n_{C-b} (obs.)−n_{C-b} (calc.) using	Hb	.00001	− .00012	− .00008	− .00010	− .00006	−0.00015	− .00012	− .00006	− .00005	− .00007	.00008
expti. n_D and n_{F-C}	HSD	− .00004	− .00005	− .00003	− .00009	− .00001	− .00008	− .00006	− .00003	.00002	.00000	.00004
Same, using only expti. n_D	HSD	− .00003	− .00010	− .00004	− .00004	.00001	− .00008	− .00005	− .00003	.00000	− .00005	.00004
n_{F-C} (obs.)−n_{F-C} (calc.)	YF	.00010	− .00005	.00004	.00023	.00007	.00002	.00008	− .00001	− .00010	− .00011	.00008
using expti. ρ	H	.00006	− .00012	− .00004	.00014	.00021	.00018	.00025	.00004	− .00003	.00000	.00011
	HSD	.00000	− .00012	− .00003	.00016	.00005	− .00001	.00001	.00002	− .00006	− .00008	.00005
Same, using calc. ρ	HSD	.00000	− .00013	− .00003	.00014	.00013	.00003	.00001	− .00009	− .00003	− .00005	.00006
n_D (obs.)−n_D (calc.) using	YF	.0000*	− .0005	.0004	.0018	.0034	.0031	.0038	.0014	.0020	.0034	.0020
expti. ρ	H	.0002*	− .0011	− .0003	.0011	.0020	.0018	.0023	.0007	.0010	.0022	.0013
	HSD	.0000*	− .0011	− .0003	.0011	.0002	− .0003	− .0001	.0003	.0002	.0008	.0004
Same, using calc. ρ	HSD	.0000*	− .0016	− .0004	.0002	.0049	.0022	− .0004	− .0059	.0018	.0025	.0020

* The index listed by Morey (Table XVI. 11) as n_D for this glass (practically pure SiO_2) is probably really N_D (the index *in air*) since it is the same as that given by Sosman as N_D for pure SiO_2. For comparison with our calculated values (H and HSD) we have therefore corrected it to vacuum; on the other hand, for comparison with the value computed by the Young and Finn constants, we have used the value given by Morey directly, since that gives better agreement and we have been unable to determine from their papers whether their constants are meant to be applicable to the air indices or to the vacuum indices.

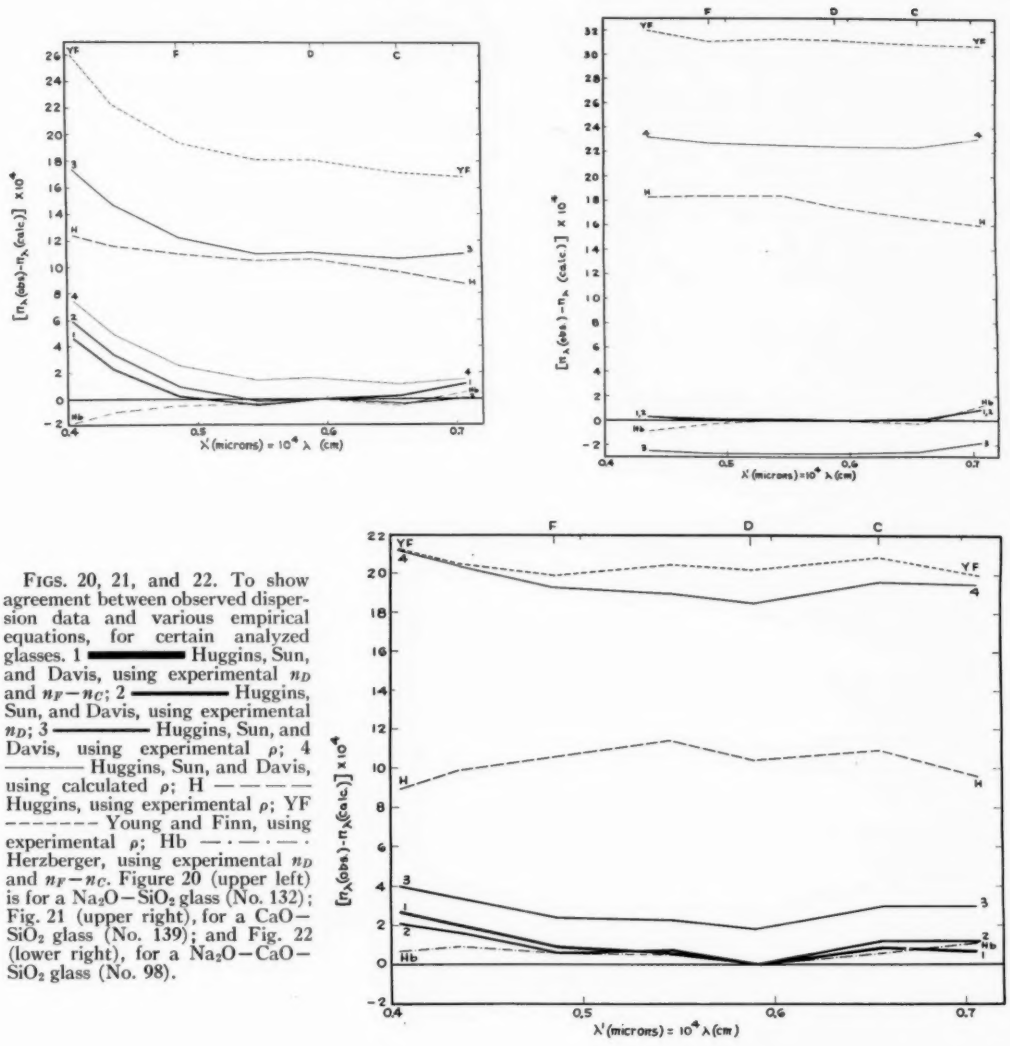

FIGS. 20, 21, and 22. To show agreement between observed dispersion data and various empirical equations, for certain analyzed glasses. 1 ▬▬▬ Huggins, Sun, and Davis, using experimental n_D and $n_F - n_C$; 2 ▬▬▬▬ Huggins, Sun, and Davis, using experimental n_D; 3 ▬▬▬▬ Huggins, Sun, and Davis, using experimental ρ; 4 ▬▬▬▬ Huggins, Sun, and Davis, using calculated ρ; H — — — — Huggins, using experimental ρ; YF - - - - - - - - Young and Finn, using experimental ρ; Hb — · — · — · Herzberger, using experimental n_D and $n_F - n_C$. Figure 20 (upper left) is for a Na_2O-SiO_2 glass (No. 132); Fig. 21 (upper right), for a $CaO-SiO_2$ glass (No. 139); and Fig. 22 (lower right), for a $Na_2O-CaO-SiO_2$ glass (No. 98).

20–22.) This is also true of calculations made with our old equations (curves H) or with Eq. (23), used by Young and Finn (curve YF).

Combination 2d

(Cf. Table III.) Our new equations and constants give a little better agreement between observed and calculated n_{F-C} values for glasses of known density and composition than was obtainable with our old equations and constants or with Young and Finn's specific dispersion factors [Eq. (42)]. With good data the deviations average less than 0.0001. If the density is unknown (combination 1d), the average deviation is only very slightly greater—in agreement with the statements in the paragraph above on "Combinations 1b, 1c, 1d, and 1e."

Combination 2e

(See curves 3.) The same remarks apply as for combination 2d, except that if one of the wavelengths is near either boundary of the visible

region, the error in the calculated dispersion is likely to be considerably greater.

Combinations 3c, 3d, and 3e

With accurate knowledge of the composition of a glass and of its n_D value, refractive indices for other wave-lengths—and so also $n_{\lambda_1-\lambda_2}$ values—can be computed without a knowledge of the density, using such a value of V_0 as will give [Eq. (1)] the observed n_D. The n_λ values so calculated are usually accurate (assuming n_D to be exactly correct) to within less than 0.0001, except for wave-lengths near the boundaries of the visible. (See curves 2.) Average errors in dispersions calculated in this way are about the same as for calculations from composition and density data (combinations 2d and 2e).

Combinations 4c and 4e

If one has accurate values of the refractive index for two wave-lengths or the refractive index for one wave-length (e.g., n_D) and the dispersion (e.g., n_{F-C}) for one pair of wave-lengths, with or without good density or composition data, one can obtain nearly as accurate n_λ and $n_{\lambda_1-\lambda_2}$ values over almost the whole visible range by making use of the equation

$$\mu_\lambda = \alpha A_\lambda - \beta B_\lambda, \tag{45}$$

where

$$A_\lambda = \sum_M \frac{d_M N_M}{g_M - 1/\lambda^2} + \sum_{\text{Ca, Ba}} \frac{d_M' N_M^2}{g_M' - 1/\lambda^2} + \frac{d_{\text{Pb}}'' N_{\text{Pb}}^3}{g_{\text{Pb}}'' - 1/\lambda^2}, \tag{46}$$

$$B_\lambda = \lambda^2 \sum d_M N_M, \tag{47}$$

and α and β are empirical factors.

If the refractive indices at two wave-lengths λ_1 and λ_2 are known, α and β can be computed from the equations

$$\alpha = \frac{\lambda_2^2 \mu_{\lambda_1} - \lambda_1^2 \mu_{\lambda_2}}{\lambda_2^2 A_{\lambda_1} - \lambda_1^2 A_{\lambda_2}} \tag{48}$$

and

$$\beta = \frac{A_{\lambda_2} \mu_{\lambda_1} - A_{\lambda_1} \mu_{\lambda_2}}{A_{\lambda_1} B_{\lambda_2} - A_{\lambda_2} B_{\lambda_1}}. \tag{49}$$

If the known experimental quantities are n_D and n_{F-C},

$$\alpha = \frac{(\lambda_F^2 - \lambda_C^2)\mu_D - \lambda_D^2(\mu_F - \mu_C)}{(\lambda_F^2 - \lambda_C^2)A_D - \lambda_D^2(A_F - A_C)} \tag{50}$$

and

$$\beta = \frac{(A_F - A_C)\mu_D - A_D(\mu_F - \mu_C)}{A_D(B_F - B_C) - (A_F - A_C)B_D}. \tag{51}$$

(If Eqs. (1) and (10) and the constants entering into them were absolutely accurate, α would equal $1/V_0$ and β would equal k_i/V_0.)

The results obtained by this procedure compare quite favorably with those obtained by the use of Herzberger's equations, as shown by a comparison of curves 1 and Hb of Figs. 20–22. (Compare also the rows labelled Hb, in Table III, with the rows immediately under them.) In this connection it may be noted that Herzberger's equations are definitely not applicable to glasses of very unusual composition, whereas we have every reason to believe that our equations and methods are not so limited.

SUMMARY AND CONCLUSIONS

We have shown that, *without any experimental data whatever*, the refractive index of a well-annealed silicate glass, for a wave-length in the visible region of the spectrum, can be fairly accurately computed from the composition by means of our equations and constants. *If the density of the glass is known*, the average accuracy of the computed index is slightly increased. n_D and $n_F - n_C$ values can then be determined more accurately than by the use of Young and Finn's specific refraction and dispersion factors. For other wave-lengths, our computed refractive indices and dispersions average considerably better than those obtained by their dispersion equation or by any other general equations known to us.

If the refractive index of the glass is known for one wave-length (e.g., n_D), our equations enable one to calculate the dispersions (for wave-lengths in the visible) with considerably greater average accuracy. The accuracy can be still further increased by a knowledge, in addition, of one dispersion value (e.g., $n_F - n_C$); it is then practically as good as that obtainable by Herzberger's method.

The Nature and Causes of Small Color Differences in Industry

Lighting for Their Detection

A. H. TAYLOR
Lighting Research Laboratory, General Electric Company, Nela Park, Cleveland
(Received July 8, 1942)

MANY types of color differences are encountered in quantity production of manufactured articles and often the allowable color tolerances are very small, necessitating accurate control and rigid inspection. The principal purpose of this paper is to discuss the nature and causes of some of these small color differences, also methods of lighting and inspection to detect them.

When radiant energy in the visible spectrum strikes any object, part of this energy is reflected at the surface with little or no change in spectral character. For glossy non-metallic surfaces approximately four percent of the incident energy is reflected in this manner. The remainder of the energy penetrates to varying depths into the material and is transmitted, absorbed, or diffusely reflected back through the surface upon which it was originally incident. The latter is chiefly responsible for the color exhibited by the article. (Colors due to fluorescence, diffraction, or interference phenomena will not be discussed here.)

If an object has a porous surface, such as cloth, for example, some of the color arises from energy which has been multiply reflected from the walls surrounding the indentations or holes in the material where spectrally selective reflection takes place. This fact may be revealed by a very simple and sensitive test of the spectral selectivity of a white pigment by making a deep, conical-shaped hole in a volume of the pigment with a pencil. If the pigment is slightly selective in its spectral reflection, the walls near the bottom of the hole will appear somewhat colored in comparison with the walls near the opening. A comparable result occurs in the case of the porous cloth.

Some of the dominant factors producing small color differences are common to various dissimilar materials. One of the most important of these is thickness of the material, the effect being the same for colored paper, paint, enamels, plastics, etc. Another important factor is the background on which a coating is applied or against which the object is viewed. Analyses of some spectral transmittance and reflectance curves will serve to illustrate and explain these facts.

Before discussing small spectral differences it may be helpful to emphasize certain facts relating wave-length and color. Upon viewing a pure spectrum it will be seen that there are no sharp boundaries between colors. Furthermore, different observers will differ in the wave-length chosen for the boundary between two adjacent colors, e.g., blue and green. With these limitations it is possible to divide the visible spectrum into the following approximate zones of color:

Violet	λ3950–4350	Yellow	λ5700–5900
Blue	4350–4775	Orange	5900–6175
Blue-green	4775–4975	Light red	6175–6400
Green	4975–5275	Dark red	6400–7050
Yellow-green	5275–5700		

The effect of thickness on the color of paper is illustrated by Figs. 1 and 2, for different numbers of sheets of colored bond paper, each sheet being approximately 0.004 inch thick. A backing of black velvet was used in making these reflectance curves and all others shown for translucent materials. It will be noted that the spectral reflectance and transmittance curves are quite similar in shape; they are both influenced principally by the spectral absorption of the paper. The reflectance is substantially the same for two and for three thicknesses of the light blue paper of Fig. 1. At λ5700, where the transmittance and reflectance for a single thickness are, respectively, 16 and 5.1 percent, the difference in reflectance between one and two thicknesses is apparently due to the energy which has been transmitted by the first sheet and reflected by the second. This energy has been transmitted twice by the first sheet and reflected once by the second and is equal to $0.16\times0.51\times0.16=0.013=1.3$ percent. However, for those spectral regions where the

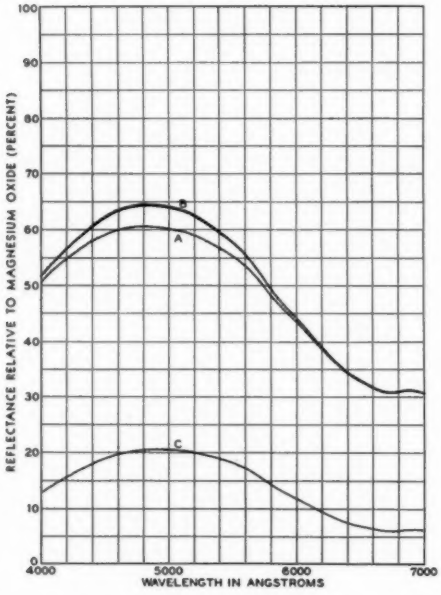

FIG. 1. Spectral reflectance of (*A*) one sheet, (*B*) two and three sheets of light blue bond paper, each sheet 0.004 inch thick. (*C*) transmittance of one sheet. (Reflectance measurements of paper and all other translucent materials were made with a backing of black velvet.)

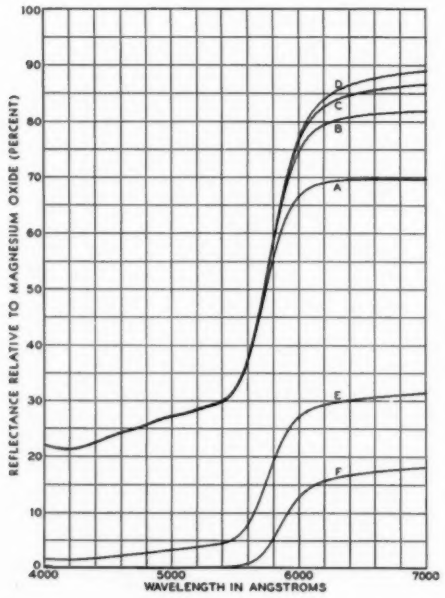

FIG. 2. Spectral reflectance of (*A*) one, (*B*) two, (*C*) three, and (*D*) four sheets of salmon pink bond paper. (*E*) transmittance of one sheet. (*F*) two sheets.

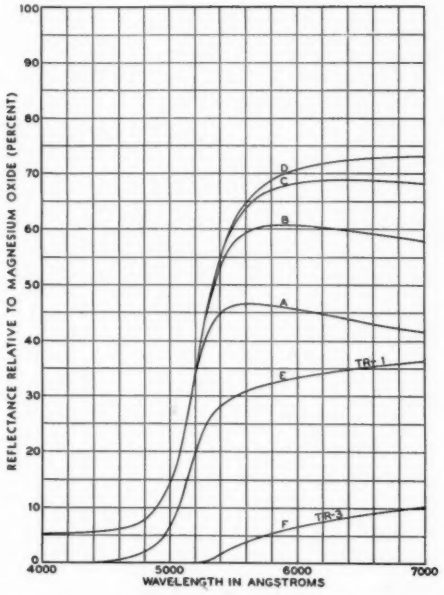

FIG. 3. Spectral reflectance of thin coats of a yellow paint on glass. (*A*) one, (*B*) two, (*C*) three, (*D*) four coats. Transmittance of (*E*) one and (*F*) three coats.

transmittance and reflectance are higher, the difference between the spectral reflectance of one and two sheets exceeds the amount accounted for in this way. The excess is probably due to energy which has been multiply reflected in the body of the two sheets and which finally emerges at the surface of incidence. Corresponding curves for salmon-pink paper are given in Fig. 2.

That paints and translucent plastics are affected in the same way by variations in thickness is clearly demonstrated by Figs. 3 and 4. Obviously, all translucent colored materials vary in color with thickness in the same manner but to varying degrees, when there is no reflection from the background.

When a paint or enamel is applied to a surface which reflects an appreciable amount of energy, the character of the background will affect the resultant color for any thickness less than complete coverage. The effects of "black" and "white" backgrounds on the spectral reflectance of different thicknesses of a thin green paint are shown by Figs. 5 and 6, respectively. It will be noted that when the background is black, increasing the thickness of the coating increases the

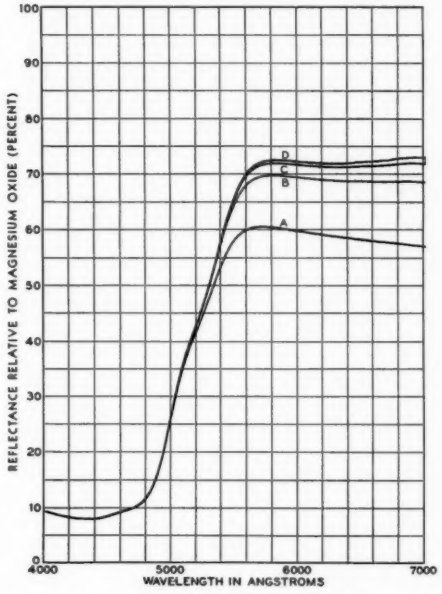

FIG. 4. Spectral reflectance (*A*) one, (*B*) two, (*C*) three, and (*D*) four sheets of translucent yellow plastic, each sheet being approximately 0.05 inch thick.

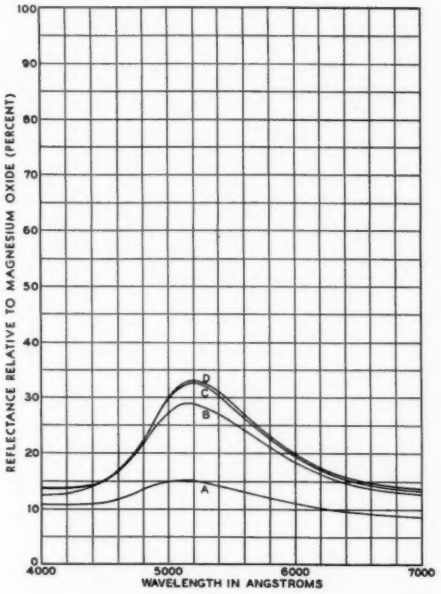

FIG. 5. Spectral reflectance of thin green paint on black cardboard. (*A*) one, (*B*) two, (*C*) three, and (*D*) four coats.

reflectance at all wave-lengths, whereas the reverse is true when the background is white.

When the applied coating (paint, enamel, etc.) is "white," the results with the so-called black and white backgrounds are as shown in Figs. 7 and 8. Figure 7 illustrates the fact that with a black background, the reflectance of a thin coat of white lacquer has a higher value in the blue end of the spectrum than in the red. This means that practically complete coverage in the blue is achieved with a thinner coating than is required for the red. Thus the object may appear bluish-white with a thin coat of white paint or enamel and a neutral or yellowish-white with a thicker coating of the same material. This accounts in large part for the variation in color appearance sometimes presented by different areas of a white porcelain enameled stove or a white enameled refrigerator since the enamel is applied on a dark background. Figure 9 confirms this conclusion.

A white enamel or paint is essentially an agglomeration of fine particles of translucent or opaque material. It is a well-established fact that such a medium transmits the light of longer wave-lengths (red) to a greater extent than it does the

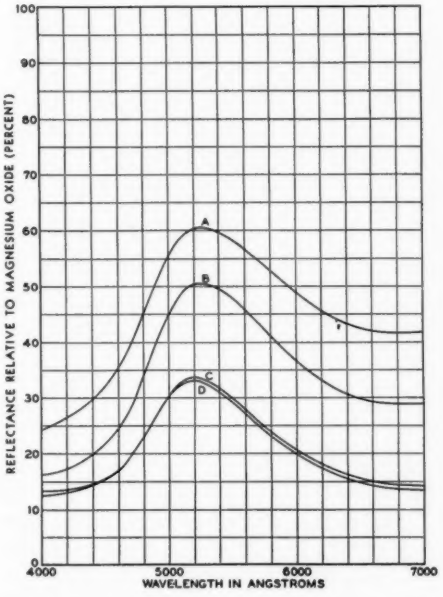

FIG. 6. Spectral reflectance of the same green paint when applied to white cardboard in (*A*) one, (*B*) two, (*C*) three, and (*D*) four coats. Compare with Fig. 5.

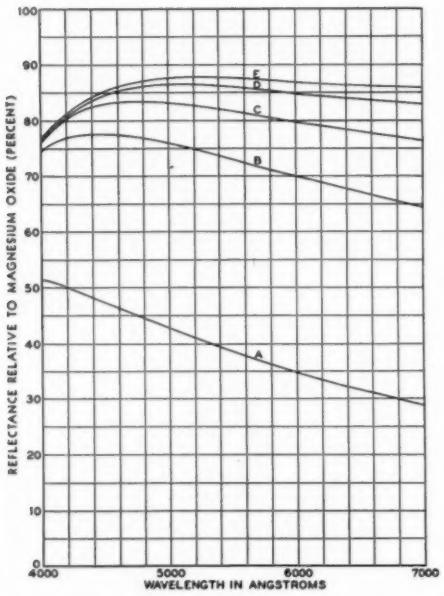

FIG. 7. Spectral reflectance of one to five coats (*A* to *E*, respectively) of thin white lacquer on black cardboard.

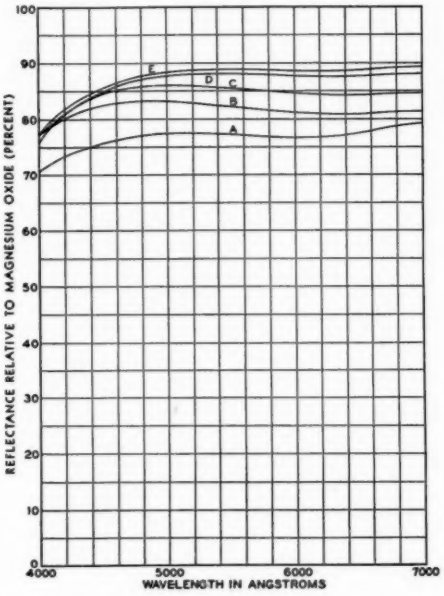

FIG. 8. Spectral reflectance of one to five coats (*A* to *E*, respectively) of thin white lacquer on white cardboard.

shorter wave-length region (blue) which is more diffusely scattered and reflected. Thus a thin coat of such a material may appear slightly reddish by transmitted light and slightly bluish by reflected light.

Figure 10 gives a more detailed illustration of what happens when thin coats of a white paint or lacquer are applied. In this case the lacquer was applied to glass so that the transmission characteristics could be studied. It will be noted that the addition of a sixth coat increased the reflectance for all wave-lengths longer than λ4800, even though the transmittance of the paint before application of the sixth coat was only 2.5 percent at this wave-length and did not exceed 8 percent at any wave-length in the visible spectrum. If the reflectance and transmittance of the thickest coating are added together, it will be found that the total absorption is less than 10 percent for all wave-lengths longer than approximately λ5000. From these considerations it follows that a thicker coating is required for a paint or lacquer having high reflectance than for one of lower reflectance, which is in accord with experience. Hence to get the highest possible reflectance with a paint as white as this, the coating should be thick enough so that the transmittance should not exceed approximately three percent at any point in the visible spectrum.

For porcelain enamels there is another important factor which affects the color, *viz.*, refiring. In the case of the blue porcelain enamel of Fig. 11 the principal effect of the refiring was to darken the surface with very little other change in color. Yellow and brown enamel showed very little spectral change upon refiring.

Another type of small color difference is that encountered in mixing paints to match a given sample. This may be illustrated by the steps in producing a light ivory paint by the addition of raw sienna to a white paint. How the spectral reflectance curve is changed by the addition of the raw sienna is illustrated by Fig. 12. The raw sienna has a high absorption in the blue, hence this is the spectral region most affected by its addition to the white paint. If a light blue paint is produced by the addition of a blue pigment to white paint, the principal change in spectral reflectance occurs in the red, where the blue pigment has a high absorption.

In the process of manufacturing colored bond paper, water is removed from the wet pulp sheet

by a "screening" process. This may remove more of the dyed water from one side of the sheet than from the other, with the result that the color of the finished sheet is not the same on the two sides. Reflectance curves for opposite sides of a light blue-green bond paper are seen in Fig. 13. The greatest changes occurred in the spectral regions of maximum absorption.

In a recent investigation of the fading of colored textiles by daylight and artificial light,[1] spectral reflectance curves before and after exposure were made for many specimens. In Fig. 14 are typical spectral reflectance curves for a pink silk specimen before and after exposure to light. For most of the specimens examined, it was found that moderate fading of the textiles *increased* the reflectance in the spectral region of low reflectance and *decreased* the reflectance in the spectral regions of high reflectance. As a result the light reflectance of the material may either increase or decrease, depending upon the wave-length regions of maximum and minimum reflectance. Thus moderate "fading" of a yellow cloth will usually make it turn somewhat darker than an unexposed specimen of the same material, whereas the opposite is true for a pink textile such as is illustrated by Fig. 14. There has been no opportunity to make a detailed study of variations occurring in the color of dyed textiles during manufacture.

The foregoing discussion pertains only to cases in which color differences are due to small differences in reflection at various parts of the visible spectrum such as may occur in quantity production of articles intended to be exactly alike. When it is necessary to match a paint or dye of unknown composition, an apparent color match may be obtained even with marked differences in the spectral reflectance characteristics if a single light source is used for viewing. Spectral reflectance curves for two dyed textiles which look alike in color in "daylight" but entirely different in unfiltered light from tungsten lamps are shown in Fig. 15. Obviously there may be a large number of such cases in industry.

Color differences of the latter type require viewing under at least two light sources, quite dissimilar in spectral energy distribution, for certainty of detection. One of these may be

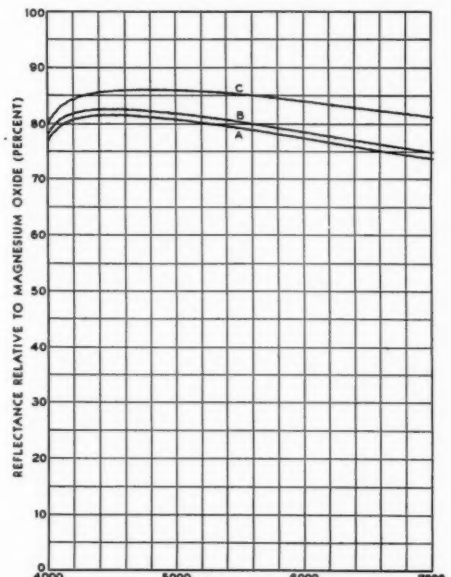

FIG. 9. Effect of coating thickness on the spectral reflectance of white porcelain enamel; (*A*) 40, (*B*) 46, and (*C*) 61 grams per square foot. Note similarity to Fig. 7.

[1] Matthew Luckiesh and A. Hadley Taylor, "Factors affecting the fading of dyed textiles by radiant energy," American Dyestuff Reporter (October 14, 1940).

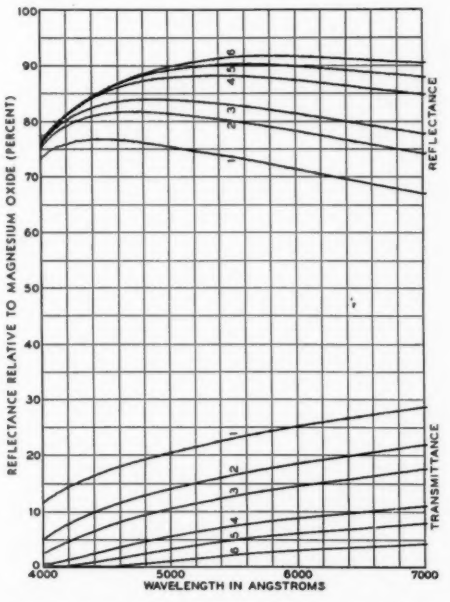

FIG. 10. Reflectance and transmittance curves for one to six coats of thin white lacquer on clear glass.

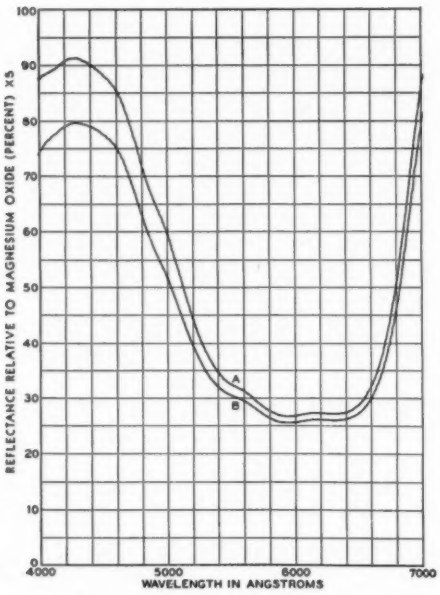

FIG. 11. Effect of refiring on the spectral reflectance of blue porcelain enamel, 50 grams per square foot (*A*) before and (*B*) after refiring.

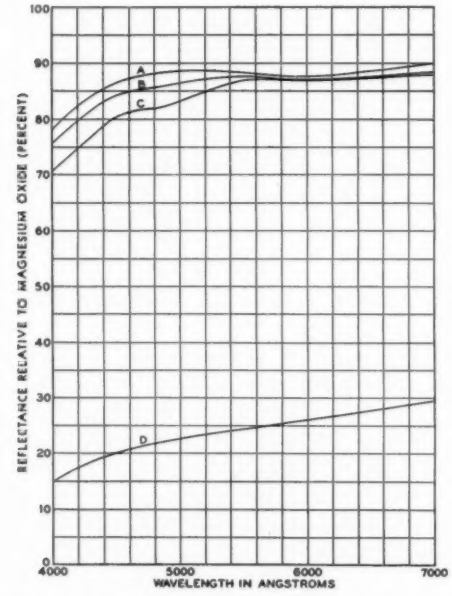

FIG. 12. Effect of tinting white paint with raw sienna to make a light ivory. (*A*) Reflectance of the unmodified white paint and (*B*) and (*C*), with the addition of raw sienna. (*D*) Transmittance of a thin coat of the light ivory paint on glass.

natural or artificial daylight and the other a tungsten filament lamp operated at normal or below normal voltage. If the two objects match in color under these two illuminants it is probable that they are very nearly alike in spectral reflectance and will match under any other light source, unless a part of the color is due to fluorescence. Many dyed textiles and some colored plastics are fluorescent when exposed to ultraviolet energy present in sunlight. Hence, in order to be certain that there are no significant spectral differences between the known and unknown colored objects, it may be desirable to compare them under a third type of illuminant, one rich in energy in the near ultraviolet.

In order to make a small color difference most easily detectable, the lighting for inspection should be such that it accentuates the color difference as much as possible. In the research on fading referred to above, it was found that a small amount of fading of a blue, purple, violet, or orchid textile was more easily seen in the light from tungsten filament lamps than in natural or artificial daylight. This is due to the fact that a small change in reflectance in the red end of the spectrum, where the reflectance is low, has a

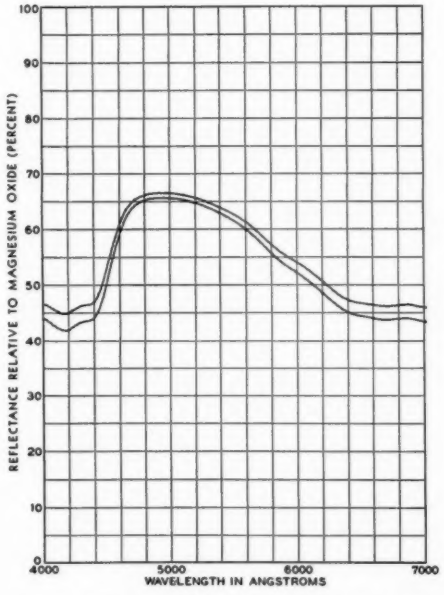

FIG. 13. Reflectance curves for opposite sides of a light blue-green bond paper.

greater effect on the dominant hue of the material than an equal percentage change in the blue, where the reflectance is high. The tungsten filament lamp, radiating more energy in the red than the blue, accentuates the color difference. It was found that small amounts of fading of red and pink textiles were more easily detected in natural or artificial daylight than with light from tungsten lamps. Referring to Fig. 14, it is seen that this should be true since the percentage change in reflectance is greatest in the blue and blue-green where the energy of daylight is relatively richer than that from tungsten filament lamps. For detecting small changes in greens and yellows there was very little choice between daylight and tungsten filament light.

Our tests indicate that small color differences are often most definitely revealed by an illuminant radiating energy throughout the visible spectrum, but being especially rich in energy in the spectral regions where the colored object has maximum *absorption*. Small changes in reflectance in those regions will often appreciably influence the color of the object. Color differences of the type shown in Fig. 12 are more easily seen in natural or artificial daylight than in light from tungsten filament lamps.

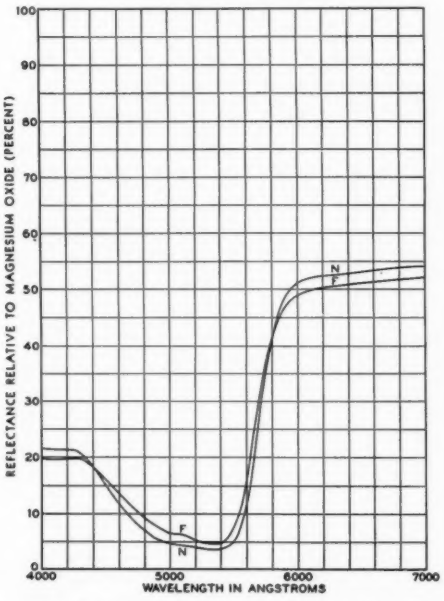

FIG. 14. Change in spectral reflectance of pink silk cloth due to fading produced by long exposure to light. (*N*) new and (*F*) faded.

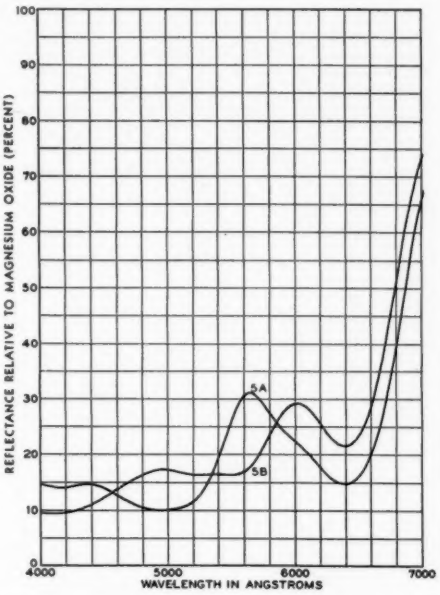

FIG. 15. Spectral reflectance of two "freakish" dyed textiles which both look brown in daylight, but under light from tungsten lamps 5*A* is greenish gray and 5*B* is brown.

In those cases where the articles on the production line may vary throughout a wide range of colors, the best type of illuminant would appear to be natural or artificial daylight *if a single illuminant is to be used*. Although instances have been pointed out above where tungsten lamps were superior to natural or artificial daylight for detecting small color differences, in general the superiority is limited to purple, violet, orchid, and blue materials. Artificial or natural daylight, with a better balance of energy throughout the spectrum, gives colors more nearly their natural appearance and on the average should be the most satisfactory single illuminant for color inspection work. The spectral energy distribution of natural daylight varies throughout a wide range;[2] hence, for constancy of illumination and color quality, artificial daylight should be more satisfactory than natural daylight.

In order to duplicate the color of a given object,

[2] A. H. Taylor and G. P. Kerr, "The distribution of energy in the visible spectrum of daylight," J. Opt. Soc. Am. **31**, 3 (1941).

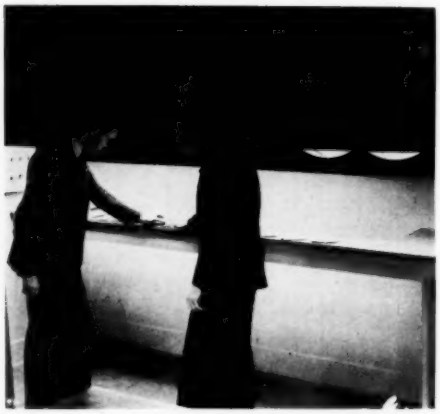

FIG. 16. Color matching booth in General Electric Lighting Institute at Nela Park, Cleveland.

e.g., a dyed textile, without any knowledge as to its spectral characteristics, it is emphasized that the comparisons should be made under *at least* two sources differing widely in spectral energy distribution. The most useful color matching booths employ these principles. It is also desirable to avoid highlights and specular reflections if possible.

Figure 16 illustrates a color matching booth developed by Mr. A. K. Gaetjens, in the General Electric Lighting Institute at Nela Park. In the left-hand booth three color temperatures are available, *viz.*, 8500 and 6500°K with fluorescent lamps and approximately 3000°K with tungsten filament lamps. At the right of Fig. 16 are shown two Macbeth color matching units employing tungsten lamps and filters. A color matching booth at the Forbes Varnish Company in Cleveland[3] shown in Fig. 17 provides three levels of illumination from fluorescent daylight lamps, 175, 350, and 500 footcandles. It is useful for comparing very dark enamel specimens. It is so arranged that all specular reflection is eliminated at the viewing position, since the area which would be imaged by a mirror is black and receives no direct light. Another booth added recently employs both fluorescent and tungsten filament lamps. Other examples might be added, but these suffice to show how proper "quality of lighting" principles have been employed.

[3] R. F. Wysocki and A. K. Gaetjens, "Color-matching at the Forbes Varnish Company," Illum. Eng. **35**, 343 (1940).

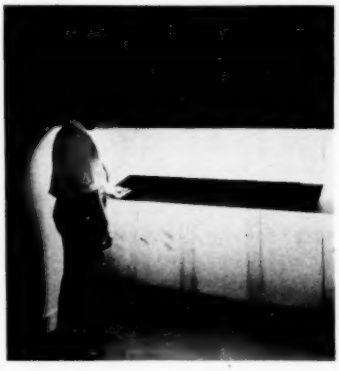

FIG. 17. Color matching booth at Forbes Varnish Company, Cleveland.

The development of fluorescent lamps makes possible the design of very satisfactory color matching booths employing two or three qualities of light. Color temperatures of 3500 and 6500°K are directly obtainable with available lamps, and a color temperature of approximately 11,000°K is obtainable by use of daylight and blue lamps in the ratio of two daylight to one blue. These three qualities of light should be adequate for most color matching tasks.

The Significance of Stray Light in Photoelectric Filter Photometers*

M. N. States and J. C. Anderson
Central Scientific Company, Chicago, Illinois
(Received July 31, 1942)

INTRODUCTION

In recent years numerous papers have been published describing photoelectric filter photometers and their application to various chemical analyses. A glance at the list of references in a recent paper by Muller[1] is a good indication of the interest in this field. The outstanding application of these devices is to the determination of the concentration of a material in solution. In such cases the concentration is related to the indications of the instrument, usually a ratio of two readings, one of which is a standard setting. If the instruments are true spectrophotometers, the ratio of the two readings corresponds to the transmittancy of the solution or, using appropriate techniques and an instrument provided with a logarithmic scale, the indications are a measure of the density of the solution. The curve relating concentration of material in solution to the indications of the instruments may be called the *analytical curve*. On the assumption that true spectrophotometers are used and that the solutions obey Beer's law, the analytical curves are linear when the results are plotted on appropriate cross-section paper. If the spectrophotometer indicates transmittancies, a graph of the solution concentrations plotted on a linear scale as ordinates against the transmittancies on a logarithmic scale is a straight line passing through the origin, $c=0$, $T=100$ percent. If the instrument has a density scale, a linear analytical curve is obtained passing through the point of zero concentration and zero density when the solution concentrations are plotted against the densities on rectilinear paper.

When the principles of spectrophotometry are applied to chemical analysis using photoelectric filter photometers, the analytical curves are in general not linear. Some authors[2] have outlined analyses to be made with filter photometers in which the solution concentration is directly proportional to the logarithm of the "transmittancy." Others,[3] using an instrument of the same manufacture for the same chemical analysis, report that the analytical curve is not linear. Filter photometers[4] have been devised and manufactured which are provided with a "density" scale, or a scale proportional to density, and the techniques suggested imply that linear analytical curves are generally obtainable. Still other experimenters,[5,6] using photoelectric filter photometers, have recognized the possibility of obtaining linear analytical curves in certain chemical analyses but indicate that such calibration curves are exceptional. They recommend the use of several standard solutions to determine the exact form of the analytical curve.

In certain instances where linear analytical curves were not obtained, it has been suggested that this may be due to the failure of the solution to follow Beer's law.[7] Others have attributed this result to the failure of the *instrument* to obey Beer's law, and still others to the lack of linear response of the photo-cell. It is well known that some solutions do not obey Beer's law, and that others exhibit discrepancies except for low concentrations. It is hardly necessary to say that no meaning can be attached to the statement that an *instrument* does not follow Beer's law. Fur-

* Presented at Tenth Summer Conference on Spectroscopy and Its Applications held at the Massachusetts Institute of Technology, Cambridge, Massachusetts, July 20–22, 1942.

[1] Ralph H. Muller, "Photoelectric methods in analytical chemistry," Ind. Eng. Chem. Anal. Ed. **11**, 1–17 (1939).

[2] W. J. Dann and K. A. Evelyn, "The determination of vitamin A with the photoelectric colorimeter," Biochem. J. **32**, 1008–17 (1938).

[3] Marian Stark Kimble, "The photocolorimetric determination of vitamin A and carotene in human plasma," J. Lab. Clin. Med. **24**, 1055–65 (1939).

[4] William H. Summerson, "A simplified test-tube photoelectric colorimeter, and the use of the photoelectric colorimeter in colorimetric analysis," J. Biol. Chem. **130**, 149–166 (1939).

[5] William S. Hoffman, *Photelometric Clinical Chemistry* (William Morrow and Company, New York, 1941), pp. 6–7.

[6] Arthur H. Sanford, Charles Sheard, and Arnold E. Osterberg, "The photelometer and its use in the clinical laboratory," Am. J. Clin. Path. **3**, 405–420 (1933).

[7] E. Leitz, Inc., Pamphlet No. 1290, *Leitz Clinical Photo-Electric Colorimeter* (1941).

thermore, it has been shown that barrier-layer cells,[8] under certain conditions, do exhibit a linear response and that they can be used successfully in true spectrophotometers. The non-linear analytical curves of photoelectric filter photometers must depend upon other factors. It is the purpose of this paper to show why the analytical curves are in general not linear and that, under certain circumstances, the analytical curves cannot be linear if the solutions obey Beer's law.

Sanford *et al.*[6] suggested that an imperfect match between the transmission band of the filter and the absorption band of the solution may account for the non-linear analytical curves obtained with filter photometers. While the difficulty is associated with the filter, the analysis to follow indicates that non-linear analytical curves may arise even when the match is perfect. To calculate the true from the apparent density of a solution, Dann and Evelyn[2] have proposed a relation between the apparent transmittancy of a solution measured on the filter photometer, the true transmittancies of the solution, and the transmission of the filter. The validity of this equation when applied to measurements on a photoelectric filter photometer is open to question, since they fail to take into account the variation in energy distribution with wave-length of the light source and the non-uniform response of the photo-cell with wave-length. This is apparent from Fig. 1 in which A is the variation with wave-length of the true transmission of a filter and B is the over-all effect of filter, photo-cell, and light source. Harris and Siegel,[9] in a recent paper, have correctly pointed out that "the linear relation is to be expected only for strictly monochromatic radiation or for the case where the absorbing species has an absorption coefficient that is constant over the whole spectral band used for analysis." Hogness[10] and his colleagues in discussing the effects of stray light in a true photoelectric spectrophotometer derive an expression relating the true and the apparent transmittancies in terms of the percentage of stray light present in the isolated light beam. Sheard and States[8] modified this expression into a more convenient form in discussing the stray light effects in a grating photoelectric spectrophotometer. When this latter equation is still further modified and applied to photoelectric filter photometers, the reason why non-linear analytical curves are obtained on these instruments becomes apparent.

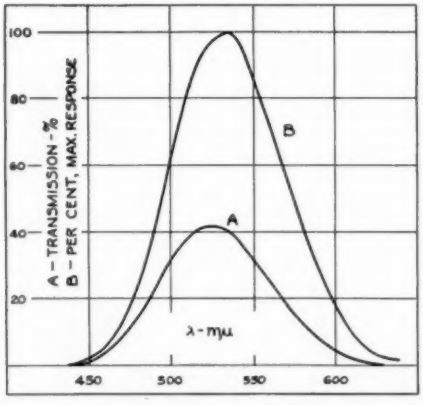

FIG. 1. A, transmission curve for a filter and B, the response curve for a photo-cell as modified by the light source and the filter.

[8] Charles Sheard and M. N. States, "A concave grating photoelectric spectrophotometer," J. Opt. Soc. Am. **31**, 64–69 (1941).

THEORETICAL ANALYSIS

Consider a transmittancy measurement T at the wave-length λ in which the spectral region isolated $\Delta\lambda$ is small as compared with the width of the absorption band of the solution or where $dT/d\lambda \cdot \Delta\lambda$ is small. On the assumption that the photoelectric current is proportional to the intensity received by the photo-cell and that the currents I_0 and I are thus observed when the solvent and solution, respectively, are placed in the light path,

$$T = I/I_0. \tag{1}$$

Suppose, however, that stray light is present so that both I_0 and I are in general larger than their true values. Then Eq. (1) must be modified,

$$T = \frac{I' - (f_1x_1 + f_2x_2 + \cdots f_nx_n)}{I_0' - (x_1 + x_2 + \cdots x_n)}, \tag{2}$$

[9] Louis Harris and Benjamin M. Siegel, "A simplified photometer for determining nitrogen dioxide concentrations," Ind. Eng. Chem. Anal. Ed. **14**, 258–260 (1942).

[10] T. R. Hogness, F. P. Zscheile, Jr., and A. E. Sidwell, Jr., "Photoelectric spectrophotometry, an apparatus for the ultra-violet and visible spectral regions: its construction, calibration, and application to chemical problems," J. Phys. Chem. **41**, 379–415 (1937).

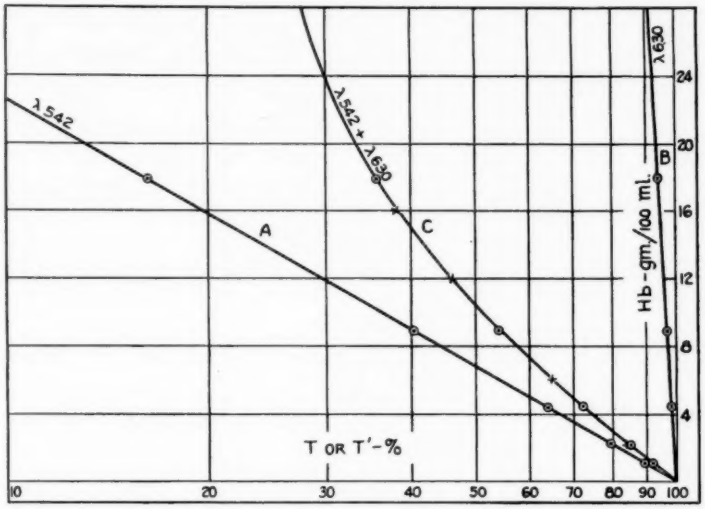

FIG. 2. Analytical curve *C* when one stray light component (λ 630) is present which is only slightly absorbed by solution. Absorption path, 1 cm.

where the series in both numerator and denominator of Eq. (2) are contributions to the photoelectric currents I_0' and I' by stray light of wave-lengths $\lambda_1, \lambda_2 \cdots \lambda_n$. At these wave-lengths the quantities $f_1, f_2 \cdots f_n$ are the true transmittancies of the solution, and $x_1, x_2 \cdots x_n$ are the photoelectric currents produced by the stray light present when the solvent is in the light path. On summing the two series in Eq. (2),

$$T=\frac{I'-f\cdot x}{I_0'-x}, \tag{3}$$

where $x=x_1+x_2+\cdots x_n$ and $f\cdot x=f_1x_1+f_2x_2+\cdots f_nx_n$, in which case f is an average transmittancy of the solution for a particular distribution of stray light.

If T', the *apparent* transmittancy of a solution, is I'/I_0', Eq. (3) reduces to

$$T'=T+\frac{x}{I_0'}(f-T). \tag{4}$$

Obviously, x is independent of the solution whereas the value of f is in general an involved function of the transmittancies of the solution at the various wave-lengths. Both depend upon the energy distribution of the light source with wave-length and the response characteristics of the photo-cell. $T'=T$ if $x=0$ or if $(f-T)=0$. In the first instance, the stray light is zero; in the second, the solution absorbs the stray light to the same extent as the spectral region isolated. T', T, and f vary with the solution concentration; x/I_0' does not. Since T is a true transmittancy, if Beer's law holds for the solution, a linear analytical curve obtains for it. On the other hand, the variation of T' and f with concentration would in general be non-linear.

EXPERIMENTAL RESULTS AND ANALYSIS

To establish the validity of Eq. (4), analytical curves were made for oxyhemoglobin using a concave grating spectrophotometer.[8] The stray light was produced by displacing laterally portions of the diffracted light beam passing through the exit slit. This was accomplished by placing narrow, small angled prisms in front of a portion of the grating surface. The amount of stray light was controlled by the width of the prism, the wave-length by the angle of the prism, and the isolated spectral region by the width of the exit slit. Analytical curves were made by varying the solution concentration using the spectral regions isolated—the radiation coming directly from the grating and the "stray light" components—independently and in various combinations.

One Stray Light Component

Referring to Fig. 2, curve *A* is the true transmittancy variation with concentration at λ 542 mμ. Curve *B* is the true transmittancy at

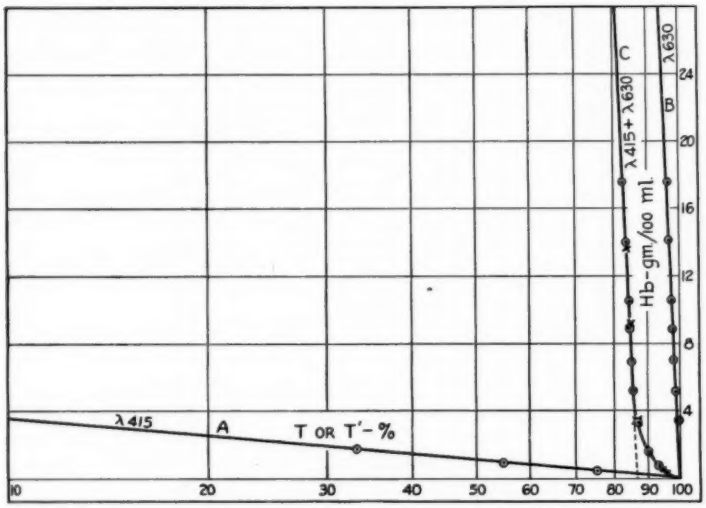

FIG. 3. Analytical curve *C* when one stray light component (λ 415) is present which is strongly absorbed by solution. Absorption path, 1 cm.

λ 630 mμ, and curve *C* is the apparent transmittancy when energy from both spectral regions is permitted to pass through the exit slit of the spectrophotometer. The stray light x/I_0' from λ 630 mμ was observed to be 24.5 percent.

On using Eq. (4), theoretical apparent transmittancy values T' corresponding to various concentrations were computed from corresponding transmittancy values T and f in curves *A* and *B* and the observed value of x/I_0'—24.5 percent. These theoretical points are the crosses on curve *C*.

In Fig. 3 a similar result is shown in which curves *A* and *B* are linear analytical curves made at wave-lengths λ 415 mμ and 630 mμ. In curve *C* stray light of wave-length 415 mμ of 13.9 percent is combined with energy from λ 630 mμ to produce the analytical curve. Computed transmittancies from Eq. (4), using transmittancy values from curves *A* and *B*, fall on curve *C*. If f is very small as compared with T, it is clear from Eq. (4) that the apparent transmittancy relationship (curve *C*) should be very nearly parallel to curve *B*. Furthermore, if curve *A* were substantially parallel to the transmittancy axis, this curve should intersect the transmittancy axis at 86.1 when x/I_0' is 13.9 percent. It is seen from the lower dotted portion of this curve that the intersection is slightly greater than this value, as it should be since the absorption in the region of the stray light is not sufficient to produce this limiting condition. In all of the curves, the spectral region of each component isolated is 9 mμ.

It is interesting to point out the wide variation in possible analytical curves obtainable with a single stray light component. Figure 4 is a

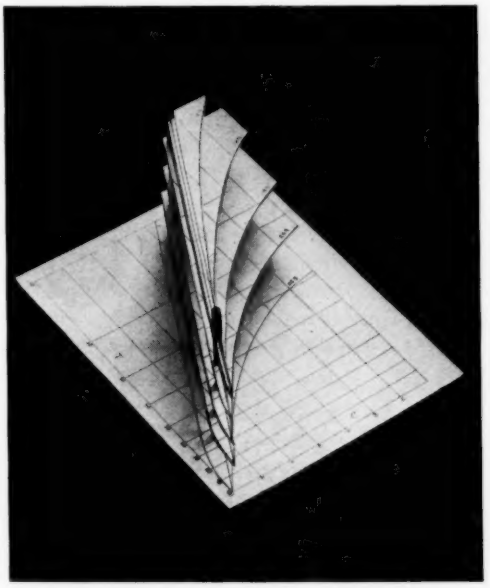

FIG. 4. Families of analytical curves obtainable with variation (in spectral region) in a single stray light component, as well as variation in the magnitude of the stray light from 0 to 25 percent of the incident radiation.

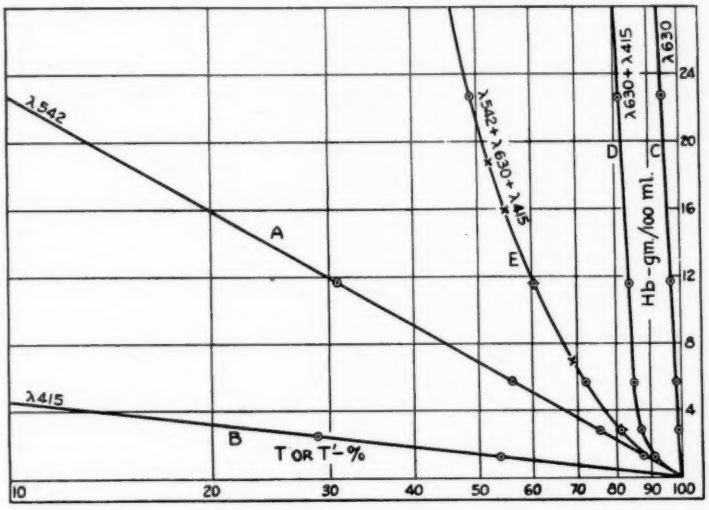

FIG. 5. Analytical curve E when two stray light components are present, one of which (λ 415) is strongly and the other (λ 630) only slightly absorbed by solution. Absorption path, 1 cm.

photograph of a model showing the families of possible analytical curves obtainable for a single stray light component in which x/I_0' varies between 0 and 25 percent and in which the absorption of the stray light component varies from nearly complete absorption to complete transmission. The small line at the top is the true analytical curve when no stray light is present. The first plane from the top is the location of the family of analytical curves for a single stray light component of 5 percent and variation in absorption of this component between the limits given. The succeeding lower planes progressively expand for 10, 15, 20, and 25 percent stray light. The limit on the right, on the curved side of the model, obtains when the stray light occurs at a wave-length for which the solution transmits perfectly. In other words, the analytical curve for the stray light under this condition would be a vertical line coincident with the concentration axis. The limit to the left arises when the stray light component is almost entirely absorbed by the solution. It is interesting to note that under this condition the apparent analytical curves are substantially linear and parallel to the true analytical curves except for low concentrations and high transmittancies. Furthermore, when the straight line portion of these limiting curves is projected on the transmittancy axis, they cut the axis at $(1-x/I_0')100$—100 minus the percentage of stray light present. These conclusions are predicted by Eq. (4). The analysis also suggests that in general a very small amount of stray light may introduce curvature or displacement or both in the analytical curves.

Two Stray Light Components

In Fig. 5 analytical curves are shown for two components of stray light. The true transmittancy is for λ 542 mμ and is shown in curve A. The true transmittancies for the two components of stray light at λ 415 mμ and λ 630 mμ are shown in curves B and C. Curve D is the apparent transmittancy of the solution when a certain mixture of the energy from λ 415 and 630 is used, while E is the analytical curve for the same relative proportion of λ 415 and λ 630 mμ with λ 542. The energy from λ 415 mμ and λ 630 mμ was 54.9 percent of the total. The crosses shown in curve E are computed values using Eq. (4) in which x/I_0' is 54.9 percent and the values of f are taken from curve D.

From this analysis it becomes apparent why analytical curves associated with the filter photometer are not in general linear. If the transmission band of the filter is wider than the absorption band of the solution, x/I' is not equal to zero and values of f in Eq. (4) are not in general equal to T and hence the analytical curves should be non-linear. In many cases the stray light x/I_0' may amount to 10 or 15 percent.

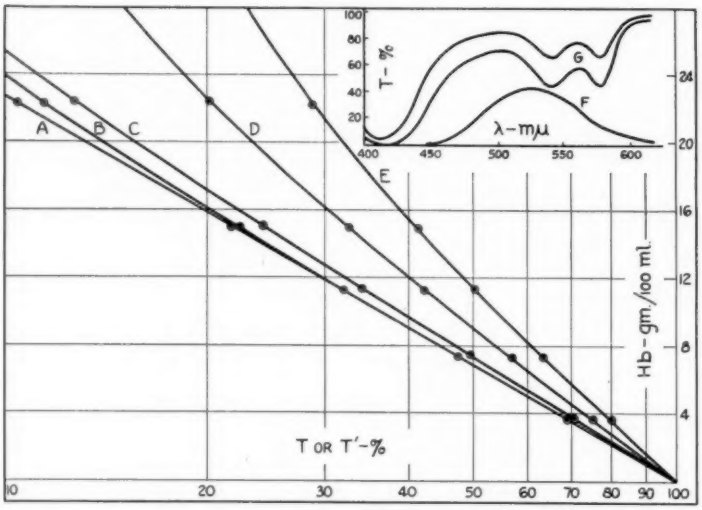

FIG. 6. Analytical curves (*A* to *E*) for same solution, in which various amounts of stray light are present. Absorption path, 1 cm.

Stray Light from a Single Wide Band

As a further test of the above analysis, analytical curves were run on varying concentrations of oxyhemoglobin using various spectral regions isolated at λ 542 mμ. These curves are shown in Fig. 6. The transmittancy curves *G* for two concentrations of oxyhemoglobin and the transmission curve *F* for a green filter are shown in the upper right-hand corner of the figure. The spectral regions isolated were 9 mμ, 14 mμ, and 24 mμ in curves *A*, *B*, and *C*. The curves are substantially linear, since the absorption band at 542 for oxyhemoglobin is quite wide, but there is a tendency for the stray light to influence the results. In curve *D* the exit slit was completely removed from the spectrophotometer, isolating a spectral region approximately 60 mμ wide. The curvature here is quite distinct. Finally the grating of the spectrophotometer was adjusted so that the direct image of the entrance slit was in focus at the exit slit. A green filter having the transmission shown in curve *F* was placed before the entrance slit. This corresponds to the use of the instrument as a filter photometer. Since the same photo-cell and measuring circuit was used in all cases, it is clear that the non-linear analytical curve *E* must be attributed to the stray light effect of the filter.

To show that it is possible to obtain linear analytical curves when the spectral region isolated by the filter is narrower than the absorption band of the solution for all concentrations involved, attention is called to Fig. 7. In this case analytical curves were made using a copper sulphate solution and a red filter. The transmittancy curves *B* for the solution and the transmission curve *C* for the filter in the upper right-hand corner of the figure indicate that ideal conditions obtain for linear analytical curves. The transmission of the filter is substantially zero at all wave-lengths at which the solution transmits light to a great extent, whereas the main transmission band of the filter is in the region where the solution absorbs strongly. Consequently, the analytical curve *A* is quite linear. It is interesting to point out that numerous filter photometers have been described showing such analytical curves for copper as proof that Beer's law is obeyed—presumably for the instrument. It is clear, however, that this is merely a fortuitous situation in which f in Eq. (4) is equal to T at all concentrations and hence stray light is of no consequence.

CONCLUSIONS

As a result of these experiments it may be desirable to point out some more or less obvious conclusions:

1. Analytical curves obtained on filter photometers are in general non-linear, and they cannot be otherwise if the solutions obey Beer's

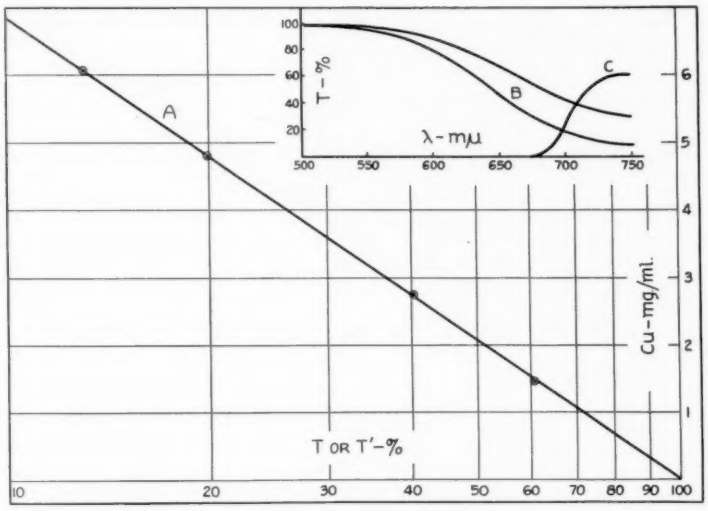

FIG. 7. Linear analytical curve for copper sulphate in which stray light effect is negligible on account of the wide absorption band of the solution. Absorption path, 1 cm.

law. When the concentration is plotted on a linear scale as ordinates against the transmittancies on logarithmic scale, the curves are concave upward. In the relatively few instances where increased concentration produces increased transmittancies,[11, 12] this conclusion is not valid.

2. Since T, x, and f in Eq. (4) in a particular filter photometer calibration are unknown, one can only estimate the stray light effects. However, if the analytical curve is substantially linear over the transmittancy range of 10 to 100 percent, x is approximately equal to 0 or f is approximately equal to T. Both of these conditions may obtain simultaneously, although the latter is the more probable explanation of a linear curve. Since f is not likely to be less than T in an actual situation, analytical curves which are linear but having a sharp break near 100 percent transmittancy are unlikely to occur.

3. The procedure of establishing an analytical curve by drawing a straight line on semi-logarithmic paper through the points $c=0$, $T'=100$ percent and one other point is open to question. The same criticism applies to the use of a single calibration point where the instrument is equipped with a density scale. It is much better practice to calibrate the instrument for a number of concentrations and to draw a smooth curve connecting the various points.

4. When linear analytical curves do not obtain for a photoelectric filter photometer, the calibration is a function of the energy distribution of the light source with wave-length. Consequently, the practice of applying a constant voltage to the incandescent light source and adjusting for the standard setting by means of an iris diaphragm is greatly to be preferred over the use of a variable resistor in the light circuit.

5. This analysis emphasizes the necessity of eliminating the effects of selective fatigue[13] of the photo-cell by appropriate instrument design. Obviously, if the spectral response of the photo-cell is a function of the cell's fatigued condition, the position of the analytical curves changes as the cell is exposed to light.

6. During the last eight or ten years filter photometers have been extensively used in clinical, steel, food, and other laboratories. Perhaps the most intensive application is the determination of molybdenum in steel. At the present time they are being used twenty-four hours a day in steel mills for this analysis. A single operator is capable of analyzing sixty samples—that is,

[11] Charles L. Guettel, "A photelometric study of the lead-dithizone system at 610 millimicrons," Ind. Eng. Chem. Anal. Ed. **11**, 639–40 (1939).

[12] William S. Hoffman, "A rapid photoelectric method for the determination of glucose in blood and urine," J. Biol. Chem. **120**, 51 (1937).

[13] M. N. States, U. S. Patent No. 2,051,320 (1936).

making one-hundred-twenty tests—in eight hours. Perhaps two-hundred different chemical analyses are now routinely performed on these instruments to varying degrees of accuracy depending upon the requirements and upon how carefully the operators adhere to fundamental principles. One may safely predict that applications of the photoelectric filter photometer will greatly increase in the future. By taking into account the factors mentioned in this paper, some of the chemical analyses now available may be improved and others may be devised.

NOVEMBER, 1942 J. O. S. A. VOLUME 32

A Stigmatic Grating Spectrograph for Industrial Laboratories*

RICHARD F. JARRELL
Jarrell-Ash Company, Boston, Massachusetts
(Received July 28, 1942)

INTRODUCTION

WADSWORTH[1] in 1896 was the first to point out what still remains the simplest and most effective method of producing a stigmatic image from a concave reflecting grating. The two formulas for the spectral and horizontal focus of such a grating are:

$$\left(\frac{\cos^2 i}{s}-\frac{\cos i}{R}\right)+\left(\frac{\cos^2 r}{s'}-\frac{\cos r}{R}\right)=0,$$
$$\left(\frac{1}{f}-\frac{\cos i}{R}\right)+\left(\frac{1}{f'}-\frac{\cos r}{R}\right)=0, \quad (1)$$

where s and s' are the distances of slit and image, respectively, from the grating, f and f' are the distances of a horizontal object and its image, R is the radius of curvature, and i and r are the angles of incidence and reflection. It will be seen that if r is put equal to 0, and if f and s are set equal to infinity, the two formulas become the same. Physically, on the grating normal, the image will be stigmatic if the light incident on the grating is first collimated. In this case the formula for either image reduces to:

$$s'=f'=\frac{R}{1+\cos i}, \quad (2)$$

the equation of a parabola in polar coordinates.

Wadsworth suggested either a collimating lens or mirror to render the light incident on the grating parallel, but actually used a lens. Fabry and Buisson[2] introduced a concave mirror to avoid the difficulty of achromatism. In their instrument a small right-angle prism was used to direct the light from the slit at the side of the spectrograph onto the mirror, but in all later instruments the slit has been set directly at the focus of the mirror. From the mirror the light is reflected back to the grating, which is mounted permanently at right angles to the axis of a long bar. The plateholder is maintained on the grating normal by locating it at the far end of this bar. With the angle of reflection thus established, the spectral region is changed by varying the angle of incidence, rotating the bar about a pivot centered under the grating face. Figure 1 showing the completed instrument will make the location of these elements clear.

It will be seen that, away from the grating normal, the spectral and visual foci are given by:

$$s'=\frac{R}{\cos r+\cos i}\cos^2 r, \quad f'=\frac{R}{\cos r+\cos 1}. \quad (3)$$

Thus $s'=f'\cos^2 r$. The difference in focus between the two images increases rather rapidly as the angle r increases. For a 21-foot radius of curvature grating, with the beam set to give an angle of incidence of 15°, the difference in focus 10 inches away from the grating normal amounts

* Presented at Tenth Summer Conference on Spectroscopy and Its Applications at Massachusetts Institute of Technology, Cambridge, Massachusetts, July 20–22, 1942.

[1] F. L. O. Wadsworth, Astrophys. J. **3**, 54–58 (1896).

[2] C. Fabry and H. Buisson, J. de Phys. **9**, 933 (1910).

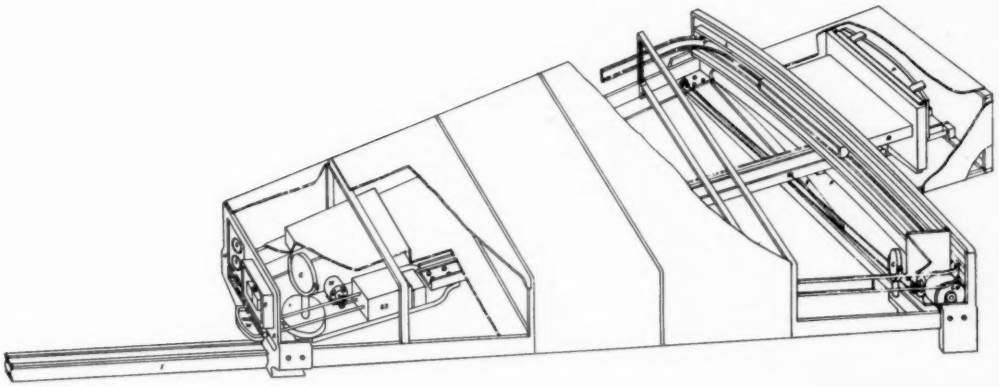

FIG. 1.

to 18 mm. This means that a horizontal line will not appear in sharp focus when the plate is bent to give the spectral lines best definition. The departure from coincidence, however, remains sufficiently small so that the distribution of light from a series of diaphragms or sector openings placed at the slit can be used to calibrate the emulsion without use of any auxiliary lenses or any stopping down of the grating aperture.

Since the collimating mirror is used slightly off axis the normal slight astigmatism resulting from such use is superimposed on the $\cos^2 r$ factor.

A perplexing feature of this type of mounting is that *higher* wave-lengths are brought to the center of the plate by moving the bar *away* from the mirror, whereas, for any one position of the bar, the *higher* wave-lengths fall *toward* the mirror. This apparent anomaly can be understood by considering the simple grating formula:

$$n\lambda = d(\sin i \pm \sin r), \qquad (4)$$

where i and r are considered positive angles measured from the grating normal, the minus sign applying when the angles are on opposite sides of the normal, the positive when they are on the same side. For the center of the plate, since $\sin r = 0$, as i is increased by moving the bar away from the mirror, the wave-length increases. At any one position of the bar, as r becomes greater on the far side of the grating normal, away from the mirror, the minus sign applies and λ decreases; while as r becomes greater on the near side of the normal the plus sign applies and λ increases.

Burns[3] constructed a spectrograph of this type at the Bureau of Standards in 1914, and Meggers, Kiess, and Stimson[4] used it in part of the work reported in their early paper on "Practical spectrographic analysis" in 1922. The Wadsworth mounting is accordingly one of the oldest in point of application to industrial analysis, yet the present spectrograph is the first commercial instrument using this mount.*

DESCRIPTION OF THE INSTRUMENT

The present spectrograph has been designed as an entirely self-contained unit. Figure 1 shows a schematic diagram of the instrument with part of the cover and camera base cut away to show the details. A rigid frame has been constructed using semi-steel castings and structural steel beams, forming a rough trapezoid, 20 inches wide at the front, 6′ 9″ wide at the back, with a perpendicular arm of 10′ 10″. The front casting carries a support on which a thrust ball bearing is mounted to act as pivot for the steel channel and casting which form the sliding bar. The channel carries a bearing which rides on a track of cold rolled steel at the rear of the spectrograph, at *F*. The grating *G* is mounted with its face centered above the ball bearing, while the col-

[3] K. Burns and W. F. Meggers, Bur. Stand. Sci. Pap. **18**, 441 (1922).

[4] Meggers, Kiess, Stimson, Bur. Stand. Sci. Pap. **18**, 444 (1922).

* Since the preparation of this manuscript the program of the Tenth Spectroscopy Conference has reached me with the notice of a paper by Forrest and Straat describing a similarly mounted instrument.

limating mirror M is supported from a base attached to the side angle iron.

In order to change spectral region it is necessary not only to rotate the bar and grating about the pivot, but also to move the plate in and out along the axis of the beam to maintain focus in accordance with formula (2). At the same time it was desired to leave the plateholder in the open where it would be accessible without opening any dark covers. This was found to be possible if the back of the spectrograph was constructed in the form of an arc of a circle centered about the pivot. In this back have been mounted light tight steel ways L in which moves a spring steel tape T fastened to an upright secured to the bar. The upright contains a box frame in which a metal open box bellows B connected to the plateholder P slides. As the channel is rotated the steel tape maintains the camera enclosure sealed from light, while the bellows permits the carriage which carries the plateholder to move to and fro along the bar to the correct focus. The carriage rides on substantial steel rods. The back of the spectrograph has been fabricated from cold finished steel bars rolled to shape and then ground to a final radius by mounting a small grinder on the channel and using the instrument as its own shaper.

A gear motor GM and sprocket chain drive pull the bar along its track. In order to maintain the plateholder in focus a strong spring holds a ball bearing contact fastened to the plateholder carriage against a cam E shaped roughly in accordance with formula (2) and finished by empirical adjustment. As the channel rotates it moves a pointer arm which projects through the front casting of the spectrograph across a wavelength scale W. Since the gear motor is controlled by a switch on the front operating panel, in changing spectral region it is only necessary to push the motor switch until the wave-length pointer indicates the desired region, and the plate is automatically in focus.

The plateholder is racked up and down by a rack and pinion and worm gear driven by the motor M and gear box GB. These have been located at the front of the instrument as shown so that a gear shift rod K can extend through the front casting. This makes it possible to shift from the normal plate racking speed to either of two slow motion drives suitable for continuously moving plate exposures, which have become increasingly more useful in recent years. The necessary manipulation can be made from the front of the spectrograph. On the front operating panel H is mounted a Veeder counter which shows the position of the plate, in mm. The motor circuit is closed through a relay operated by a rotating contact driven by the plate drive shaft. Switches on the front operating panel make it possible to select contacts which will break the circuit in steps of 1 mm, 2 mm, 3 mm, or 6 mm as desired. A push button short circuit starts the motor again. For moving plate exposures or in rapid racking of the plate a short circuit switch can be thrown. The plate dark slide is operated automatically by the plate drive or can be manipulated by hand.

The plateholder accommodates two $4'' \times 10''$ plates. A 35-mm filmholder can be supplied instead, covering a twenty-inch length of spectrum. For appearance sake the plateholder and its carriage and bellows have been enclosed partially by a cover matching the spectrograph itself.

The bilateral symmetrical slit S regularly supplied is a modification of the design described by Elliott,[5] employing jaws which ride on balls in hardened and ground steel ways. It is spring closing, with a stop to prevent damage to the jaws. The drum subdivisions correspond to 0.0025 mm. The slit is provided with an electromagnetic shutter which may be controlled by the electric timer shown on the front panel. A shield projecting from the front casting protects the slit from accidental blows. The jaws, which come flush with the front of the shield so that sectors can be used directly before the slit, are covered with a thin quartz window to keep out dust.

The figure will show how the operating mechanism has been segregated from the camera itself. The gear motor is in a separate compartment by itself. The bar and pivot, motor and gear box, track for the bar, and focus cam are all below the camera bottom. The grating and mirror supports project up through this bottom through light tight seals, while the plateholder bellows admits the front of the plate to the camera. The only other part in the camera enclosure is the back of the slit mount, with its shutter electromagnet.

[5] A. Elliott, J. Sci. Inst. **10**, 358 (1933).

Thus the camera is shielded from the heat of the motors and from the light which the brushes emit in starting and stopping. Only the essential optical elements are in the camera.

OPTICAL CHARACTERISTICS

A 6″ diameter 21-foot radius of curvature, 15,000-line per inch grating is employed. It is aluminum on Pyrex, ruled by Dr. R. W. Wood at Johns Hopkins. Dr. Wood has made a special effort to produce a grating with high intensity in the first-order ultraviolet, as well as visible. The first grating shows a very bright first-order spectrum on one side, extending well down into the ultraviolet. It has a ghost intensity of about 1/900 in the first order and the target pattern appears unusually uniform.

The spectrograph has a dispersion in the ultraviolet of 5.0A/mm in the first order. In the red, where the plateholder moves further from the grating, the dispersion increases to 4.8A/mm. At one setting the spectrum is practically normal and the dispersion essentially linear. The range of the instrument is from 1800A to 9000A in the first order, which means that it will photograph up to 4500A in the second order or 3000A in the third. At one setting the plates cover approximately 2500A in the first order. The optical characteristics will vary slightly from instrument to instrument because it is difficult to standardize rigidly the focal length of such long radius mirrors.

GRATING INTERCHANGER

In closing it might be said that a grating interchanger has been designed which would make it possible to exchange gratings without opening the spectrograph merely by turning a handle at the front of the instrument. This would revolve the new grating into position and would at the same time substitute a new ball bearing contact for the focus cam, so that the spectrum would be automatically in focus. This would make it possible to shift to lower or higher dispersions at will, or to substitute gratings of more favorable intensity distribution for the particular region being examined. The device has not been tested as yet so that it is not described in detail.

NOVEMBER, 1942 J. O. S. A. VOLUME 32

A Grating Spectrograph of Fabricated Steel*

J. W. Forrest and H. W. Straat
Bausch and Lomb Optical Company, Rochester, New York

(Received July 22, 1942)

IT is the purpose of this paper to describe very briefly the mechanical structure of a recently completed grating spectrograph of the Wadsworth type. This unit uses a grating of four-meter radius, one hundred millimeters in length, and ruled with ten thousand lines per centimeter. A similar grating of fifty-nine hundred lines per centimeter was used in the model but the chassis is designed to accept the grating of higher dispersion. With the ten thousand line grating the dispersion at one end of the arc is 4.8A/mm and at the other end 3.6A/mm.

The original design plan was to provide an instrument which would be a completely integral unit in the same sense that the Littrow prism instrument is a unit, and to do this with a sand-casting structure. However, difficulties due to excessive weight and to the machining of the arc prevented this design from getting beyond the paper stage. It was with some fear of vibration troubles that the possibility of a welded unit was taken under consideration. Contrary to expectation the finished unit has shown exceptional freedom from the thing that was most feared. It was necessary, due to the present floor space requirements, to assemble and test the unit in a portion of the plant where vibration was very

* Presented at the Tenth Summer Conference on Spectroscopy and Its Applications held at the Massachusetts Institute of Technology, Cambridge, Massachusetts, July 20–22, 1942.

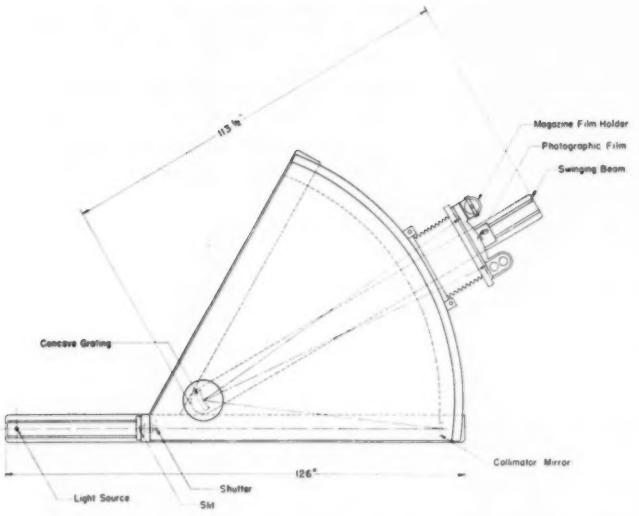

FIG. 1. Plan view of grating spectrograph.

noticeable. In spite of this no troubles due to this factor have been detected and no attempt has been made at any time to reduce the vibration by the use of shock-absorbing devices.

The instrument as designed was fabricated for us by the William J. Meyer Company of Rochester, specialists in sheet metal work. The main chassis consists of two beams of rectangular section (Fig. 1) welded to each other and to the arc which is also entirely of a welded structure. A traveling beam carrying the camera is of the same type and is supported at one end by the main bearing under the grating (*7*) and at the other by Torrington needle bearings (*9*) running on a machined horizontal surface. One of the fixed beams is extended back of the slit (*1*) to provide a support for the arc and auxiliary apparatus. The entire unit is supported on three formed and welded pedestals. The actual points of support are three small convex portions at the center of the pedestals. Suitable strengthening members (Fig. 2) are welded in throughout the structure and the unit is completed and made light-tight by means of a sheet metal cover. The material used throughout is $\frac{3}{16}$-inch sheet steel. The estimated weight of the completed unit is under 1500 pounds.

In addition to the unexpected advantage of freedom from vibration, the unit as constructed avoids the use of large boring mills to fashion the machined surfaces on the arc. When the chassis first came into the plant, the main bearing (*10*) was built and installed. A heavy radius bar was then mounted and the arc surfaces machined about the bearing center without the use of anything other than the ordinary small tools found in precision shops. This manner of machining the arc offers the second advantage that each instrument will be absolutely true about its own bearing center and later difficulties of assembly will be avoided.

The remainder of the structure consists of standard sand cast parts, the only one meriting description being the film holder. This unit (Fig. 3) was originally designed for use on the Littrow prism instrument and was carried over

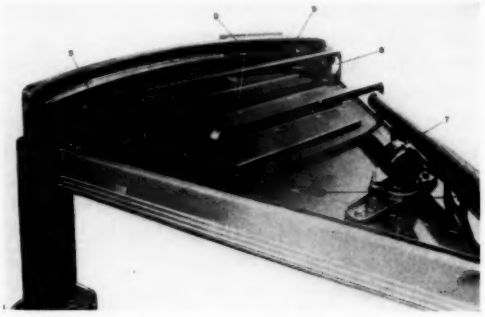

FIG. 2. Internal welded structure.

with proper size alterations to the grating model. It utilizes 35-mm film carried in a storage container (*2*). The container will accept 100 ft. of film which may be used as desired without removing the main holder from the instrument. The receiving drum (*3*) on the right is arranged to be removed and taken to the dark room. Its removal automatically cuts the film and effects a light-tight closure of the exit port of the holder. Return of the receiving unit (*3*) again opens the port. A footage counter which can be set when the new roll is put in the holder indicates the amount of film remaining. This counter is provided with a double dial and gear system permitting maximum utilization of film. If several pictures are to be taken before the removal of the chamber for development, the fast dial is given a three-quarter turn. If the film is to be removed after each picture it is given a full turn. The exposed area is 15 inches long. In the first case with a three-quarter turn, 17 inches of film are used and in the second case, where pictures are cut off individually, 22.5 inches are used. The entire holder is manually adjustable (*4*) along the beam for focusing purposes. Flexible steel curtains (*5*) operating on spring rollers close the slot in the chassis as the film holder is moved from position to position.

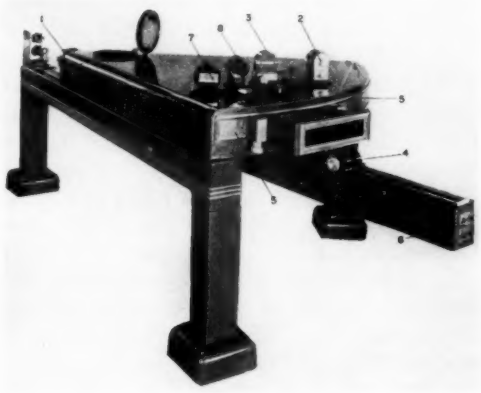

FIG. 3. Instrument with optical units removed.

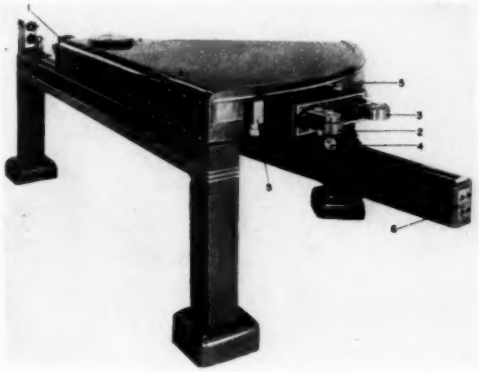

FIG. 4. Assembled instrument.

The traveling beam (Fig. 4) is operated in either direction by motor driven screw. A switch on the end of the beam when thrown completely over snaps into place on either side and the motor will then drive the camera across the arc in about two minutes. Over-run is prevented by automatic cut-out switches at either end. If the same switch is held in the half-way position the motor is operated at slow speed and precise setting on the arc scale is possible. The shutter is also operated electrically from either the plate or the arc position and is provided with a pilot light to indicate its position.

To summarize briefly, the characteristics of the instrument described may be tabulated as follows:

Grating size —10 cm with 10,000 lines per cm;
Grating radius —4 meters (13.3 ft.);
Dispersion —4.8 to 3.6A per mm (first order);
Weight —1500 lb. approximately;
Maximum length—4.3 m approximately;
Film length —380 mm;
Film capacity —standard 100-ft. roll;
Total spectrum length (first order 2100A to 8000A) 1.4 m.

Spectrochemical Determination of Silicon, Iron, and Aluminum in Mineral Powders with a High Voltage Direct Current Arc* [1]

HOWARD I. OSHRY,[2] JAMES W. BALLARD,[3] AND H. H. SCHRENK[4]
Central Experiment Station, Bureau of Mines, Pittsburgh, Pennsylvania
(Received July 25, 1942)

INTRODUCTION

IN the evaluation of health hazards due to atmospheric contaminants, it is important to know the composition of the air-borne material. This requires the analysis of samples whose components may vary over a wide range. Moreover, samples encountered in the analysis of air-borne materials may range in size from a fraction of a milligram for samples collected in an impinger[5] to several hundred milligrams for samples collected with an electrostatic precipitator.[6] In addition, the study of atmospheric contamination may involve a study of the material from which the dust is generated, in which case several pounds of material must be sampled and analyzed. Chemical methods for determining many of the constituents are difficult and time consuming, especially for very small samples.

The nature of spectrochemical analysis has generally limited its use to two types of determinations—determination of the concentration of minor constituents in a sample or identification of the constituents of small samples. The application of spectrographic techniques to the quantitative determination of the major constituents of mineral samples generally has had limited success, although some have been reported in the literature.[7]

This paper describes a spectrochemical technique for the determination of silicon, iron, and aluminum as oxides in powder samples, which was suggested by a series of papers by Breckpot and others[8] describing a study of the impurities in copper, using the oxide as a powder. The technique to be described uses less than 12 mg of sample and may be employed for concentrations between about 1.0 and 100 percent of the elements determined. It involves dilution of the sample in a known amount of specially purified nickel oxide and the determination of the silica, iron oxide, and alumina as impurities in the nickel oxide.

APPARATUS

The spectrograph used is a large Littrow prism-type instrument with quartz optics, giving a 700-mm spectrum between 2100A and 8000A. The spectrograph, arc stand, and various controls for safe and convenient operation of the installation have been described.[9]

The requirements for a source of power for obtaining satisfactory spectra of the nickel oxide mixtures are that it volatilize an amount of sample large enough to reduce sampling errors to a reasonable value, that the burning conditions in the arc be reproducible, and that the variables in the arc be easily controlled. The low rate of sample volatilization in the high voltage, low current spark made it necessary to find some other source that would give comparable reproducibility and burn more sample in a reasonable time. Attempts to use a 250-volt d.c. arc were not very successful, since the variations in the current of the low voltage d.c. arc could not be controlled sufficiently to permit its use in quantitative work without recourse to expensive and

* Presented at the Tenth Summer Conference on Spectroscopy and Its Applications held at the Massachusetts Institute of Technology, Cambridge, Massachusetts, July 20–22, 1942.

[1] Published by permission of the Director, Bureau of Mines, U. S. Department of the Interior, Washington, D. C.

[2] Former Assistant Physicist, Gas and Dust Section, Central Experiment Station, Bureau of Mines, Pittsburgh, Pennsylvania; present address: Mine Safety Appliances Company, Pittsburgh, Pennsylvania.

[3] Associate Physicist, Gas and Dust Section, Central Experiment Station, Bureau of Mines, Pittsburgh, Pennsylvania.

[4] Chief Chemist, Health Division, Bureau of Mines.

[5] Carlton E. Brown and H. H. Schrenk, "A technique for the use of the impinger method," Bureau of Mines Inf. Circ. 7026 (1938), 20 pp.

[6] E. C. Barnes and G. W. Penney, "An electrostatic dust weight sampler," J. Ind. Hyg. and Tox. **20**, 259–265 (1938).

[7] Morris Slavin, "Quantitative analysis based on spectral energy," Ind. Eng. Chem. Anal. Ed. **10**, 407–411 (1938).

[8] R. Breckpot, "Spectrographic determination of some secondary constituents in copper," Am. Soc. Sci. Bruxelles **B53**, 219–247 (1933), and other papers.

[9] H. I. Oshry, J. W. Ballard, and H. H. Schrenk, "Spectrochemical determination of lead, cadmium, and zinc in dusts, fumes, and ores," J. Opt. Soc. Am. **31**, 627–633 (1941).

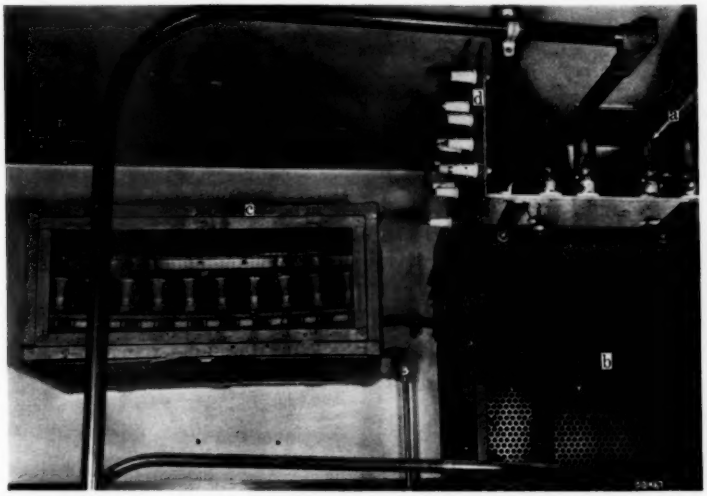

FIG. 1. Photograph of high voltage arc source.

elaborate control methods.[10] The high voltage a.c. arc[11] was tried and found to be considerably more reproducible than the low voltage d.c. arc.

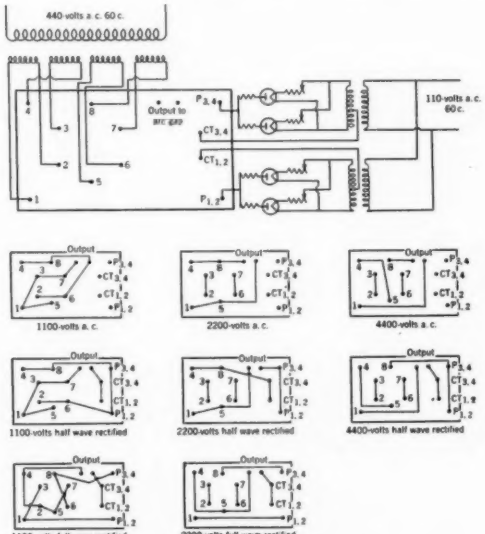

FIG. 2. Panel connections for high voltage arc source.

It was found, however, that it did not give results reproducible enough to warrant its adoption. The source finally adopted is a high voltage d.c. arc obtained by full-wave rectification of a 2200-volt a.c. arc. This supplies an interrupted arc with 120 ignitions per second. The rectifier unit (Fig. 1) uses four Type WL 872-A mercury-vapor rectifier tubes *a*, which have an inverse plate-voltage rating of 10,000 volts and a peak plate-current rating of 5.0 amperes, and will carry an average d.c. plate current of 1.25 ampere. The tubes are used in pairs and balanced in the circuit by the introduction of a 3-ohm resistor in series with the plate of each tube. The tubes and their filament transformers are mounted alongside the high voltage transformer *b*, on a platform near the ceiling. The current in the arc is limited by the resistance bank *c* of cone-type heaters.

The high voltage transformer is a 15-kva dry-type unit with a secondary consisting of four 1100-volt coils for an applied primary voltage of 440 volts. The secondary coils may be connected so that 1100, 2200, or 4400 volts are available at the full capacity of the transformer. Connections from the secondary coils of the high voltage transformer, the rectifier-tube plates, the center taps of the rectifier-tube filament transformers, and the arc gap are brought to porcelain-insu-

[10] C. G. Suits, "Measurement of some arc characteristics at 1000 atmospheres pressure," J. App. Phys. **10**, 203–206 (1939).

[11] O. S. Duffendack and K. B. Thompson, "Developments in the quantitative analysis of solutions by spectrographic means," Proc. A. S. T. M. **36**, part 2, 301–309 (1936).

lated jack plugs mounted on a transite panel (*d*, Fig. 1).

Figure 2 shows the circuit diagram of the high voltage arc source and the number of power supplies that may be applied to the arc gap by changing connections on the panel. Current in the circuit for the a.c. arc is limited by the capacity of the transformer to 13.6 amperes at 1100 volts, 6.8 amperes at 2200 volts, and 3.4 amperes at 4400 volts. For the d.c. arc at 1100 or 2200 volts, half- or full-wave rectified, the current is limited by the capacity of the rectifier to 5.0 amperes. The half-wave rectified 4400-volt arc is limited by the capacity of the transformer to 3.4 amperes.

Since the rectifier tubes require a preheating period before voltage is applied to the plates, a time-delay relay has been incorporated into the control circuit for the arc. Figure 3 shows the 110-volt, 60-cycle control circuit that actuates the contactor in the 440-volt, 60-cycle circuit of the high voltage transformer primary and supplies the primaries of the rectifier-tube filament transformers. The manual control switch for changing over from d.c. to a.c. operation is mounted near the high voltage panel. The use of the d.c. power supply described gives a stable arc whose current can be maintained within less than 0.03 ampere of a predetermined value.

To obtain current density high enough to volatilize the samples in a reasonable time without exceeding the capacity of the rectifier circuit, electrodes are used similar to those described by Strock.[12] These electrodes are cut from 4.75-mm ($\frac{3}{16}$-inch) high purity graphite rods supplied by the Dow Chemical Company. A tool, made in three parts, shown in Fig. 4, is used to shape and bore the electrodes in a single operation. The

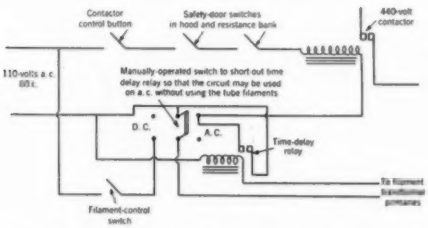
Contactor control button
Safety-door switches in hood and resistance bank
440-volt contactor
110-volts a.c. 60 c.
Manually-operated switch to short out time delay relay so that the circuit may be used on a.c. without using the tube filaments
D.C.
A.C.
Time-delay relay
To filament transformer primaries
Filament-control switch

FIG. 3. Control circuit for high voltage arc source.

[12] L. W. Strock, *Spectrum Analysis with the Carbon Arc Cathode Layer* (A. Hilger, Ltd., London, 1936), 54 pp.

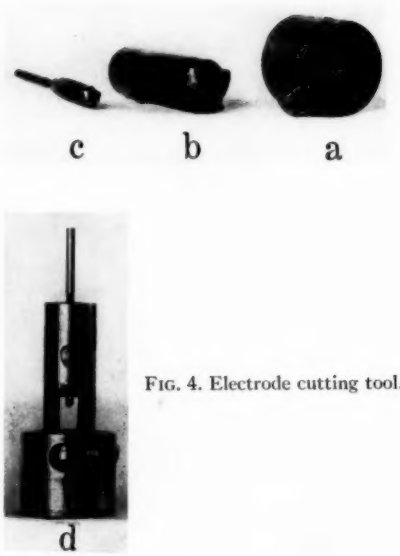

FIG. 4. Electrode cutting tool.

part *a* is a guide that supports the electrode while it is being cut; the part *b* is the shaper that reduces the diameter of the electrode from 4.75 mm to 3.20 mm; the part *c* is the boring cutter that drills a 1.30-mm diameter hole in the electrode to a depth of 1.5 mm and faces off the end of the electrode at right angles to its length; the assembled tool is shown in *d*. Figure 5 shows a section of a completed electrode used to hold a sample.

The upper electrode is 4.75 mm in diameter, with a flat end faced off perpendicular to its length by a tool similar to the one described. Experiments showed that results are influenced by the shape of the upper electrode; the flat shape was chosen because it was most easily and accurately reproducible. The tools mount in a sleeve that fits over the shaft of a small electric motor. The cuttings from electrode preparation are collected and separated into size fractions to get the pure graphite powder used in preparing samples. With a tool such as that described, as many as 15 electrodes may be prepared in a minute. Since it has been found necessary to keep the size and shape of the electrodes the same to obtain consistent analytical results, some device such as the one described should be employed to prepare electrodes.

The densitometer used to measure the spectra

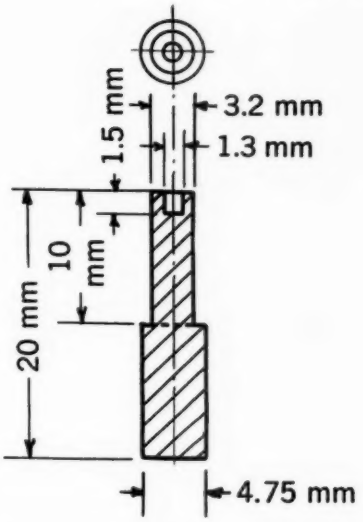

FIG. 5. Section of electrode used to hold sample.

is a projection-type instrument which has been described.[13] The optical system has been modified by the introduction of an additional slit to cut down the effect of scattered light.

PREPARATION OF SAMPLES

The samples of mineral powder or air-borne dust are prepared for analysis by mixing them into a matrix of nickel oxide and graphite powder. The nickel oxide serves as an internal standard and is present in such excess that it also acts as a spectroscopic buffer.[14] The graphite powder serves as a stabilizer in the arc, prevents spattering, and insures uniform burning of the sample. The graphite powder used is the fraction recovered from preparation of electrodes that passes through a 400-mesh sieve. Nickel was chosen as the base material for this study because its oxide has physical characteristics about the average of those for materials commonly found in mineral powders, it does not occur widely in nature as a major constituent of minerals, and its spectrum is complex enough to give a wide choice of comparison lines without too many interferences with the sensitive lines of other elements.

The nickel oxide was prepared[15] from cobalt-free nickel shot dissolved in hot, concentrated hydrochloric acid. The solution of nickel chloride in hydrochloric acid is treated with cupferron to precipitate the iron present, the solution filtered with suction to remove the cupferron precipitate and the carbon which had been present in the original shot, and the filtrate evaporated to dryness. The nickel chloride is converted to the nitrate by repeated boiling in concentrated nitric acid. The nitrate solution is evaporated to dryness, dissolved in distilled water, and filtered to remove the silica which was dehydrated. The filtrate is evaporated to dryness and the dry nickel nitrate converted to the oxide by heating in a muffle furnace. All the above operations are carried out in Pyrex vessels. The final product is a very finely divided powder containing less than 0.009 percent SiO_2, 0.008 percent Fe_2O_3, 0.008 percent Al_2O_3, and similar quantities of other impurities not of immediate interest. The structure of the nickel oxide checked by x-ray diffraction patterns was found to be essentially NiO.

The mixing of a sample with the matrix is accomplished in small ball mills, which were fabricated from nickel castings and will be

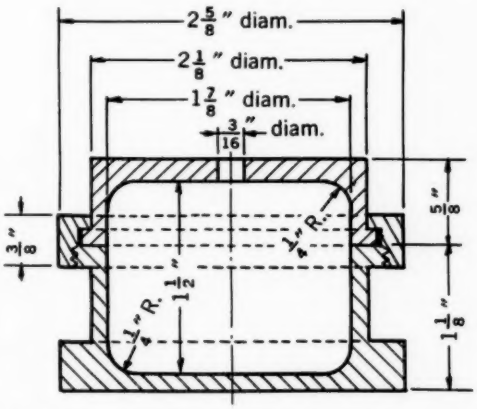

FIG. 6. Section of nickel mill used to mix sample.

[13] James W. Ballard, Howard I. Oshry, and H. H. Schrenk, "Some photometric instruments used in x-ray diffraction and spectrographic methods of analysis," Bureau of Mines Report of Investigations 3638 (1942), 13 pp.

[14] G. O. Langstroth, and D. R. McRae, "Transport of materials in sources for spectroscopic analysis," Can. J. Research **A16**, 61–74 (1938).

[15] The purified nickel oxide was prepared by H. A. Watson and R. L. Beatty, Assistant Chemists, Gas and Dust Section, Bureau of Mines.

described in a subsequent paper on sampling, mixing, and grinding. Figure 6 shows a sectional drawing of one of the mills. Nickel is used for the mills to reduce contamination of the sample during the mixing process. Any material ground off the mills in the course of mixing is principally nickel, and the addition of a small quantity to the gram of nickel oxide added to the sample as internal standard and buffer has little effect on the result of the analysis. Chemically pure nickel shot between 3 and 5 mm in diameter is used in the mills to mix the sample. The design of the mills eliminates sharp corners difficult to clean and makes possible a liquid-tight seal without the use of gaskets. A hole in the top of the mill permits evaporation of the liquid used as a dispersing agent during the mixing period.

In preparing a sample, 70 grams of the nickel shot is put in a clean mill, and 1 gram of the nickel oxide is weighed and transferred to the mill with ½ gram of the graphite powder. A weighed portion of sample, usually between 8 and 12 mg (less material may be used), is added along with 10 ml of reagent-grade methanol, introduced to act as dispersing agent during the mixing process. The flange of the bottom section of the mill is coated with a thin film of petrolatum, the top is put on, and the mill is sealed by screwing on the ring that holds the top and bottom sections together. The mill is placed on motor-driven rollers with heating coils mounted below the mill. The rollers are started, and the heater is turned on; in 35 to 40 minutes the sample is mixed and the methanol completely evaporated. The mill is removed from the rollers, allowed to cool, and opened, and the contents removed with the aid of a rubber policeman. The sample is separated from the nickel shot by screening through a 12-mesh stainless steel screen onto a piece of glazed paper. The sample is stored in a small vial until it is to be analyzed.

The electrodes are filled with the prepared samples by pouring a portion of sample onto a piece of glazed paper, pressing the electrode into the powder, and packing the powder into the electrode with a steel rod of the same diameter as the hole in the electrode. This operation is repeated until the hole in the electrode has been completely filled. The quantity of sample packed into the electrode in this manner is rather uniform so that the intensity of the nickel lines in the spectrum of a sample is nearly the same in several exposures. This facilitates the density measurements.

The mixture of sample and matrix introduced into an electrode for an exposure weighs about 10 mg; but only about 0.08 mg of this mixture is the original sample. The mixing technique described above mixes the sample into the matrix homogeneously enough so that the 0.08-mg portion is representative of the amount introduced into the mill if the particle size of the sample is small enough so that an appreciable number of sample particles are present in the 0.08 mg, and the probability of the presence of an excess of some single constituent of the sample is small. Experiments showed that uniform mixing is not obtained until the samples are reduced to pass through a 400-mesh screen. For samples reduced to this size, there are several thousand particles in the 0.08-mg portion burned in the arc.

The amount of sample added to the nickel oxide is relatively small, so that no effect on the intensity of the lines of one element due to the presence of another element has been found. This has made it possible to analyze samples of widely varying composition with consistent results.

PREPARATION OF THE SPECTROGRAMS

The prepared electrodes are placed in the holders in the arc stand. The lower one contains the sample and is at a positive potential with respect to the other. The electrodes are aligned on the optic axis, and the separation between them is fixed at 1.25 mm, using a source-aligning system previously described.[16] The spectrograph shutter is opened, the arc turned on, an exposure made through a 0.050-mm slit with a step sector rotating before the slit at about 2250 r.p.m., and the arc focused on the collimating lens. The exposure is continued until the sample is completely burned—between 95 and 105 seconds. The end of the exposure is indicated by the disappearance of the characteristic green color of the arc due to nickel and by the sudden rise in the temperature of the lower electrode. The arc current is maintained at 4.5 amperes and the

[16] See footnote 9, p. 3.

TABLE I. Line pairs used for analysis.

Unknown		Internal standard	
Element	Wave-length, angstroms	Element	Wave-length, angstroms
Silicon	2516.12	Nickel	2540.02
Iron	2522.85	Nickel	2540.02
Aluminum	3082.16	Nickel	2540.02

electrode separation at 1.25 mm during the entire exposure, using the controls previously described. Eastman Type 103-0 plates are used to obtain high sensitivity. The plates are developed in Eastman D-19 developer in a thermostatically controlled constant temperature tank. After processing, the plates are dried in a blast of warm air.

PLATE MEASUREMENT

Table I shows the line pairs used for analysis. The same nickel line is used as a comparison standard for the determination of all three elements. Although the aluminum line used is considerably separated from the nickel line, it was found that the results obtained using this line pair were just as reproducible from plate to plate and over long periods of time as the results obtained using a nickel line close to the aluminum line. This indicates that the plate response remains relatively the same within the wave-length range employed, which accords with the findings of Pierce and Nachtrieb.[17]

The method of plate measurement, using a step sector and restricting measurements to densities less than 0.5, has been described.[18] This method has been found to give intensity ratios relatively independent of the magnitude of the Schwarzchild-Villiger effect, provided the amount of scattering is not changed by disturbing the densitometer adjustments during the course of a set of measurements. If a single spectrum is measured first with one amount of scattered light and then with a different amount, the magnitude of the galvanometer deflections for the two sets of measurements may differ appreciably; but there is no significant change in the value of the intensity ratio computed from these deflections. Corrections for background were found necessary for all three elements and gave consistent results. The background is measured in a step of the spectrum where it is dense enough for reliable measurement. The actual correction for other steps is obtained using the exposure ratios of the step sector.

DEVELOPMENT OF METHOD

In preliminary studies to determine which of the available power supplies would give the most satisfactory results, both the half- and full-wave rectified arcs were studied. It was found that the half-wave rectified source allowed too great an interval to elapse between ignitions of the arc so that the sample cooled excessively and the rate of volatilization was decreased below a useful value. Therefore, the full-wave rectified arc was used in all further studies. It was found also that the intensity ratio between a line due to one of the unknowns and a nickel line was affected by changes in the electrode separation and the arc current in the high voltage d.c. arc, as has been reported previously for the high voltage a.c. arc.[19,20] Investigation disclosed that factors other than the arc current and the electrode separation were affecting the reproducibility of the method. Observation of the arc during an exposure showed that the nickel oxide alone showed some tendency to burn irregularly, spattering parts of the sample out of the arc. Graphite powder was added to the nickel oxide in varying proportions in an attempt to eliminate the irregularity in the arc. It was found that the addition of the graphite had a stabilizing effect, but that the background on the plate was increased. The minimum background for a satisfactorily stable arc was obtained by mixing $\frac{1}{2}$ gram of the graphite powder with 1 gram of the nickel oxide.

Observation of the electrodes after they had been used in the arc disclosed that the sample tended to condense on the upper electrode where part of it was revolatilized and re-excited during the course of the exposure. Comparison of the appearance of the electrodes with the results obtained from samples burned in the electrodes

[17] W. C. Pierce, and N. H. Nachtrieb, "Photometry in spectrochemical analysis," Ind. Eng. Chem. Anal. Ed. **13**, 774–781 (1941).

[18] See footnote 9, p. 3.

[19] O. S. Duffendack, and R. A. Wolfe, "Analysis of caustic liquors for traces of impurities," Ind. Eng. Chem. Anal. Ed. **10**, 161–164 (1938).

[20] See footnote 9, p. 3.

showed a correlation between the amount of sample remaining on the electrodes and the intensity ratios. In an attempt to prevent condensation of the sample on the electrodes, experiments were performed varying the flow of air across the arc. It was found that the velocity of the air stream has a marked effect on the reproducibility of the results as well as on the absolute values of the intensity ratios. The most satisfactory results were obtained with an air velocity just below that which would make the arc unstable and tend to extinguish it. For an electrode separation of 1.25 mm and an arc current of 4.5 amperes, it was found that an air stream moving across the arc at about 500 f.p.m. gave the most satisfactory results.

The precision of the method was tested under the exposure conditions found to give optimum reproducibility. A series of 30 exposures was made, using portions of the same sample mixture. Intensity measurements were made, and the relative intensities were computed for silicon, iron, and aluminum with respect to nickel. The probable error of a single observation was found to be 4.6 percent for the silicon ratio, 3.1 percent for the iron ratio, and 4.7 percent for the aluminum ratio. These errors are due to mixing, variations in the arc, photographic materials, and photometric procedure. To reduce them in the report of an analysis the average of the results of five separate spectra is used to determine the concentration of an element in a sample.

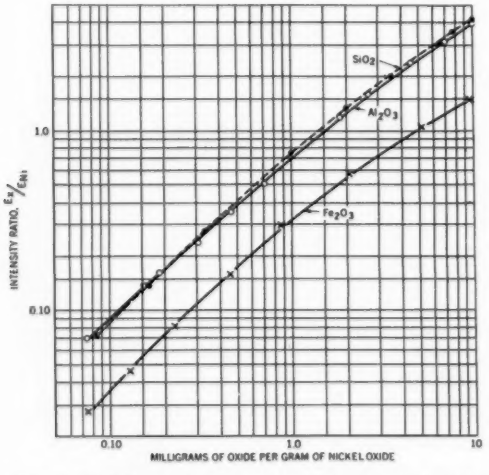

FIG. 7. Relation between relative intensity and oxide content per gram of nickel oxide.

PREPARATION OF ANALYTICAL CURVES

Figure 7 shows the analytical curves prepared from samples containing weighed amounts of test materials. The curves are plotted showing relative intensity against weight of element as oxide in 1 gram of nickel oxide; this simplifies the computations required to determine the percent of the test materials in the sample.

Corrections are made for the residual impurities in the nickel oxide[21] and for impurities introduced by the mixing process. The sum of these contaminations remains the same for all samples from a single batch of nickel oxide when the standardized procedure is used for preparing samples. The extent of the contamination amounts to a correction of 0.085 mg of SiO_2, 0.075 mg of Fe_2O_3, and 0.075 mg of Al_2O_3 in 1 gram of the nickel oxide used. The presence of the residual contamination in the nickel oxide determines the lower limit of the range over which analyses may be made. Use of more nearly pure nickel oxide extends the lower limit appreciably, since the contamination from the mixing process is only a small fraction of the total impurities. Although the sensitivity of the method extends below 0.05 mg of test material in 1 gram of nickel oxide (0.5 percent of a 10-mg sample), the accuracy of determination of such small amounts is limited by the fact that the correction due to the residual impurities is the same order of magnitude as the amount being determined. For example, a 5 percent error in the value read off the analytical curve may, after the correction is made, result in a considerably larger error in the actual amount of test material in a mineral sample containing about 0.1 mg of the material. A secondary factor restricting the lower limit is the background upon which the lines are superimposed. This is most important in the case of aluminum but is not significant in its effect on the lower limit as long as the correction for residual impurities is the order of magnitude described. The upper limit for the determinations is imposed by the change in slope of the working

[21] See footnote 19, p. 14.

TABLE II. Spectrographic analysis of National Bureau of Standards samples.

Bureau of Stand. No.	Nature of sample	SiO_2, percent Chem.	Spec.	Error, percent	Fe_2O_3, percent Chem.	Spec.	Error, percent	Al_2O_3, percent Chem.	Spec.	Error, percent
1a	Argillaceous limestone	14.1	14.7	+4.3	1.63	1.66	+ 1.8	4.16	4.11	− 1.2
26	Crescent iron ore	5.03	5.18	+3.0	83.8	81.8	− 2.4	1.02	1.03	+ 1.0
29	Magnetite iron ore	12.0	11.5	−4.2	79.7	73.1	− 8.3	1.91	1.82	− 4.7
69	Bauxite	6.32	6.15	−2.8	5.66	5.69	+ .5	55.1	58.4	+ 6.0
70	Feldspar	66.7	70.0	+5.1	.03	.07	——	18.0	18.2	+ 1.1
76	Burnt refractory	54.7	53.2	−2.7	2.38	2.24	− 5.9	37.7	39.2	+ 4.0
78	Burnt refractory	20.7	19.1	−7.7	.79	.94	+19.0	70.0	65.8	− 6.0
97	Flint clay	42.9	41.0	−4.4	.98	.93	−5.1	38.8	36.5	− 5.9
103	Chrome refractory	8.24	8.64	+4.9	16.0	15.9	− .6	20.8	20.1	− 3.4
104	Burned magnesite	2.54	2.69	+5.9	7.07	7.12	+ .7	.84	.99	+17.9
	Average error			4.5			4.9			5.1

TABLE III. Comparison between spectrographic and chemical analysis of coal ash and limestone.

Sample No.	SiO_2, percent Chem.	Spec.	Diff., percent	Fe_2O_3, percent Chem.	Spec.	Diff., percent	Al_2O_3, percent Chem.	Spec.	Diff., percent
1	33.8	32.9	−2.7	9.3	9.61	+ 3.2	35.2	37.3	+ 6.0
2	16.8	17.4	+3.6	24.7	23.9	− 3.2	9.0	7.48	−16.7
3	53.4	51.2	−4.1	4.4	4.54	+ 2.3	35.7	35.4	− .8
4	2.1	2.32	+9.5	.5	.21[1]	−60.0	.80	.83	+ 3.8
5	55.7	56.0	− .5	1.9	1.97	+ 5.0	28.7	29.7	+ 3.5
		Averages	4.1			3.4[2]			6.2

[1] A second spectrographic analysis gave 0.24.
[2] Neglecting the value for sample No. 4.

curves which lowers the precision of determinations at the higher concentrations. For more precise determinations in the high range, a smaller amount of sample may be introduced into the mill.

RESULTS OF ANALYSES

To test the validity of the technique and to improve the precision of the analytical curves, a set of 10 standard mineral samples from the National Bureau of Standards was analyzed. Table II gives the results of these analyses. The average error in the determination of SiO_2 in these samples is 4.5 percent of the amount present; for Fe_2O_3, 4.9 percent; and for Al_2O_3, 5.1 percent.

Table III gives the results of analyses of five samples of coal ash and limestone which had been analyzed chemically.[22] The average difference between the spectrographic and the chemical analyses for the five samples is 4.1 percent of the amount present for SiO_2, 3.4 percent for Fe_2O_3, and 6.2 percent for Al_2O_3. As a further test of the accuracy of the technique, six synthetic samples were made up by mixing various portions of the Bureau of Standards standard samples. The composition of these samples was unknown to the analyst. Table IV shows the results of the analyses of the synthetic samples. The average errors for these six samples are 5.9 percent, 5.8 percent, and 6.9 percent for silica, iron oxide, and alumina, respectively. If the range of the method is restricted to determinations greater than 1 percent, the average error for all the samples is as follows:

	Percent
Silica	4.8
Iron oxide	3.7
Alumina	5.4

DISCUSSION AND SUMMARY

A method has been described for the spectrographic determination of silica, iron oxide, and alumina in mineral powders. The technique has been tested with analyzed samples of minerals

[22] These samples were analyzed in the Analytical Laboratory of the Central Experiment Station of the Bureau of Mines under the supervision of Mr. W. A. Selvig, Supervising Chemist, Coal Constitution and Miscellaneous Analysis Section.

TABLE IV. Spectrographic analysis of synthetic samples.

Sample No.	SiO_2, percent Added	Found	Error, percent	Fe_2O_3, percent Added	Found	Error, percent	Al_2O_3, percent Added	Found	Error, percent
1	5.50	5.41	− 1.6	11.7	11.5	− 1.7	11.2	12.1	+ 8.0
2	22.5	20.8	− 7.5	4.06	3.50	−13.8	19.6	20.9	+ 6.6
3	10.1	9.94	− 1.6	38.2	37.2	− 2.6	2.76	2.48	−10.0
4	57.2	48.7	−14.9	.42	.46	+ 9.5	26.4	29.9	+13.2
5	7.68	7.46	− 2.9	23.4	22.0	− 6.0	42.4	42.1	− .7
6	34.1	31.9	− 6.5	19.9	19.6	− 1.5	30.2	31.1	− 3.0
		Averages	5.9			5.8			6.9

and refractory materials and is being used for determining the composition of atmospheric contamination. It is being extended to include the determination of other important elements. The sample required is less than 12 mg and may be of the order of 1 mg. The average accuracy of the method in the range between 1.0 and 100 percent has been found to be about 5 percent of the amount present for all three components.

The samples are mixed with a large excess of nickel oxide, which acts both as an internal standard and as a spectroscopic buffer. Graphite powder is added to the samples to increase the uniformity of burning in the arc and to prevent spattering of the sample during an exposure. A stream of air passing across the arc during an exposure carries away the volatilized material and prevents its condensation on the electrodes. A method of mixing is described which gives a homogeneous combination of the sample, nickel oxide, and graphite without the introduction of excessive contamination. The technique described makes it possible to analyze powder samples of widely different composition without finding appreciable effect on the determination of one element due to the presence of another.

The source of power which is used, a full-wave rectified 2200-volt arc, has been found eminently suitable for the complete volatilization of mineral samples and should have further application in the analysis of refractory materials. The rectifier circuit is simple and inexpensive, and provides a variety of power supplies for the arc. The 2200-volt d.c. circuit gives an arc in which the current can be controlled to within 0.03 ampere.

The technique described will give consistent results, but over a period of time it has been found that unexplained shifts of the analytical curves may occur. This shift had been reported previously for other methods.[23,24] The analytical curves should therefore be checked from time to time with samples of known composition.

The required time for an analysis of the three components of a sample is about 1½ hours for one analyst when several samples are run consecutively. The determination of other constituents does not increase the time appreciably, since the time used in measuring the spectrograms and computing the results is a small fraction of the total time involved. The time for an analysis is decreased by more than a factor of 2 if the work is divided between two analysts.

[23] J. T. Mereles Malpica, "Quantitative spectrographic analyses," G. E. Rev. **43**, 288–297 (1940).

[24] Talk by H. V. Churchill, Aluminum Company of America, reported in *Crucible*, (Feb. 1942), pp. 40–41.

Quantitative Spectroscopy Applied to Some Impurities in 70–30 Cupro-Nickel*

WALTER D. FRANCE
Scovill Manufacturing Company, Waterbury, Connecticut
(Received July 25, 1942)

DUE to the present emergency, the increased production of ships has made it necessary to speed up, in every way possible, the manufacture of copper-alloy seamless condenser tubes. These tubes are used in surface condensers, evaporators, and heat exchangers. One of the alloys used in their manufacture is 70–30 Cupro-Nickel, designated under A.S.T.M. B111-40T as requiring the chemical analysis given in Table I.

TABLE I.

Alloy	Cu %	Sn %	Ni %	Pb %	Fe %	Zn %	Mn %
70–30 Cupro-Ni.	Remainder	1.50 max.	29.0 to 33.0	0.05 max.	0.5 max.	1.0 max.	1.0 max.

Of the minor elements, determination of zinc, lead, and iron considerably lengthens a chemical analysis. The percentages of these elements fall within the range best suited for spectrographic procedures and a great deal of work has been done in certain laboratories developing various methods for such an analysis, but nothing definite has yet been published. The purpose of this report is to present one such method that will give reproducible results economically and accurately. The method described below was developed to handle as many as one hundred samples of cupro-nickel a day.

APPARATUS

The spectrograph used in the investigation was a Bausch and Lomb large Littrow type having a dispersion in the range used of about 2.5A per mm. The slit width used in the work was 0.02 mm and the Hartsman diaphragm was set to give spectral lines of 1.4 mm. The optical bench of the spectrograph was equipped with a quartz spherical condensing lens and a rotating sector run by a universal motor at 1800 r.p.m. All density readings were made on an Adam Hilger microphotometer using a storage battery connected to a General Electric Tungar trickle charger for illumination of the bulb. The xyonolite slide on the microphotometer was set at 10 mm and the slit before the photo-cell at 0.06 mm.

Throughout the work, Eastman No. 33 plates were used and were developed in Eastman D-11 developer. The darkroom was equipped with a Dietert developing machine, thermostatically controlled to keep the solutions at 70°F, a plate washer, and a plate dryer. Developing, fixing, and washing times were accurately controlled in order to keep the plates as uniform as possible.

ELECTRODES AND SAMPLE

Type of electrode and excitation is somewhat dependent on the kind of sample that is supplied for an analysis. For example, an analysis of condenser tubes is run from milled samples taken from every lot of 600 tubes. Sometimes other prefabricated or mill samples are in the form of drillings or thin sheet. To accommodate the various sizes and shapes of samples, it seemed best to use the carbon arc electrode, similar to that reported by Smith,[1] Hitchen,[2] and Milbourn.[3]

The positive and lower electrodes were made from $\frac{1}{4}''$ carbon rods sold by the National Carbon Company. With a specially designed lathe tool a 0.225″ diameter hole was drilled to a depth of 0.150″, thereby leaving a thin side wall. It is very important to have the hole drilled in the center of the carbon to give uniform side walls. Uneven side walls burn down non-uniformly and cause erratic results. The upper negative electrodes were made by pointing $\frac{1}{8}''$ carbons in a pencil sharpener.

To facilitate putting drillings, etc., in the small carbon cups, all samples were weighed and then briquetted into a pellet 0.210″ in diameter. The pilling operation was done by hand with a punch and die. It was found that much more

* Presented at the Tenth Summer Conference on Spectroscopy and Its Applications, held at the Massachusetts Institute of Technology, Cambridge, Massachusetts, July 20–22, 1942.

[1] D. M. Smith, J. Inst. Metals **55**, 119 (1935).
[2] C. S. Hitchen, Am. Inst. Min. Met. Eng. Tech., p. 494 (1933).
[3] M. Milbourn, J. Inst. Metals **55**, 403 (1934).

TABLE II. Plate 2333B. Iron determination.

Conc.	0.06	0.09	0.11	0.15	0.22	0.32	0.44	0.50
Fe 2966.9	32.0	29.5	20.8	17.4	12.5	7.8	13.4	9.7
Fe 2966.9	30.9	28.5	19.5	13.5	15.0	9.8	11.0	8.3
Fe 2966.9	28.8	30.8	14.5	13.7	15.8	9.4	10.7	9.5
Ni 2865.5	11.5	13.0	10.0	10.7	10.1	7.7	15.7	12.2
Ni 2865.5	10.0	12.4	8.9	9.7	11.7	10.5	14.5	10.7
Ni 2865.5	9.6	12.5	7.0	8.5	12.0	8.7	13.2	13.4
Fe 2966.9	2.78	2.27	2.08	1.63	1.24	1.01	0.86	0.80
Ni 2865.5	3.09	2.30	2.19	1.55	1.28	0.93	0.76	0.78
	3.00	2.46	2.08	1.62	1.32	1.08	0.81	0.71
Fe 2788.1						19.4	30.8	21.8
Fe 2788.1						26.2	28.0	18.6
Fe 2788.1						22.3	25.7	22.0
Ni 2865.5						7.7	15.7	12.2
Ni 2865.5						10.5	14.5	10.7
Ni 2865.5						8.7	13.2	13.4
Fe 2788.1						2.52	1.96	1.79
Ni 2865.5						2.50	1.93	1.74
						2.56	1.95	1.64

TABLE III. Lead determination.

Conc.	0.03	0.06	0.07	0.12
Pb 2873.3	24.0	9.5	8.4	7.4
Pb 2873.3	22.6	11.0	6.0	6.3
Pb 2873.3	24.0	12.0	9.0	7.0
Cu 2768.9	21.6	20.0	20.5	21.2
Cu 2768.9	19.8	20.4	15.0	20.2
Cu 2768.9	22.8	21.8	19.2	21.7
Pb/Cu	1.11	0.48	0.41	0.35
	1.14	0.54	0.40	0.31
	1.05	0.55	0.47	0.32

TABLE IV. Plate 2334B. Zinc determination.

Conc.	0.70	0.93	1.13	1.37	1.75
Zn 2756.5	13.2	9.7	14.3	14.2	9.5
Zn 2756.5	14.2	15.2	14.0	8.0	7.0
Zn 2756.5	14.3	18.0	12.8	11.8	8.8
Cu 2768.9	12.0	11.5	22.6	26.5	21.6
Cu 2768.9	13.0	20.8	20.0	16.3	19.8
Cu 2768.9	13.7	21.5	20.3	23.2	22.8
Zn/Cu	1.10	0.85	0.64	0.54	0.44
	1.09	0.73	0.70	0.49	0.35
	1.04	0.84	0.63	0.51	0.39

reproducible results were obtained by having all the samples the same size, since this made the distance from the top of the electrode wall to the sample the same, thereby causing fusion of the pellet to start at the same time for every sample. In another work[4] it was found that the mass of sample was important since mechanical losses were almost constant for similarly weighed samples. The weight of sample that gave best results for Cupro-Nickel pellets in the above described carbons was 200 mg weighed within ± 10 mg.

EXCITATION

A 220-v d.c. arc excitation system having a variable resistance supplied a current from 2.5 to 10 amperes. Arc excitation is used universally in most of the spectrographic laboratories because of its high degree of sensitivity compared to spark excitation. The general criticism of arc excitation is its lack of reproducibility. However, for the analysis of Cupro-Nickel which burns very quietly in the arc the reproducibility of the spectra is good. It is important in quantitative work, however, with this type of excitation to strike the arc with an external carbon rod, instead of by drawing the electrodes together. Since the top electrode is a point, the latter method makes a hot spot on the sample which melts instantly and produces an erratic spectrum compared to one that was produced by the former method of striking the arc.

A current of 10 amperes was used for this work since it gave a more steady arc than with a lower current. Furthermore, by using a high amperage a hotter arc was produced and therefore the exposure time could be held at a minimum. To carry off the dense fumes produced by such an excitation an exhaust system was used.

SLIT ILLUMINATION

A quartz spherical lens was adjusted on the optical bench so that an image of the arc is formed on the quartz window before the slit. With the lens used the magnification of the arc on the slit is $3\frac{1}{2}$ times. An investigation of the variation of electrode spacings of $\frac{1}{8}''$, $\frac{1}{4}''$, and $\frac{3}{8}''$ showed that the effect of electrode spacing was negligible but was another variable that could be easily controlled. An electrode spacing of $\frac{1}{4}''$ was used and was held as constant as possible by continual adjustment of the electrodes during the exposure. The $\frac{1}{4}''$ spacing gave an image of $\frac{7}{8}''$. Only a small fraction of the central part of the

[4] W. E. Milligan and W. D. France, Ind. Eng. Chem. Anal. Ed. **13** (1941).

image was photographed since the Hartman diaphragm was set to produce spectra 1.4 mm high.

EXPOSURE

Since it was desired to develop a spectrographic procedure for the simultaneous quantitative analysis of three elements—namely zinc, iron, and lead—care had to be taken to obtain exposures that would produce usable spectral lines of each element. The conditions of electrodes and sample, excitation, and slit illumination described above were designed to give reproducible spectra in a minimum total time of 30-seconds exposure. Actual exposure time was arrived at by a study of the density of the spectral lines of the elements in question. From a series of 30-second exposures it was found that with the rotating sector set at $\frac{1}{2}$, thereby making an actual exposure of 7.5 seconds, the density of the line pairs listed below were within the straight line portion of the blackening curve:

Cone	Line Pairs
0.01–0.08	Pb 2873.316/Cu 2768.878
Max. 1.20	Zn 2756.452/Cu 2768.878
Max. 0.69	Zn 2770.984/Cu 2768.878
Max. 0.25	Fe 2966.900/Ni 2865.502
Max. 0.60	Fe 2788.105/Ni 2865.502

Not only did the line pairs conform to the requirements of density but also registered a suitable charge in density for changes in concentration.

The rotating sector has a twofold purpose. Its use constitutes good sampling of the exposure and makes it possible to maintain a constant total exposure time by changing the setting of the sector openings. The latter variable is very important since the plates used varied somewhat

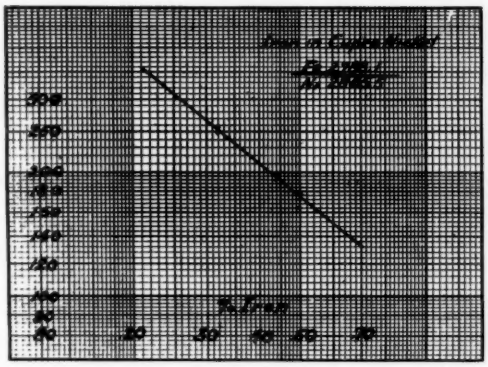

Fig. 2.

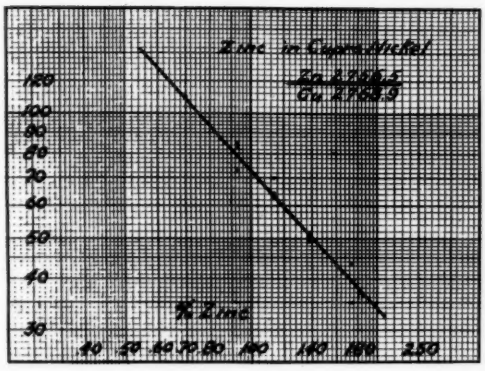

Fig. 3.

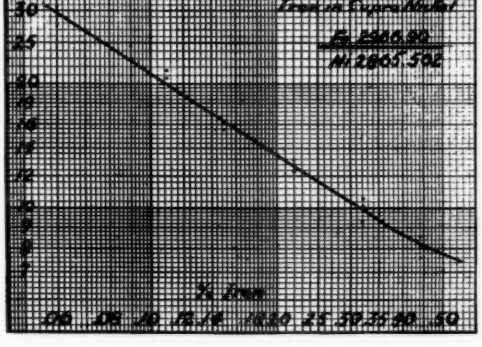

Fig. 1.

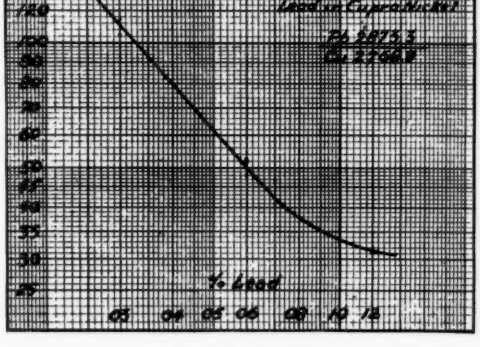

Fig. 4.

TABLE V. Plate 2423B. Percent iron.

Observation	% Iron	Dev.	Observation	% Iron	Dev.
0.10	0.11	0.01	0.14	0.11	0.03
.10	.11	.01	.11	.11	.00
.12	.11	.01	.10	.11	.01
.12	.11	.01	.10	.11	.01
.11	.11	.00	.11	.11	.00
.10	.11	.01	.10	.11	.01
.12	.11	.01	.16	.11	.05
.14	.11	.03	.12	.11	.01
.12	.11	.01	.10	.11	.01
.11	.11	.00	.11	.11	.00

$$\text{p.e.} = 0.6745\left(\frac{\Sigma D^2}{N-1}\right)^{\frac{1}{2}}$$
$$= 0.011 = 10 \text{ percent.}$$
$$\text{P.E.} = 0.6745\left[\frac{\Sigma D^2}{N(N-1)}\right]^{\frac{1}{2}}$$
$$= 0.0025 = 2.3 \text{ percent.}$$

in sensitivity from one batch to the next. As an example of this, some boxes of plates require that the rotating sector be set at $\frac{3}{4}$ in order to obtain the proper density of lines.

PHOTOGRAPHIC PROCESSING

All plates were developed for four minutes in Eastman D-11 solution at a temperature of 70°F, which was controlled by the thermostat on the Dietert Developing machine. Before this machine was obtained ice baths were used to keep the temperature of the solutions constant, but since such practice was difficult to control, the plates varied measurably in contrast. Our experience has shown that temperature control of the solutions is a major factor in obtaining reproducible results. The volume of developer used in the machine was 500 cc, and only five plates were processed in one batch, which constituted a day's work. The partially used developer was saved for work other than spectrographic.

An alternative developer which gives just as good contrast as D-11 is the DK-50. With this developer a volumetric replenisher is used which helps to keep the relative proportion of the developers close to that of a fresh solution.

The suspected effect of the wave motion due to the rocking of the machine was investigated. It was noticed that the plates developed by the machine were just as uniform as those developed in trays and agitated by a camel hair brush. These remarks although only qualitative are the interpretation of our experimental results.

RESULTS

All final photometer readings were made on the Hilger microphotometer. Before making readings the instrument was set to give a clear plate reading of 50. This reading on a routine plate might vary as much as 0.5 cm. Tables II–IV show the results of a test plate that was run for the purpose of testing this method. Galvanometer deflections and ratios of deflections of the working and internal standard spectral lines are given in the tables. All of the deflections were made with a clear plate reading of 50.0 cm. With these data any method of plotting the results may be used. No mention was made of background because with the short exposures it was negligible.

The data were given in triplicate so that an idea of the reproducibility could be seen from the tables and the following curves. All the curves were plotted on log-log paper using the concentration and ratio values (see Figs. 1–4). All of the values given were obtained from standard samples that were run just as a routine plate. The values obtained fell either side of the ideal working curves.

For routine work 36 samples and 8 standard samples are put on each plate taken. In this way every plate is actually calibrated by means of the known standards. Since the standards represent the limits of concentration, a rough working curve could be drawn for each plate; however by keeping all variables as constant as possible the use of the standards to check the working curves, as shown in the diagrams, is sufficient. Sometimes the curves have to be shifted to compensate for plate sensitivity or developing conditions.

In using the calculating board the concentra-

TABLE VI. Plate 2423B. Percent lead.

Observation	% Lead	Dev.	Observation	% Lead	Dev.
0.05	0.06	0.01	0.04	0.06	0.02
.07	.06	.01	.06	.06	.00
.06	.06	.00	.05	.06	.01
.04	.06	.02	.04	.06	.02
.05	.06	.01	.05	.06	.01
.05	.06	.01	.09	.06	.03
.04	.06	.02	.06	.06	.00
.04	.06	.02	.06	.06	.00
.05	.06	.01	.07	.06	.01
.04	.06	.02	.05	.06	.01

p.e. = 0.0095 = 16 percent.
P.E. = 0.0021 = 3.5 percent.

tion *vs.* ratio curve is made as directed by the Dietert Company. For calibrating the plates the galvanometer readings from the iron standards are used. According to our hypothesis a series of concentrations of iron should give an iron spectral line of stepped intensities. Using a blackening curve drawn from a 1 : 1.5 stepped sector as a basis for the zero setting of the horizontal scale and the ratio from the working curve for the particular concentration, a blackening curve for each plate was drawn from the galvanometer readings of the Fe 2966.900A and the Ni 2865.502A lines for each concentration of the iron standards. A line results which usually parallels or closely approximates the original blackening curve. Once the new curve is located, the concentrations of the unknown samples can be obtained from their galvanometer readings.

Two concentration *vs.* ratio curves were presented for the determination of iron since the iron line 2966.900A, the more sensitive line, gives more reproducible results for the lower concentrations, while the iron line 2788.105A gives better results for the high concentrations.

PRECISION OF THE METHOD

In order to determine the reproducibility of the method a series of twenty exposures was made on an analyzed sample of Cupro-Nickel containing 0.06 percent lead, 0.11 percent iron, and 1.11 percent zinc. By the method of least squares and the curve of probability[5] the probable error of a single observation (p.e.) and the probable error of the mean (P.E.) are shown for the determination of the three elements in Tables V–VII.

Although one might conclude from the precision data p.e. that the errors are large, actually they are acceptable for "go and no go" analysis since the impurities very seldom come within 50 percent of the maximum allowable concentration. When the concentration of iron, lead or zinc approaches their maximum specification, within their respective probable error, these samples are re-run chemically to make sure that no bad metal is released. By following this procedure an average of one or two samples a week have to be checked chemically.

If, however, chemical means are not available or there is doubt about an analysis of one sample it can be run 16–20 times on one plate thus securing a result whose precision is of the order of P.E. shown in Tables V–VII.

[5] H. M. Goodwin, *Precision of Measurements and Graphical Methods* (McGraw-Hill, Inc., 1920).

TABLE VII. Plate 2423B. Percent zinc.

Observation	% Zinc	Dev.	Observation	% Zinc	Dev.
1.24	1.11	0.13	0.99	1.11	0.12
0.90	1.11	.21	1.32	1.11	.21
1.00	1.11	.11	0.99	1.11	.12
1.13	1.11	.02	0.85	1.11	.26
1.04	1.11	.07	1.10	1.11	.01
1.20	1.11	.09	1.24	1.11	.13
1.04	1.11	.07	1.24	1.11	.13
1.04	1.11	.07	1.20	1.11	.09
1.13	1.11	.02	1.40	1.11	.29
1.13	1.11	.02	0.98	1.11	.13

p.e. =0.095 =8.6 percent.
P.E. =0.021 =1.9 percent.

ACKNOWLEDGMENTS

The author wishes to express his gratitude to W. B. Price and F. M. Barry for their interest in the work and to the Scovill Manufacturing Company for permission to publish it. Acknowledgment is due to R. K. Bailey and E. D. Wade also of the Scovill Manufacturing Company for their cooperation and assistance in making the various tests necessary for the preparation of the paper.

On Precision in Spectrochemical Analysis*

H. B. VINCENT AND R. A. SAWYER
University of Michigan, Ann Arbor, Michigan†

(Received August 24, 1942)

IN the examination of spectrochemical procedures with a view toward improving the precision of the analyses performed, the importance is apparent of segregating the uncertainties entailed in the various steps of the analytical process so that attention may be directed to those operations whose contributions to the total error are significant. Statistical methods for the division of deviations among several possible sources are not new, but it is thought that their use in spectrochemistry may be less extensive than might be recommended.

It is hoped that the present paper may assist in promoting interest in the use of statistical methods for the study and reporting of spectrochemical data.

Arguments may be advanced to show that probable errors may be expected to be strictly reproducible only if the aggregation of data is very large, and that, in consequence, statistical methods should never be applied to short series. These contentions may be less than cogent. It is true that some uncertainty in the magnitude of the deviations themselves results from a paucity of readings, but, since often short series only are available, it is thought that even if the treatment may lack the highest mathematical rigor, it may be accepted as applicable if it provides useful information.

In the demonstration of a proposed procedure for the segregation of spectrochemical errors, it has appeared suitable to choose for discussion certain data obtained in the examination of a NBS standard steel. Since these data were obtained with a discharge circuit other than that previously mentioned[1] by the authors, a description of operating conditions may be of interest.

Cylindrical electrodes of $\frac{7}{32}$ of an inch in diameter having conical ends of 148° included angle were opposed in axial alignment across a discharge gap of $\frac{5}{32}$ of an inch and subjected to the action of the circuit shown diagramatically in Fig. 1. This circuit has been under industrial test for several months, with gratifying results. In performing the analyses listed below, the following elements were used: T, a 25-kva oil-cooled transformer, power line to 33,000 volts r.m.s. adjusted by a primary resistor to produce a peak secondary voltage of 30,000 volts; C, a capacitance of 0.001 microfarad; R_1, a resistor of 1000 ohms; C, a capacitance of 0.011 microfarad; I, a synchronous interrupter; L, an inductance of about 50 microhenries, and G, the discharge gap mentioned above. An exposure time of 30 seconds for the recording of spectra followed a preexposure operation for 5 seconds.

Test electrodes were obtained from the following source. Under date of July 1, 1941, the National Bureau of Standards shipped to the Ford Motor Company one bar, 32 inches long by $1\frac{1}{2}$ inches diameter, of their standard sample 30C. This bar was drawn to rod of $\frac{7}{32}$-inch diameter; the rod was cut to six-inch lengths. Six lengths were selected at random and submitted to the University of Michigan for spectroscopic test.

The rods were numbered from 1 to 6, inclusive, and each rod was divided into three substantially equal portions. For rod 1, the surfaces adjoining one of the cuts provided the test location 11, the surfaces adjoining the other cut, the test location 12, while the original ends of the rod were opposed to provide electrodes for the test location

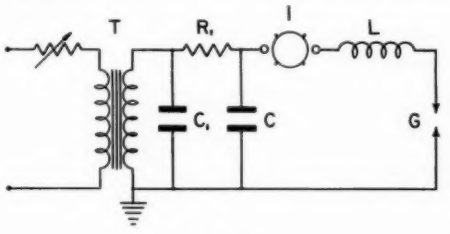

FIG. 1.

* Presented at the Tenth Summer Conference on Spectroscopy and its Applications held at the Massachusetts Institute of Technology, Cambridge, Massachusetts, July 20–22, 1942.

† The data presented in this paper are taken from work carried forward in the Department of Physics on a project sponsored through the Department of Engineering Research.

[1] H. B. Vincent and R. A. Sawyer, J. App. Phys. **8**, 163 (1937).

TABLE I. Computation of total uncertainty.

Test point	Percent chromium				Dev. $\times 10^2$				Dev.$^2 \times 10^6$			
	R_1	R_2	R_3	R_4	d_1	d_2	d_3	d_4	d_1^2	d_2^2	d_3^2	d_4^2
11	0.9777	0.975	0.985	0.970	0	2	8	7	0	4	64	49
12	0.988	0.974	0.982	0.972	11	3	5	5	121	9	25	25
13	0.975	0.977	0.987	0.975	2	9	10	2	4	0	100	4
21	0.975	0.977	0.977	0.981	2	0	0	4	4	0	0	16
22	0.967	0.975	0.966	0.967	10	2	11	10	100	4	121	100
23	0.971	0.980	0.979	0.975	6	3	2	2	36	9	4	4
31	0.979	0.975	0.984	0.985	2	2	7	8	4	4	49	64
32	0.967	0.980	0.979	0.979	10	3	2	2	100	9	4	4
33	0.972	0.995	0.962	0.970	5	18	15	7	25	324	225	49
31	0.974	0.980	0.977	0.970	3	3	0	7	9	9	0	49
42	0.987	0.975	0.980	0.983	10	2	3	6	100	4	9	36
43	0.977	0.967	0.982	0.969	0	10	5	8	0	100	25	64
51	0.971	0.967	0.969	0.983	6	10	8	6	36	100	64	36
52	0.987	0.967	0.975	0.973	10	10	2	4	100	100	4	16
53	0.967	0.977	0.972	0.981	10	0	5	4	100	0	25	16
61	0.994	0.982	0.987	0.986	17	5	10	9	289	25	100	81
62	0.984	0.972	0.977	0.975	7	5	0	2	49	25	0	4
63	0.962	0.980	0.977	0.983	5	3	0	6	25	9	0	36
									1102	735	819	653

13. Similar test locations were chosen for each of the other rods.

Using the spectral lines Cr 2822.01 and Fe 2811.27, four independent analyses were made at each test point, yielding the readings R_1, R_2, R_3, and R_4 of Table I. Readings R_1 for the test points 11 to 33, inclusive, were made on one photographic plate; readings R_1 for the test points 41 to 63, inclusive, were made on a second photographic plate. Analyses for R_2, R_3, and R_4 were arranged similarly.

An analytical curve for reduction of the log relative intensity values to percentage content was drawn from the average values obtained for the 72 readings for 30C steel and the average values for 16 readings, two on each photographic plate, for a sample of N.B.S. Standard 106 steel. The chromium contents were assumed to be those listed by the Bureau.

Computations show that the root mean square deviation from the average concentration of 0.977 percent Cr amounts to 0.69 percent of the content.

$$\sum d^2 = 0.003309,$$
$$\sigma_1 = (100/C)(\sum d^2/n)^{\frac{1}{2}}.$$

Where C is percentage concentration and n total number of readings

$$\sigma_1 = (100/0.977)(0.003309/72)^{\frac{1}{2}}$$
$$= 0.69 \text{ percent of content.}$$

The standard deviation σ_1 may be related to the probable error of a single determination, if the distribution can be shown to be Gaussian. In a short series of readings, such demonstrations are likely to be less than conclusive, but the comparison given in Table II indicates a reasonably close agreement, which is confirmed by the results published by Kaiser[2] on more extensive data. The values listed as observed were obtained by proportioning the number of errors falling in the interval which the stated deviation divides.

In the computation of σ_1, a uniform content of 0.977 percent Cr is assumed for each test point; the deviation includes, obviously, any error which may arise from non-uniformity of the sample. To segregate the error due to lack of

TABLE II. Distribution of errors.

Distribution	Number of observations	Number of errors exceeding $0.67\sigma_1$	σ_1	$\sqrt{2}\sigma_1$	$2\sigma_1$
Observed	72	35	22	10	3
Gaussian	72	36	23	11	3

[2] H. Kaiser, Zeits. f. tech. Physik **17**, 227 (1936).

TABLE III. Computation of analytical uncertainty.

Test point	Percent chromium				Average	Dev. $\times 10^2$				Dev.$^2 \times 10^4$			
	R_1	R_2	R_3	R_4	R	d_1	d_2	d_3	d_4	d_1^2	d_2^2	d_3^2	d_4^2
11	0.977	0.975	0.985	0.970	0.977	0	2	8	7	0	4	64	49
12	0.988	0.974	0.982	0.972	0.979	9	5	3	7	81	25	9	49
13	0.975	0.977	0.987	0.975	0.979	4	2	8	4	16	4	64	16
21	0.975	0.977	0.977	0.981	0.978	3	1	1	3	9	1	1	9
22	0.967	0.975	0.966	0.967	0.969	2	6	3	2	4	36	9	4
23	0.971	0.980	0.979	0.975	0.976	5	4	3	1	25	16	9	1
31	0.979	0.975	0.984	0.985	0.981	2	6	3	4	4	36	9	16
32	0.967	0.980	0.979	0.979	0.976	9	4	3	3	81	16	9	9
33	0.972	0.995	0.962	0.970	0.975	3	20	13	5	9	400	169	25
41	0.974	0.980	0.977	0.970	0.975	1	5	2	5	1	25	4	25
42	0.987	0.975	0.980	0.983	0.981	6	6	1	2	36	36	1	4
43	0.977	0.967	0.982	0.969	0.974	3	7	8	5	9	49	64	25
51	0.971	0.967	0.969	0.983	0.972	1	5	3	11	1	25	9	121
52	0.987	0.967	0.975	0.973	0.976	11	9	1	3	121	81	1	9
53	0.967	0.977	0.972	0.981	0.974	7	3	2	7	49	9	4	49
61	0.994	0.982	0.987	0.986	0.987	7	5	0	1	49	25	0	1
62	0.984	0.972	0.977	0.975	0.977	7	5	0	2	49	25	0	4
63	0.982	0.980	0.977	0.983	0.981	1	1	4	2	1	1	16	4
										545	814	442	420

homogeneity, σ_h, a standard deviation σ_2 may be computed about the mean observed content for each test point, as shown in Table III. Since $\bar{R}$ is not an established value, but is subject, rather, to the uncertainty of the readings from which it derives, division by the factor $n-1$ is indicated.

$$\sum d^2 = 0.002221,$$
$$\sigma_2 = (100/C)[\sum d^2/(n-1)m]^{\frac{1}{2}},$$

where C is percentage concentration, n is number of readings per test point, and m is the number of test points.

$$\sigma_2 = (100/0.977)(0.002221/3\times 18)^{\frac{1}{2}}$$
$$= 0.66 \text{ percent of content.}$$

The homogeneity error σ_h may now be computed from the formula

$$\sigma_h^2 = \sigma_1^2 - \sigma_2^2,$$

whence

$$\sigma_h = 0.20 \text{ percent of the content.}$$

In view of its derivation from two substantially larger deviations, the probable precision of σ_h is not high. However, information on the order of magnitude of the concentrational uncertainty may be important.

The deviation of σ_2 may be apportioned among the various steps of the analytical procedure by a study of the uncertainties involved in each step. One error which may be segregated quite readily is that due to the microphotometer used for density measurement. The data given below have been chosen to demonstrate a method of computation alternate to that used in connection with Table III.

Table IV shows the microphotometer scale reading in centimeters for three repeat readings, R_1, R_2, and R_3 on each of 66 spectral lines, D_1, D_2, and D_3 are the differences in readings of successive lines in the columns R_1, R_2, and R_3, respectively. The deviations d_1, d_2, and d_3 are computed as follows: $d_1 = |D_1 - D_2|$, $d_2 = |D_1 - D_3|$, and $d_3 = |D_2 - D_1|$. The last three columns give the squares of the deviations.

$$\sum d^2 = 0.5850.$$

It is apparent that each deviation involves the error present in the reading of four separate lines. Hence,

$$\sigma_m = (\sum d^2/4n)^{\frac{1}{2}}.$$

Where n is the total number of deviations

$$\sigma_m = (0.5850/4\times 195)^{\frac{1}{2}}$$
$$= 0.027 \text{ cm.}$$

TABLE IV. Computation of microphotometer error.

Readings			Differences			Dev. $\times 10^2$			Dev.$^2 \times 10^4$		
R_1	R_2	R_3	D_1	D_2	D_3	d_1	d_2	d_3	d_1^2	d_2^2	d_3^2
33.75	33.75	33.75	6.75	6.80	6.75	5	0	6	25	0	25
27.00	26.95	27.00	0.25	0.35	0.35	10	10	0	100	100	0
27.25	27.30	27.35	9.55	9.55	9.50	0	5	5	0	25	25
17.70	17.75	17.85	1.75	1.70	1.70	5	5	0	25	25	0
19.45	19.45	19.55	14.70	14.70	14.60	0	10	10	0	100	100
34.15	34.15	34.15	0.40	0.40	0.50	0	10	10	0	100	100
34.55	34.55	34.65	2.45	2.40	2.45	5	0	5	25	0	25
32.10	32.15	32.20	5.60	5.50	5.55	10	5	5	100	25	25
26.50	26.65	26.65	5.75	5.60	5.65	15	10	5	225	100	25
32.25	32.25	32.30	8.10	8.00	8.05	10	5	5	100	25	25
24.15	24.25	24.25	9.90	9.85	9.90	5	0	5	25	0	25
34.05	34.10	34.15	0.05	0.00	0.05	5	0	5	25	0	25
34.00	34.10	34.10	13.00	13.05	13.05	5	5	0	25	25	0
21.00	21.05	21.05	7.20	7.20	7.25	0	5	5	0	25	25
28.20	28.25	28.30	2.95	2.95	2.95	0	0	0	0	0	0
31.15	31.20	31.25	0.65	0.60	0.60	5	5	0	25	25	0
31.80	31.80	31.85	3.55	3.55	3.60	0	5	5	0	25	25
28.25	28.25	28.25	6.10	6.10	6.10	0	0	0	0	0	0
22.15	22.15	22.15	11.90	11.90	11.90	0	0	0	0	0	0
34.05	34.05	34.05	0.80	0.75	0.70	5	10	5	25	100	25
34.85	34.80	34.75	6.20	6.10	6.05	10	15	5	100	225	25
28.65	28.70	28.70	5.80	5.85	5.80	5	0	5	25	0	25
22.85	22.85	22.90	12.95	13.00	12.95	5	0	5	25	0	25
35.80	35.85	35.85	3.50	3.55	3.50	5	0	5	25	0	25
32.30	32.30	32.35	10.60	10.50	10.60	10	0	10	100	0	100
21.70	21.80	21.75	5.45	5.50	5.45	5	0	5	25	0	25
16.25	16.30	16.30	8.55	8.60	8.60	5	5	0	25	25	0
7.70	7.70	7.70	8.25	8.30	8.30	5	5	0	25	25	0
15.95	16.00	16.00	2.10	2.10	2.10	0	0	0	0	0	0
13.85	13.90	13.90	5.95	6.05	6.00	10	5	5	100	25	25
19.80	19.95	19.90	8.95	9.05	9.05	10	10	0	100	100	0
10.85	10.90	10.85	4.60	4.60	4.70	0	10	10	0	100	100
15.45	15.50	15.55	6.40	6.40	6.40	0	0	0	0	0	0
21.85	21.90	21.95	8.90	8.90	9.00	0	10	10	0	100	100
12.95	13.00	12.95	23.70	23.65	23.75	5	5	10	25	25	100
36.65	36.65	36.70	4.90	4.90	4.95	0	5	5	0	25	25
21.75	21.75	21.75	5.50	5.50	5.50	0	0	0	0	0	0
16.25	16.25	16.25	0.20	0.20	0.20	0	0	0	0	0	0
16.05	16.05	16.05	15.90	15.90	15.90	0	0	0	0	0	0
13.95	31.95	31.95	18.00	18.10	18.00	10	0	10	100	0	100
13.95	13.85	13.95	5.90	6.00	5.90	10	0	10	100	0	100
19.85	19.85	19.85	8.95	9.00	9.00	5	5	0	25	25	0
10.90	10.85	10.85	4.60	4.65	4.60	5	0	5	25	0	25
15.50	15.50	15.45	6.30	6.35	6.40	5	10	5	25	100	25
21.80	21.85	21.85	9.85	9.90	9.90	5	5	0	25	25	0
12.95	12.95	12.95	6.35	6.45	6.45	10	10	0	100	100	0
19.25	19.35	19.35	5.65	5.60	5.55	5	10	5	25	100	25
24.90	24.95	24.90	11.90	11.90	11.85	0	5	5	0	25	25
13.00	13.05	13.05	2.10	2.10	2.10	0	0	0	0	0	0
10.90	10.95	10.95	10.15	10.15	10.15	0	0	0	0	0	0
21.05	21.05	21.05	3.10	3.05	3.10	5	0	5	25	0	25
17.95	18.00	17.95	1.30	1.35	1.30	5	0	5	25	0	25
16.65	16.65	16.65	1.90	1.95	1.95	5	5	0	25	25	0
18.55	18.60	18.60	7.35	7.35	7.30	0	5	5	0	25	25
25.90	25.90	25.90	8.40	8.40	8.35	0	5	5	0	25	25
17.50	17.55	17.55	5.00	4.95	4.95	5	5	0	25	25	0
22.50	22.50	22.50	4.25	4.25	4.30	0	5	5	0	25	25
18.25	18.25	18.20	5.80	5.80	5.85	0	5	5	0	25	25
24.05	24.05	24.05	1.75	1.70	1.70	5	5	0	25	25	0
22.30	22.35	22.35	13.25	13.30	13.25	5	0	5	25	0	25
9.05	9.05	9.10	16.20	16.25	16.20	5	0	5	25	0	25
25.25	25.30	25.30	0.90	0.95	0.85	5	5	10	25	25	100
24.35	24.35	24.45	5.60	5.60	5.70	0	10	10	0	100	100
18.75	18.75	18.75	5.20	6.15	6.10	5	10	5	25	100	25
12.55	12.60	12.65	1.60	1.60	1.60	0	0	0	0	0	0
14.15	14.20	14.25									

TABLE V. Computation of error from photographic plate.

R_1	R_2	D_1	D_2	kD_1	Dev. $\times 10^2$ d	Dev.^{2} $\times 10^4$ d^2
15.95	15.75	5.05	5.00	4.95	.05	.0025
10.90	10.75	1.55	1.60	1.50	.10	100
9.35	9.15	4.65	4.50	4.55	.05	25
14.00	13.65	6.30	6.05	6.15	.10	100
7.70	7.60	2.85	2.65	2.80	.15	225
10.55	10.25	5.20	5.20	5.10	.10	100
15.75	15.45	7.05	6.85	6.90	.05	25
8.70	8.60	2.55	2.50	2.50	.00	0
6.15	6.10	6.30	6.15	6.15	.00	0
		$\Sigma D=41.50$	40.50			$\Sigma d^2=.0600$
12.25	12.20	4.50	4.55	4.45	.10	.0100
16.75	16.75	4.20	4.10	4.15	.05	25
12.55	12.65	5.95	5.75	5.90	.15	225
18.50	18.40	1.80	1.85	1.80	.05	25
16.70	16.55	3.05	3.10	3.05	.05	25
19.75	19.65	1.10	1.05	1.10	.05	25
18.65	18.60	5.80	5.90	5.75	.15	225
12.85	12.70	4.45	4.35	4.40	.05	25
8.40	8.35	.90	.85	.90	.05	25
9.30	9.20					
		$\Sigma D=31.75$	31.50			$\Sigma d^2=.0700$
19.55	19.75	5.60	5.55	5.65	.10	.0100
25.15	25.30	12.00	12.00	12.15	.15	225
13.15	13.30	2.15	2.20	2.20	0	0
11.00	11.10	10.25	10.45	10.35	.10	100
21.25	21.55	8.90	9.25	9.00	.25	625
12.35	12.30	5.85	6.05	5.90	.15	225
18.20	18.35	1.45	1.40	1.45	.05	25
16.75	16.95	2.05	2.00	2.05	.05	25
18.80	18.95	7.40	7.40	7.50	.10	100
26.20	26.35					
		$\Sigma D=55.65$	56.30			$\Sigma d^2=.1425$
13.35	13.60	5.50	5.65	5.60	.05	.0025
18.85	19.25	9.85	10.20	10.00	.20	400
9.00	9.05	6.00	6.30	6.10	.20	400
15.00	15.35	2.65	2.60	2.70	.10	100
12.35	12.75	1.10	1.20	1.10	.10	100
11.25	11.55	1.60	1.70	1.60	.10	100
12.85	13.25	7.25	7.20	7.35	.15	225
20.10	20.45	2.70	2.75	2.75	0	0
17.40	17.70	8.70	8.65	8.85	.20	400
26.10	26.35	3.85	3.85	3.90	.05	25
29.95	30.20	4.00	4.00	4.05	.05	25
25.95	26.20	5.40	5.40	5.50	.10	100
31.35	31.60					
		$\Sigma D=58.60$	59.50			$\Sigma d^2=.1900$
12.20	12.30	4.85	5.00	4.90	.10	.0100
17.05	17.30	4.50	4.65	4.55	.10	100
12.55	12.65	6.35	6.50	6.40	.10	100
18.90	19.15	2.35	2.40	2.40	.00	0
16.55	16.75	3.65	3.60	3.70	.10	100
20.20	20.35	1.00	1.00	1.00	.00	0
19.20	19.35	5.85	5.90	5.90	.00	0
13.35	13.45	3.85	3.80	3.90	.10	100
9.50	9.65	15.00	15.05	15.15	.10	100
24.50	24.70	2.80	2.85	2.85	.00	0
21.70	21.85					
		$\Sigma D=50.20$	50.75			$\Sigma d^2=.0600$

R_1	R_2	D_1	D_2	kD_1	Dev. $\times 10^2$ d	Dev.^{2} $\times 10^4$ d^2
15.55	15.75	4.70	4.65	4.75	.10	.0100
10.85	11.10	.10	.20	.10	.10	.0100
10.75	10.90	16.75	16.85	16.90	.05	25
27.50	27.75	18.15	18.20	18.35	.15	225
9.35	9.55	4.85	4.90	4.90	.00	0
14.20	14.45	6.60	6.70	6.65	.05	25
7.60	7.75	3.05	3.15	3.10	.05	25
10.65	10.90	5.60	5.50	5.65	.15	225
16.25	16.40	7.25	7.35	7.35	.00	0
9.00	9.15	4.00	4.05	4.05	.00	0
13.00	13.20	1.55	1.80	1.55	.25	625
14.55	15.00					
		$\Sigma D=72.60$	73.35			$\Sigma d^2=.1350$
33.70	33.75	6.65	6.75	6.55	.20	.0400
27.05	27.00	.45	.25	.45	.20	400
27.50	27.25	9.75	9.55	9.60	.05	25
17.75	17.70	1.80	1.75	1.75	.00	0
19.55	19.45	14.70	14.70	14.50	.20	400
34.25	34.15	.55	.40	.55	.15	225
34.80	34.55	2.55	2.45	2.50	.05	25
32.25	32.10					
		$\Sigma D=36.45$	35.85			$\Sigma d^2=.1475$
26.95	26.50	5.65	5.75	5.70	.05	.0025
32.60	32.25	8.05	8.10	8.10	.00	0
24.55	24.15	9.85	9.90	9.95	.05	25
34.40	34.05	.10	−.05	.10	.15	225
34.50	34.00	12.90	13.00	13.00	.00	0
21.60	21.00	7.05	7.20	7.10	.10	100
28.65	28.20	2.90	2.95	2.95	.00	0
31.55	31.15	.70	.65	.70	.05	25
32.25	31.80	3.70	3.55	3.75	.20	400
28.55	28.25	6.00	6.10	6.05	.05	25
22.55	22.15	11.85	11.90	11.95	.05	25
34.40	34.05	.75	.80	.75	.05	25
35.15	34.85	6.10	6.20	6.15	.05	25
29.05	28.65	5.60	5.80	5.65	.15	225
23.45	22.85	12.80	12.95	12.90	.05	25
34.25	35.80	3.45	3.50	3.50	.00	0
32.80	32.30					
		$\Sigma D=97.45$	98.30			$\Sigma d^2=.1150$
36.50	36.65	14.85	14.90	14.95	.05	.0025
21.65	21.75	5.50	5.50	5.55	.05	25
16.15	16.25	.15	.20	.15	.05	25
16.00	16.05	15.80	15.90	15.90	.00	0
31.80	31.95	18.05	18.00	18.15	.15	225
13.75	13.95	6.00	5.90	6.05	.15	225
19.75	19.85	8.80	8.95	8.85	.10	100
10.95	10.90	4.50	4.60	4.55	.05	25
15.45	15.50	6.20	6.30	6.25	.05	25
21.65	21.80	8.55	8.85	8.60	.25	625
13.10	12.95					
		$\Sigma D=88.40$	89.10			$\Sigma d^2=.1300$
17.75	17.50	4.95	5.00	4.90	.10	.0100
22.70	22.50	4.25	4.25	4.20	.05	25
18.45	18.25	6.10	5.80	6.00	.20	400
24.55	24.05	1.80	1.75	1.75	.00	0
22.75	22.30	13.50	13.25	13.30	.05	25
9.25	9.05	16.40	16.20	16.15	.05	25
25.65	25.25	.80	.90	.80	.10	100
24.85	24.35	5.80	5.60	5.70	.10	100
19.05	18.75	6.30	6.20	6.20	.00	0
12.75	12.55	1.55	1.60	1.55	.05	25
14.30	14.15					
		$\Sigma D=61.45$	60.55			$\Sigma d^2=.0800$

TABLE V.—*Continued.*

R_1	R_2	D_1	D_2	kD_1	Dev. $\times 10^2$ d	Dev.^{2} $\times 10^4$ d^2
8.95	9.15	11.85	12.05	12.00	.05	.0025
20.80	21.20	7.25	7.35	7.35	.00	0
13.55	13.85	4.10	4.25	4.15	.10	100
17.65	18.10	.55	.50	.55	.05	25
17.10	17.60	.95	.90	.95	.05	25
18.05	18.50	3.95	4.00	4.00	.00	0
22.00	22.50	1.75	2.00	1.75	.25	625
20.25	20.50	1.55	1.35	1.55	.20	400
18.70	19.15					
		$\Sigma D = 31.95$	32.40			$\Sigma d^2 = .1200$
19.35	19.25	5.60	5.65	5.60	.05	.0025
24.95	24.90	11.85	11.90	11.80	.10	100
13.10	13.00	2.15	2.10	2.15	.05	25
10.95	10.90	7.10	7.02	7.05	.00	0
18.05	17.95	1.35	1.30	1.35	.05	25
16.70	16.65	1.95	1.90	1.95	.05	25
18.65	18.55	7.40	7.35	7.35	.00	0
26.05	25.90					
		$\Sigma D = 37.40$	37.25			$\Sigma d^2 = .0200$
18.65	18.60	4.65	4.75	4.70	.05	.0025
23.30	23.35	.90	.90	.90	.00	0
24.20	24.25	7.60	7.50	7.65	.15	225
16.60	16.75	.40	.50	.40	.10	100
16.20	16.25					
		$\Sigma D = 13.55$	13.65			$\Sigma d^2 = .0350$
		$\Sigma d^2 = 1.3050$				

This deflection error may be reduced quite readily to the equivalent uncertainty in the determination of concentration.

From the calibration curve for the photographic emulsion, 1-mm error in the deflection difference for a line pair gives 1/21 of a unit error in the log relative intensity.

The standard samples yielded the following data:

Log rel. intensity	Conc. %	Log conc. %
2.490	1.29	0.1105897
0.425	0.977	$\bar{T}$.9898946
2.065		0.1206951

From Table IV

$\sigma_m = 0.027$ cm
$= (0.27/21)$ log rel. intensity units
$= (0.27/21) \times (.1206951/2.065)$ log percent concentration units
$\sigma_m = 0.00076222$ log percent concentration units.

If an error of the magnitude of σ_m be applied to a sample of unit concentration, we have

$$\text{log indicated concentration} = \log 1 + \sigma_m = 0.00076222$$

and

$$\text{indicated concentration} = 1.00176.$$

Thus

$$\sigma_m = 0.18 \text{ percent of content.}$$

Since the light-sensitive component of the photographic plate is made up of a substantial number of discrete particles, distributed, presumably, at random, statistical fluctuations in the relative sensitivity of small adjacent regions may be anticipated. The procedure detailed below appears suitable for the study of such fluctuations.

If spectral lines of adequate length are recorded on a photographic plate, readings may be made on each of a group of lines for two mutually exclusive regions along their lengths. Due to imperfection in the imaging provided by the spectrograph, the two regions measured may have been recorded at slightly different intensities; correction may be introduced by multiplying either set of readings by a factor k to render the sum of the readings equal for both sets. The remaining r.m.s. deviation σ_3 includes then the deviation due to the grain of the photographic place σ_p as well as the measurement uncertainty σ_m.

In Table V, R_1 and R_2 are readings taken on mutually exclusive sections of long spectral lines; D_1 and D_2 are differences of readings of successive lines while kD_1 represents the adjusted value of D_1 to make $kD_1 = D_2$. The deviation d is $|D_2 - kD_1|$, while the last column gives the square of the deviation.

It is apparent that each deviation involves four line measurements. Thus,

$$\sigma_3 = (\sum d^2/4n)^{\frac{1}{2}}.$$

TABLE VI. Summary of deviations.

Source of uncertainty	Standard deviation Designation	% of content
Total error	σ_1	0.69
Inhomogeneity of sample	σ_h	0.20
Spectroscopic source	σ_s	0.46
Plate grain	σ_p	0.28
Microphotometer	σ_m	0.18

TABLE VII.

Source of uncertainty	Contribution to total deviation Designation	% of content
Total error	$\sqrt{2}\sigma_1$	0.98
Inhomogeneity	$\sqrt{2}\sigma_h$	0.28
Analytical error	$\sqrt{2}\sigma_2$	0.93
Spectroscopic source	$\sqrt{2}\sigma_3$	0.65
Plate grain	$2\sigma_p$	0.56
Microphotometer	$2\sigma_m$	0.36

Where n is the total number of deviations

$$\sigma_3=(1.3050/4\times122)^{\frac{1}{2}}$$
$$=0.052 \text{ cm.}$$

In a manner similar to that used for σ_m, the deflection error σ_3 may be transformed into the corresponding uncertainty in the measurement of percentage content, yielding

$$\sigma_3=0.33 \text{ percent of content.}$$

The standard deviation σ_p is, then

$$\sigma_p=(\sigma_3^2-\sigma_m^2)^{\frac{1}{2}}$$
$$=0.28 \text{ percent of content.}$$

The deviation σ_p checks quite closely, 0.28 percent *vs.* 0.31 percent, with the results of previous data, for a photometered area of 1.40×10^5 square microns, published last year.[3]

While several uncertainties, such as the least count of reading of scales and graphs, might be considered, it is thought that, with care, these may be kept quite small compared to the errors arising from the spectroscopic source, the photographic plate and the microphotometer. Under such assumption, a source error σ_s may be computed from σ_2. Since each analytical determination of Table III involves the reading of two spectral lines, *viz.*, the element line and the reference line, the microphotometer and plate-grain deviations to be associated with these results are, respectively, $\sqrt{2}\sigma_m$ and $\sqrt{2}\sigma_p$, and the source error is

$$\sigma_s=(\sigma_2^2-2\sigma_m^2-2\sigma_p^2)^{\frac{1}{2}}$$
$$=0.46 \text{ percent of content.}$$

The standard deviations assigned to the major sources of uncertainty are recapitulated in Table VI.

In assigning the contributions which each step in the analytical process makes to the total error, due account must be taken of recurrence. It is apparent that for σ_p and for σ_m, two uncertainties will be entailed in each analysis since each determination involves two spectral lines—an element line and a matrix line. In estimating the precision which may be anticipated in application to routine analytical procedure, sight must not be lost of the fact that each such analysis includes, explicitly or implicitly, a comparison of two samples, *viz.*, a test sample and a standard sample of known content. Hence, the total uncertainty may be expected to yield a value of $\sqrt{2}\sigma_1$ with contributions from the major sources of uncertainty approximating those shown in Table VII.

In view of the addition of deviations as the square root of the sum of squares, it is apparent that a major improvement in the analytical uncertainty may be effected only through a decrease in the more important errors. For example, if the microphotometer described last year[3] were substituted for the quite reliable laboratory instrument[4] used in test, σ_m would be reduced from 0.18 percent of content to 0.05 percent of content, and the analytical uncertainty of 0.93 would become 0.91; reduction by the same factor of the source and plate grain errors would yield, respectively, standard deviations of 0.69 and 0.76 percent of content.

The segregation of errors and the designation of those sources where improvement might be undertaken most profitably is thought to be so important in the attainment of higher analytical precision that the use of statistical treatment, applicable rigorously only to long series of measurements, might be accepted generally for the study of short series as well.

[3] H. B. Vincent and R. A. Sawyer, J. Opt. Soc. Am. **31**, 639 (1941).

[4] H. B. Vincent and R. A. Sawyer, J. Opt. Soc. Am. **27**, 193 (1937).

Stereo-Movies Without Camera Accessories

GORDON L. WALLS
Ophthalmic Research Laboratory, Wayne University College of Medicine, Detroit, Michigan
(Received September 28, 1942)

I. PREPARATION OF THE FILMS

THE method here described was devised as a makeshift, for the production of sample stereoscopic motion-picture films in monochrome and color. Such films were needed for demonstrating the writer's stereo-movie system;* but no stereoscopic camera or accessories were available. Certain features of the method seem to commend it to those interested in the fundamentals of stereo-cinematoscopic vision—particularly, to the investigator whose purse does not fit his urge to experiment with inter-lens distances, screen magnifications, viewing methods, and so on.

When a "one-eyed" camera is used for making stereoscopic still pictures, two exposures are ordinarily made with the camera moved, between times, an extent approximating the human interpupillary distance. An alternative method, which is occasionally more convenient, is to keep the camera stationary and rotate the object slightly on its axis between the two exposures, which then represent right- and left-eyed views of it. This rotation method was extended, for the production of stereoscopic motion pictures, in the following way:

A wooden disk about 30″ in diameter was mounted as a turntable and was driven slowly by an electric phonograph motor with a rubber-stopper pulley bearing upon the edge of the disk. The disk made about two revolutions per minute; but its size and speed were of no great consequence—the one important consideration was constancy of speed. The turntable was loaded either with a single large, irregular object (e.g., a vase of flowers) or a group of small objects (toy animals, canned goods, or the like) arranged in merry-go-round fashion.

With a stationary 16-mm camera loaded with reversible monochrome or Kodachrome film, two (or a multiple of two) revolutions of the disk were photographed. After processing, the portions of the film bearing separate turntable revolutions (or series thereof) were cut apart and aligned with homologous frames side by side. The two strips were then trimmed equal in length, and leaders were attached.

Two films were now in hand which were as nearly identical as the constancy of turntable speed allowed. They were screened by a pair of 16-mm sound projectors. Such machines can usually be borrowed or rented, and their speeds are so constant and so nearly equal that there will seldom be a difference of more than a frame or two per minute of run.

If projected side by side on a screen, and "fused" through the viewing goggles described below, the homologous frames would now be identical and a two-dimensional image would result. But, by simply advancing one film a few frames ahead of the other before starting the projectors, the angular difference produced between simultaneous frames makes them, respectively, left- and right-eyed, and the fusion image becomes stereoscopic.

An important feature is the ease with which one can alter the scale of the third dimension by varying the amount of advancement of one film before projecting—or even during projection, where the machines happen to be provided with brakes capable of brief actuation. From the film speed, the turntable speed (read from the film), and the disparity (in number of frames) of the two films as projected, the equivalent inter-lens distance of the hypothetical two-lens camera can readily be computed. Obviously too, a pseudoscopic effect of any desired extent can be produced at will.

II. VIEWING

Entirely satisfactory observation has been obtained by the use of a pair of 10-diopter prisms mounted in a spectacle frame, base in. Hinged

* In an attempt to persuade manufacturers to build a special camera and offer it on the amateur market. The camera would employ a single 35-mm film, fed at 16-mm rate, and a pair of rhomboidal prisms behind the two lenses, to bring the left- and right-eyed images side by side on the film in the proper relationship for viewing with the criss-cross goggles described herein.

to the temporal margins of the frame are matte black celluloid blinders. The film images are placed side by side on the screen with a few inches of darkness between them, and with the left-eyed image on the right and the right-eyed image on the left. With the 10-diopter wedges, the observer will find that he can station himself conveniently between the two projectors, and will need to exercise only a normal amount of convergence to secure and maintain fusion.

As the films are started, the observer holds the goggle blinders open, and then sees three pictures—the middle one, stereoscopically. Swinging the blinders inward cuts off the outlying monocular images, and the blurred free edges of the blinders conceal themselves in the dark area between the two screen images. The effect is then obtained of "looking through a window" at an actual scene.

III. NOTES

All objects in the camera field except the turntable and its cargo will be seen only two-dimensionally. A flat background should therefore be provided, unless for special purposes it is desired to secure a direct comparison of two- and three-dimensional appearances.

If a steady turntable speed cannot be attained, one may photograph only a single revolution and build up suitably lengthy projection films from a number of prints; but one is then restricted to the use of printable types of film.

Any method of viewing may be employed. The two screen images may be superimposed through filters or polarizing materials, and viewed through corresponding devices, though there seems no point to thus sacrificing brilliancy and colors.

If experiments demand that the observer-to-screen distance be flexible, a Risley prism may be substituted for one of the 10-diopter wedges; or, a phorometer may be employed.

An interesting illusion is obtained if one eye is occluded temporarily during observation: the turntable at once appears to accelerate. When observed binocularly, objects on either the near or far edge of the turntable are naturally rendered unclear through physiological diplopia. Seen monocularly, the near and far objects are equally sharp (granting good photography), and their movement in opposite directions mutually exaggerates their apparent speeds.

It will be found that stereopsis plus color is rather disappointing. Stereoscopic monochrome pictures are startlingly more "real" than flat ones, with flat color pictures intermediate in illusory perfection. Properly illuminated Kodachrome scenes have a depthy quality which binocular stereopsis does not materially enhance.

NOVEMBER, 1942 J. O. S. A. VOLUME 32

American War Standard Specification and Description of Color

FOR almost half a century, spectrophotometry has been the accepted method for the determination of those characteristics of an object which relate to its color. The National Bureau of Standards pioneered in this type of measurement and has continued its use as a primary method.

Color standardization and specification for technical purposes have been an accomplished fact for at least twenty years. The 1922 Report of the Colorimetry Committee of the Optical Society of America codified and published a standard procedure based on scientific investigations carried out by leading investigators in this and other countries since the middle of the nineteenth century. In 1931 the International Commission on Illumination adopted essentially the same procedure, with details modified on the basis of the most recent and reliable investigations, incorporating almost completely the recommendations of the National Bureau of Standards and the British National Physical Laboratory. This system has been widely published, elaborated for convenience in practical applications, and extensively used during the past decade in academic and industrial laboratories both here and abroad.

The chief criticism of this basic system of color

specification has been due to its technical character, very little provision having been made for its interpretation in familiar terms. This limitation has been overcome in the present standardization by recognition of the correlation between the basic system and the useful and readily comprehensible system of colored samples embodied in the *1929 Munsell Book of Color*. Reference to the *Munsell Book of Color*, supplemented by the basic specifications of the colors exhibited therein, provides a convenient, readily comprehended interpretation of the basic specifications, and facilitates their visualization. This is especially important for those who are not familiar with the basic specifications of color. Used in this manner, the *1929 Munsell Book of Color* bridges the gap between the aesthetic and qualitative comprehension of color employed by artists, designers, and the general public, and the basic specifications employed by and necessary for the purposes of science and industry.

When a numerical specification of color is undesirable, the use of a correlated system of color names adapted from common language and proposed by the Inter-Society Color Council is recommended. This system of color names has been defined in terms of the Munsell system and provides a literary method for the description of color where general comprehensibility is desired and precision is not important.

1. PURPOSE

To recognize and recommend a basic method for the specification of color and to facilitate its popular interpretation.

2. PROVISIONS

2.1* The spectrophotometer shall be recognized as the basic instrument in the fundamental standardization of color.

Note: Specifications of the spatial distributions of the incident and collected light are essential to the standardization of spectrophotometry. Until standard conditions are established by agreement the particular conditions employed in each instance should be stated clearly.

2.2* Color specifications computed from spectrophotometric data shall be found by means of the standard observer and coordinate system adopted in 1931 by the International Commission on Illumination.

In the absence of a special reason for adopting some other illuminant in reducing spectrophotometric data, standard I.C.I. Illuminant *C*, representative of average daylight, shall be used.

The basic specifications of color shall consist of the tristimulus value Y and the trichromatic coefficients x and y of the I.C.I. coordinate system, or they shall consist of the tristimulus value Y and the dominant wave-length and purity.

Note: Dominant wave-length and purity are obtainable by computation from the trichromatic coefficients x and y. Several methods of expressing purity have been proposed and used to some extent. In this standardization purity refers to the quantity which is called excitation purity in discussions of the several possible purity scales. For the sake of uniformity the symbol p and expression in terms of percent are recommended for purity. Likewise when Y is specified in terms of reflection factor it should be expressed in percent, symbol R. It is customary to express dominant wave-length in millimicrons μ, and this practice is recommended, together with the symbol λ.

2.3* For the popular identification of color, material standards may be used. The only system of material standards that has been calibrated in terms of the basic specification is represented by the 1929 edition of the *Munsell Book of Color*. The use of this book is recommended wherever applicable to the specification of the color of surfaces. Approximate identifications of Munsell hue, value, and chroma may be secured by direct visual comparison with the samples in the *1929 Munsell Book of Color*. When the most accurate visual comparisons are needed, the mask method is recommended. Wherever more exact Munsell notations are desired, they shall be found from the basic specification Y, x and y by interpolation among the smoothed curves for Munsell hue, value, and chroma.

Note: Most surfaces whose colors fall outside the range covered by the samples of the *1929 Munsell Book of Color*

---

* The alternative but coordinated systems of color specification described in 2.1, 2.2, and 2.3 are each adequate for specification of color tolerance in those cases for which each system is useful and convenient. As in all engineering specifications, the tolerances in different industries vary and depend upon the uses for which the products are intended. Color specifications according to 2.2 and 2.3 are, strictly speaking, appropriate only for products viewed by normal vision, but in the absence of agreement on standards for anomalous color vision or vision at low illuminations no more appropriate color specifications are available.

cannot be assigned Munsell notations by reference to the smoothed curves. For such surfaces, for transparent media, and for illuminants, only the basic specification Y, x and y, or Y, dominant wave-length and purity are recommended.

2.4 A descriptive name according to the ISCC-NBS system of color designation may be derived from the Munsell notation. This name is recommended wherever general comprehensibility is desired and precision is not important. The use of color names for color specification is not recommended.

Note: It should be emphasized that the ISCC-NBS names are descriptive only and are not adapted to sales promotion nor intended to replace names that are developed for that purpose.

For further information address: AMERICAN STANDARDS ASSOCIATION, *29 West Thirty-Ninth Street, New York, New York.*

Book Review

Optical Methods of Chemical Analysis. THOMAS R. P. GIBB, JR. First edition, pp. xiv+391, Figs. 300. Published by McGraw-Hill Book Company, Inc., New York, 1942 as 45th volume of the International Chemical Series. Price $5.00.

According to the author "the purpose of this book is to present a compact, abridged survey of the field of optical methods of analysis in a style suited both to the practical analyst and the advanced student of analytical chemistry. An attempt has been made to cover the construction, the fundamental theory, and the analytical uses of those instruments which have proved of most value to the chemist."

The ten instruments dealt with in detail are: 1. spectrograph, 2. spectrophotometer, 3. colorimeter, 4. turbidimeter, 5. nephelometer, 6. fluorophotometer, 7. microscope, 8. polarizing microscope, 9. refractometer, and 10. polariscope. A chapter is devoted to each type of instrument, except that 3 to 6 inclusive are treated together in Chapter III because they all depend on the measurement of light intensity, and an extra chapter, V, is devoted to Elementary crystallography as an introduction to the identification of crystals with the polarizing microscope. Each chapter is concluded with illustrative laboratory experiments, a group of practical problems, and a list of references selected usually "on the basis of simplicity, recency, and extent of bibliography." The references are admittedly incomplete, but this reviewer feels that they should have included a companion volume of the International Chemical Series, namely, *Crystal Chemistry* by C. W. STILLWELL.

The first edition of a scientific book is almost certain to contain some errors, no matter how conscientiously the proof has been read and corrected. Thus on page 24, the statement that the light-gathering power of a spectroscope is proportional to the focal length divided by the diameter of the collimator (aperture ratio) is followed by "the smaller the aperture, the brighter the spectrum, other factors being equal." Following the elementary theory of the diffraction grating we find on page 34 the statement that "a first-order line of 8000A will appear in the same place as a second-order line of 4000A and an exceedingly faint third-order line of 2000A." Perhaps all textbooks should contain some more or less obvious misstatements as a challenge to the students.

The author's course in "Optical Methods of Chemical Analysis" is required at M.I.T., of third-year students of chemistry and biology, and is elected by students pursuing courses in chemical engineering. This textbook is without doubt an important and opportune contribution to the teaching of optical chemistry. The ever-increasing demand for speed and sensitivity in analytical chemistry will continue to force the use and development of optical methods, and it may be expected that all progressive educational institutions will, in the future, train optical chemists in increasing numbers. The possibility that this will happen is assured by the timely appearance of this textbook on *Optical Methods of Chemical Analysis.*

W. F. MEGGERS
National Bureau of Standards